การประเมินปริมาณรังสีที่ผู้ป่วยขนาดต่างๆได้รับจากการตรวจทรวงอกด้วยเครื่องเอกซเรย์คอมพิวเตอร์ชนิด 320 สไลซ์

นางสาวเสาวภาคย์ ย้อยแก้ว

วิทยานิพนธ์นี้เป็นส่วนหนึ่งของการศึกษาตามหลักสูตรปริญญาวิทยาศาสตรมหาบัณฑิต
สาขาวิชาฉายาเวชศาสตร์ ภาควิชารังสีวิทยา
คณะแพทยศาสตร์ จุฬาลงกรณ์มหาวิทยาลัย
ปีการศึกษา 2559

Size-Specific Dose Estimates for Thoracic Imaging in 320 Row Detector Computed Tomography

Miss Saowapark Yoykaew

A Thesis Submitted in Partial Fulfillment of the Requirements
for the Degree of Master of Science Program in Medical Imaging
Department of Radiology
Faculty of Medicine
Chulalongkorn University
Academic Year 2016

Thesis Title	Size-Specific Dose Estimates for Thoracic Imaging in 320 Row Detector Computed Tomography
By	Miss Saowapark Yoykaew
Field of Study	Medical Imaging
Thesis Advisor	Associate Professor Anchali Krisanachinda, Ph.D.

Accepted by the Faculty of Medicine, Chulalongkorn University in Partial Fulfillment of the Requirements for the Master's Degree

.... Dean of the Faculty of Medicine
(Professor Suttipong Wacharasindhu, M.D.)

THESIS COMMITTEE

.... Chairman
(Associate Professor Panruethai Trinvarat, M.D.)

.... Thesis Advisor
(Associate Professor Anchali Krisanachinda, Ph.D.)

.... Examiner
(Associate Professor Kosuke Matsubara, Ph.D.)

.... External Examiner
(Professor Franco Milano, Ph.D.)

เสาวภาคย์ ย้อยแก้ว : การประเมินปริมาณรังสีที่ผู้ป่วยขนาดต่างๆได้รับจากการตรวจทรวงอกด้วยเครื่องเอกซเรย์คอมพิวเตอร์ชนิด 320 สไลซ์ (Size-Specific Dose Estimates for Thoracic Imaging in 320 Row Detector Computed Tomography) อ.ที่ปรึกษาวิทยานิพนธ์หลัก: รศ. ดร.อัญชลี กฤษณจินดา, 111 หน้า.

ในปัจจุบันนี้ ปริมาณรังสีที่ผู้ป่วยได้รับจากเครื่องเอกซเรย์คอมพิวเตอร์ แสดงในรูปของค่าปริมาณรังสีตลอดช่วงความยาวของการสแกนหรือ ค่า DLP (dose length product) และ ค่า CT dose index volume ($CTDI_{Vol}$) ซึ่งค่า $CTDI_{Vol}$ เป็นค่าที่ใช้ประเมินปริมาณรังสีโดยเฉลี่ยสำหรับตัวกลางที่มีค่าการดูดกลืนคล้ายมนุษย์ ซึ่งอ้างอิงจากหุ่นจำลองที่มีขนาดเส้นผ่านศูนย์กลาง 16 และ 32 ซม. โดยไม่มีการคำนึงถึงขนาดของผู้ป่วย ในขณะที่ปริมาณรังสีที่ผู้ป่วยได้รับขึ้นอยู่กับการตั้งค่าพารามิเตอร์ เช่น ค่าความต่างศักย์หลอด (kVp), ค่ากระแสไฟฟ้าหลอด (mA) เป็นต้น และขนาดของผู้ป่วย ดังนั้นการแสดงค่าปริมาณรังสีโดยประเมินจากหุ่นจำลองจึงไม่ถูกต้องและไม่ตรงกับความเป็นจริง

AAPM no.204 และ 220 ได้รายงาน การประเมินปริมาณรังสีที่ผู้ป่วยขนาดต่างๆได้รับ โดยแนะนำเทอม SSDEและคำนึงถึงขนาดของผู้ป่วยและการลดทอนปริมาณรังสีสำหรับการตรวจด้วยเครื่องเอกซเรย์คอมพิวเตอร์ วัตถุประสงค์ของงานวิจัยนี้เพื่อประเมินปริมาณรังสีที่ผู้ป่วยขนาดต่างๆได้รับจากการตรวจด้วยเครื่องเอกซเรย์คอมพิวเตอร์ส่วนทรวงอก (CT Chest) และศึกษาความสัมพันธ์ของปัจจัยต่างๆที่มีผลต่อปริมาณรังสีที่ผู้ป่วยได้รับ

งานวิจัยนี้เป็นการศึกษาแบบการเก็บข้อมูลย้อนหลัง โดยศึกษาในผู้ป่วยจำนวน 230 ราย (ผู้ชาย 115 ราย และผู้หญิง 115 ราย) ซึ่งมีอายุ ในช่วง 18 ถึง 93 ปี และ มีน้ำหนักในช่วง 40 ถึง70 กิโลกรัม ได้รับการตรวจ จากเอกซเรย์คอมพิวเตอร์ส่วนช่องอกด้วยการฉีดสารทึบรังสี (Venous phase protocol) ที่โรงพยาบาลจุฬาลงกรณ์ สภากาชาดไทย จากเครื่องเอกซเรย์คอมพิวเตอร์ชนิด 320 แถวของหัววัด ผลิตภัณฑ์ของบริษัทโตชิบา รุ่น Aquilion One และ การประเมินปริมาณรังสีที่ผู้ป่วยขนาดต่างๆได้รับ (SSDE) คำนวณโดย พิจารณาขนาดตัวของผู้ป่วยและขนาดของเส้นผ่านศูนย์กลางสมมูลน้ำจากภาพตัดขวางเอกซเรย์คอมพิวเตอร์ ได้นำค่าแก้ของขนาดตัวของผู้ป่วยมาจากการรายงานของ AAPM no.204 และ 220 มาคำนวณ

การประเมินปริมาณรังสีที่ผู้ป่วยขนาดต่างๆได้รับ (SSDE) ได้คำนวณจากภาพตัดขวางของผู้ป่วยในตำแหน่งตรงกลางทรวงอกและตรงกลางของระยะสแกน โดยจากการทดลองพบว่า ค่า SSDE ที่ได้จากการคำนวณจากภาพตัดขวางของตำแหน่งตรงกลางของระยะสแกนสูงกว่าตำแหน่งตรงกลางทรวงอกเล็กน้อย ค่าSSDE จากภาพตัดขวางของตำแหน่งตรงกลางของทรวงอก มีค่า $SSDE_{AP+LAT}$ $SSDE_{EFF}$ และ$SSDE_{Dw}$ คือ 10.50-24.45, 10.43-24.25 และ 11.66-26.83 มิลลิเกรย์ ตามลำดับ และ SSDE จากภาพตัดขวางของตำแหน่งตรงกลางของระยะสแกน มีค่า $SSDE_{AP+LAT}$ $SSDE_{EFF}$ และ $SSDE_{Dw}$ คือ 10.83-24.85, 10.70-24.70 และ 11.33-27.13 มิลลิเกรย์ ตามลำดับ การศึกษาความสัมพันธ์ของปัจจัยต่างๆ เช่น ค่า $CTDI_{vol}$, น้ำหนัก, ดัชนีมวลกาย, ความกว้างและระยะจากซ้ายไปขวา, เส้นผ่านศูนย์กลาง และ ขนาดของเส้นผ่านศูนย์กลางสมมูลน้ำ ต่อปริมาณรังสีที่ผู้ป่วยได้รับ(SSDE) อยู่ในระดับปานกลาง

สรุป การประเมินปริมาณรังสีบริเวณช่องอกที่ผู้ป่วยขนาดต่างๆได้รับ (SSDE) โดยคำนึงถึงขนาดตัวของผู้ป่วยจาก 3 วิธี ($SSDE_{AP+LAT}$, $SSDE_{EFF}$ and $SSDE_{Dw}$) พบว่า $SSDE_{Dw}$ เหมาะสมที่สุดในการแสดงค่าการประเมินปริมาณรังสีของผู้ป่วยขนาดต่างๆ มากกว่า ค่า $CTDI_{vol}$ ซึ่งสามารถให้ผลที่ถูกต้องเพราะจากการพิจารณาร่วมทั้งขนาดตัวของผู้ป่วยและส่วนประกอบภายในช่องอก

ภาควิชา รังสีวิทยา ลายมือชื่อนิสิต ....

สาขาวิชา ฉายาเวชศาสตร์ ลายมือชื่อ อ.ที่ปรึกษาหลัก ....

ปีการศึกษา 2559

5874086330 : MAJOR MEDICAL IMAGING
KEYWORDS: MULTI-DETECTOR COMPUTED TOMOGRAPHY / SIZE-SPECIFIC DOSE ESTIMATE / THORACIC CT EXAMINATION / PATIENT SIZE

SAOWAPARK YOYKAEW: Size-Specific Dose Estimates for Thoracic Imaging in 320 Row Detector Computed Tomography. ADVISOR: ASSOC. PROF. ANCHALI KRISANACHINDA, Ph.D., 111 pp.

The patient dose from CT scan is normally displayed in Dose Length Product (DLP) and volume CT dose index ($CTDI_{vol}$). Actually, $CTDI_{vol}$ represents the scanner output, does not address patient size, can be used to estimate patient radiation dose but the dose value is inaccurate as it is estimated from the cylindrical phantom of particular size. AAPM Report no.204 [1] introduced in 2011 and AAPM Report no.220 [2] introduced in 2014 on the size-specific dose estimates (SSDEs) for CT examination in order to provide high accuracy on radiation dose to the patient. The purpose of this study was to determine the patient radiation dose using SSDEs for thoracic imaging in 320 MDCT and the parameters influenced SSDEs.

This study is retrospective analysis with 230 patients, 115 male and 115 female of the age range from 18 to 93 years old, the selected weight range from 40 to 70 kg. All of the patients underwent the thoracic contrast enhancement with venous phase protocol scanned by 320 MDCT. The patient radiation dose in terms of SSDE was calculated based on AP+LAT dimension, effective diameter, and water equivalent diameter. The conversion factors following the body size and composition according to the AAPM no.204 and 220 recommendations were applied.

SSDE was measured from middle slice of chest and middle slice of scan range. The results showed that the SSDE calculated from the middle of scan range was a little higher than SSDE calculated from middle of organ. At the middle slice of organ, the range of $SSDE_{AP+LAT}$ $SSDE_{EFF}$ and $SSDE_{Dw}$ were 10.50-24.45, 10.43-24.25 and 11.66-26.83 mGy respectively. At the middle slice of scan range, the range of $SSDE_{AP+LAT}$, $SSDE_{EFF}$ and $SSDE_{Dw}$ were 10.83-24.85, 10.70-24.70 and 11.33-27.13 mGy respectively. The correlation of $CTDI_{vol,}$ body weight, BMI, AP+LAT dimension, effective diameter and water equivalent diameter with SSDE were moderately linear relationship.

In conclusions, SSDE had been estimated using 3 methods ($SSDE_{AP+LAT}$, $SSDE_{EFF}$ and $SSDE_{Dw}$) of body configurations in CT dosimetry. $SSDE_{Dw}$ is most appropriate for determination as the CT patient dose indicator further from $CTDI_{vol}$ especially in various body sizes and body composition in thorax region.

Department:	Radiology	Student's Signature	....
Field of Study:	Medical Imaging	Advisor's Signature	....
Academic Year:	2016		

ACKNOWLEDGEMENTS

I would like to express gratitude and deepest appreciation to Associate Professor Anchali Krisanachinda, Ph.D., Department of Radiology, Faculty of Medicine, Chulalongkorn University, my advisor, for her guidance, helpful suggestion, constructive comments and polishing of the thesis writing to improve the English expression.

I would like to deeply thank Dr. Kitiwat Khamwan, Department of Radiology, Faculty of Medicine, Chulalongkorn University, for his guidance and contribution in this research.

I would like to deeply thank Associate Professor Panruethai Trinavarat, MD., Department of Radiology, Faculty of Medicine, Chulalongkorn University, for her recommendation and comments in this research.

I would like to deeply thank Professor Franco Milano, University of Florence Italy, who is the external examiner of the thesis defense for his constructive comments.

I would like to deeply thank Associate Professor Dr. Kosuke Matsubara, Department of Quantum Medical Technology, Faculty of Health Sciences, Kanazawa University, JAPAN, who is the examiner of the thesis defense for his constructive comments, recommendation and teaching in principles of CT dosimetry.

I would like to thank Miss Hataipat Jantawong, Ph.D. student in Medical Physics programme, Faculty of Medicine, Chulalongkorn University, Bangkok, Thailand for her guidance and contribution. Sincere thanks to Mrs.Petcharleeya Suwanpradit and Mrs.Walaiporn Suksancharoen, the medical physicists at Department of Radiology, King Chulalongkorn Memorial Hospital for their kind guidance and support in this study.

I would like to thank all Radiology Technologist in CT room at King Chulalongkorn Memorial Hospital for their kind supports.

I would like to deeply thank Department of Radiology, Songklanagarind Hospital for support during the entire course of the study.

Finally, I am greatly thankful to my family for their invaluable encouragement and understanding during the entire course of the study.

CONTENTS

Page

Page

LIST OF TABLES

Table **Page**

LIST OF FIGURES

Figure **Page**

LIST OF ABBREVIATION

Abbreviation	Terms
SSDE	Size specific dose estimate
$SSDE_{AP+LAT}$	Size specific dose estimate based on AP+LAT dimension
$SSDE_{EFF}$	Size specific dose estimate based on effective diameter
$SSDE_{DW}$	Size specific dose estimate based on water equivalent diameter
f_{size}	Size-dependent conversion factor
f_{Dw}	Conversion factor as a function of water equivalent diameter, Dw
AP	Anteroposterior
LAT	Lateral
Dw	Water equivalent diameter
A_w	Water equivalent attenuation
A_{ROI}	Total area of ROI
A_{pixel}	Area of a pixel in the CT image
$\overline{CT(x,y)}_{ROI}$	Mean CT number in the ROI
AAPM	American Association of Physicists in Medicine
AEC	Automatic exposure control
CT	Computed Tomography
MDCT	Multi-Detector Computed Tomography
CTDI	Computed tomography dose index
$CTDI_{vol}$	Volume computed tomography dose index
$CTDI_w$	Weighted computed tomography dose index
DLP	Dose-length product
mGy	Milligray
mSv	Millisievert
mGy.cm	Milligray-centimeter
DRL	Diagnostic reference level
GL	Guidance level
FOV	Field of view
PMMA	Polymethylmethacrylate
ROI	Region of interest
SD	Standard deviation

cm	Centimeter
cm^2	Square centimeter
R^2	R-squared value
BMI	Body mass index
BW	Body weight
Kg/m^2	Kilogram per meter square
HU	Hounsfield unit
PACS	Picture archiving and communication system
QC	Quality control

CHAPTER I

INTRODUCTION

1.1 Background and Rationale

CT is the best modality for low contrast imaging in human and the clinical applications. The CT scanner has increased rapidly because of the short scan time and best image quality resulting in the major source of human exposure and highest collective effective dose from medical exposure [1].

The radiation dose from CT scan can damage the cells and tissues causing stochastic effect and cancer induction [2]. The probability of this effect depends on the quantity of radiation dose. Therefore, the radiation dose determination is very important and would be more accurate.

CT chest examination can demonstrate lung disorders such as nodules and lesions in the lung. The radiation dose delivered to the patient should be concerned because the increasing use of MDCT in patient studies and the thoracic region has several sensitive organs to radiation with high risk of fatal cancer such as lung and breast [3].

The patient dose estimation from CT scan is displayed in terms of Dose Length Product (DLP) with the unit of mGy.cm and the volumetric CT dose index ($CTDI_{vol}$) in mGy. $CTDI_{vol}$ represented the scanner output, depends on several parameters such as tube current time product (mAs), tube potential (kVp), pitch, gantry rotation time, slice collimation and filters. Actually, $CTDI_{vol}$ has not been considered to the actual patient size and only be used to estimate patient radiation dose based on the determination from the polymethyl methacrylate (PMMA) cylindrical phantom of particular size. One phantom size is 16 cm diameter to approximate the size of head and the other is 32 cm diameter to approximate the size of body. Both phantom is 15 cm length. Moreover, the composition inside the phantoms is constructed from homogeneous materials. As a result, the radiation dose value to the patient is inaccurate [4].

In fact, patient radiation dose should take into account for both output radiation dose and the patient characteristics, therefore patient size and tissue as well as organ composition should be considered to estimate patient radiation dose by using the concepts of the size-specific dose estimates (SSDEs).

AAPM Report number 204[5] introduced on the SSDEs for estimation of patient dose based on $CTDI_{vol}$ and patient size. Later on, AAPM Report number 220 [6] allows the estimation of patient dose based on $CTDI_{vol}$ and the body composition, water equivalent diameter (Dw) for CT examination to provide more accurately on radiation dose to the patient.

$CTDI_{vol}$ and DLP have been used for the patient radiation dose estimation at most institutions in Thailand. It is not realistic and inaccurate. When the radiation delivered to small or large patients displayed the same amount of $CTDI_{vol}$, estimated from same cylindrical phantom size.

At King Chulalongkorn Memorial Hospital (KCMH), the patients had been examined for the diagnosis and follow up of the lesions in thoracic region by using thoracic contrast enhancement with venous phase protocol in CT study. Regarding to scanner, the radiation output ($CTDI_{vol}$) had been determined and verified by using 32 cm in diameter of homogeneous cylindrical phantoms. On the contrary human thoracic region is not cylindrical shape, uniform in size and density, therefore, SSDE should be implemented for patient dose from CT scan in thoracic region.

1.2 Research objectives

1.2.1 To determine the patient dose using SSDE for thoracic imaging in 320 row detector computed tomography.
1.2.2 To determine parameters influence SSDE.

1.3 Definition

Volume CT dose index ($CTDI_{vol}$)	The multiplication of weighted CT Dose Index ($CTDI_w$) by pitch factor, the unit is mGy and it is used to compare radiation output level between different CT scanners.
Dose Length Product (DLP)	The product of $CTDI_{vol}$ and scan length, the unit mGy.cm, is related to the total ionizing energy imparted to the referenced phantom.
Size-specific dose estimates (SSDEs)	SSDE is patient dose estimated from the factors that take into account to the patient size and the body composition of different attenuation during CT scan.
320 MDCT	CT scanner with detector array of 320 row detector that allows the simultaneous scanning of more than one slice.

CT chest with venous phase protocol	Thoracic contrast enhancement using iodine contrast media and scan at 70-90 seconds after injection to separate lesion and surrounding tissue. This sequence is performed through the liver in the portal venous phase of enhancement.
AP+LAT dimension	The sum of anterior-posterior (AP) dimension demonstrates the thickness of patient body and lateral (LAT) dimension demonstrates left side to right side dimension of patient body.
Effective diameter	The diameter of the patient at a given the z-axis of the patient, assuming that the patient has a circular cross section. $Effective\ diameter = \sqrt{AP \times LAT}$
Water equivalent diameter (D_w)	The x-ray attenuation of a patient in terms of a water cylinder having the same x-ray attenuation. The diameter of such a cylinder of water are referred to as the Water equivalent diameter (Dw)
Attenuation	The reduction in radiation from passing through a tissue or material. This takes place through absorption or scatter of x-ray photons.

CHAPTER II

REVIEW OF RELATED LITERATURE

2.1 Theory

2.1.1 Introduction of computed tomography

Computed Tomography (CT) imaging is also known as "CAT imaging" (computed axial tomography). The word "tomography" is derived from the Greek word "tomos" (act of cutting) and "graphos" (image). Tomography refers to the cross-sectional imaging of an object from either transmission or reflection data collected by illuminating the object from many different directions [1].

Since the first CT scanner was developed in 1972 by Sir Godfrey Hounsfield, the modality has become established as an essential radiological technique applicable in a wide range of clinical situations. X-rays had been used to generate cross-sectional, two-dimensional images of the body. Images are acquired by rapid rotation of the x-ray tube 360° around the patient. The transmitted radiation is then measured by the ring of sensitive radiation detectors located on the gantry around the patient. The final image is generated from these measurements utilizing the basic principle that the internal structure of the body can be reconstructed from multiple x-ray projections.

Early CT scanners acquired images a single slice at a time (sequential scanning). However, during the 1980s significant advancements in technology heralded the development of slip ring technology, which enabled the x-ray tube to rotate continuously in one direction around the patient. This has contributed to the development of helical or spiral CT.

The first clinically available CT device was installed at London's Atkinson Morley Hospital in September 1971, after further refinement on the data acquisition and reconstruction techniques. Images could be produced in 4.5 minutes. On October 4, 1971, the first patient as in Figure 2.1, who had a large cyst, was scanned and the pathology was clearly visible in the cross-sectional image [2].

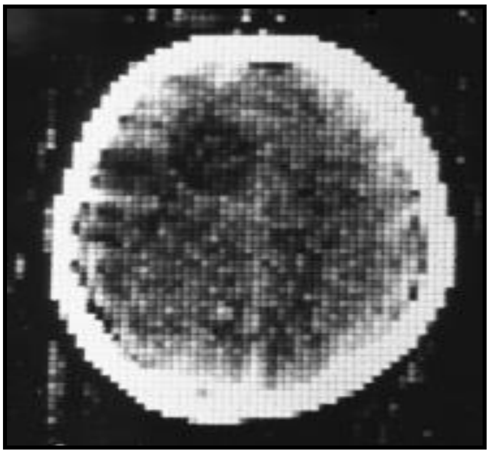

Figure 2.1 CT head images acquired of the first CT scanners [2].

CT has evolved into an indispensable imaging method in clinical routine. It was the first method to non-invasively acquire images of the inside of the human body that were not biased by superposition of distinct anatomical structures. This is due to the projection of all the information into a two-dimensional imaging plane, as typically seen in planar x-ray fluoroscopy. Therefore, CT yields images of much higher contrast compared with conventional radiography. Additionally, due to its ease of use, clear interpretation in terms of physical attenuation values, progress in detector technology, reconstruction mathematics, and reduction of radiation exposure, computed tomography will maintain and expand its established position in the field of radiology. [2, 7]

2.1.2 Principle of CT

2.1.2.1 X ray projection, attenuation and acquisition of transmission profiles

The process of CT image acquisition involves the measurement of x- ray transmission profiles through a patient for a large number of views. A profile from each view is achieved primarily by using a detector arc generally consisting of 800–900 detector elements (dels), referred to as a detector row. By rotation of the x-ray tube and detector row around the patient, a large number of views can be obtained. The use of tens or even hundreds of detector rows aligned along the axis of rotation allows even more rapid acquisition (Figure 2.2). The acquired transmission profiles are used to reconstruct the CT image, composed of a matrix of picture elements (pixels).

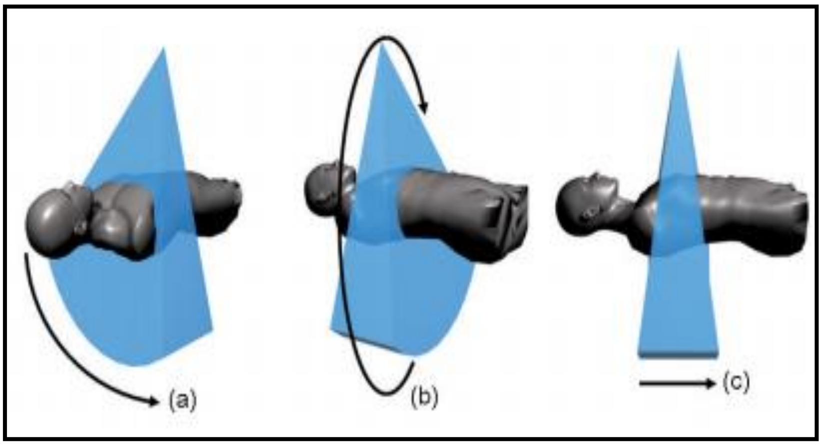

Figure 2.2 CT image acquisition showing the transmission of X-rays through the patient by using a detector row (a), with rotation of the x-ray tube and detector (b) and by multiple detectors (c) [7].

The values assigned to the pixels in a CT image are associated with the attenuation of the corresponding tissue, or, more specifically, to their linear attenuation coefficient μ (m^{-1}). The linear attenuation coefficient depends on the composition of the material, the density of the material and the photon energy, as seen in Beer's law:

$$I(x) = I_0 e^{-\mu x}$$

Where I(x) is the intensity of the attenuated x- ray beam, I_0 the unattenuated x-ray beam and *x* the thickness of the material. As an x- ray beam is transmitted through the patient, different tissues are encountered with different linear attenuation coefficients. If the pathway through the patient ranges from 0 to d, then the intensity of the attenuated x- ray beam, transmitted a distance d, can be expressed as:

$$I(d) = I_0 e^{-\int_0^d \mu(x) d(x)}$$

From the above, it can be seen that the basic data needed for CT are the intensities of the attenuated and unattenuated x-ray beams, respectively I(d) and I_0 , and that these can be measured. Image reconstruction techniques can then be applied to derive the matrix of linear attenuation coefficients, which is the basis of the CT image.

2.1.2.2 Hounsfield units

In the CT image, the matrix of reconstructed linear attenuation coefficients ($\mu_{material}$) is transformed into a corresponding matrix of Hounsfield units ($HU_{material}$), where the HU scale is expressed relative to the linear attenuation coefficient of water at room temperature (μ_{water}):

$$HU_{materail} = \frac{\mu_{material} - \mu_{water}}{\mu_{water}} \times 1000$$

It can be seen that $HU_{water} = 0$ ($\mu_{material} = \mu_{water}$), $HU_{air} = -1000$ ($\mu_{material} = 0$) and HU = 1 is associated with 0.1% of the linear attenuation coefficient of water. From the definition of the HU, it follows that for all substances except water and air, variations of the HU values occur when they are determined at different tube voltages. The reason is that, as a function of photon energy, different substances exhibit a non-linear relationship of their linear attenuation coefficient relative to that of water. This effect is most notable for substances that have a relatively high effective atomic number, such as contrast enhanced blood and bone.

CT images are usually visualized on a monitor using an eight-bit greyscale offering only 256 grey values. Each pixel HU value then has to undergo a linear mapping to a 'window' 8 bit value. The window width defines the range of HUs that is represented by the mapped values (ranging from white to black) and the window level defines the central HU value within the selected window width. Optimal visualization of the tissues of interest in the image can only be achieved by selecting the most appropriate window width and window level. Consequently, different settings of the window width and window level are used to visualize soft tissue, lung tissue or bone. The greyscale, as defined by window level and window width, is adapted to the diagnostic task and is thus dependent on the clinical question. [2, 4, 7, 8]

2.1.3 Components of Computed Tomography Scanner

The components of CT scanner include the gantry, X-ray source, a high-powered generator, detectors and detector electronics, data transmission systems (slip rings) and the computer system for image reconstruction and manipulation, as shown in Figure 2.3.

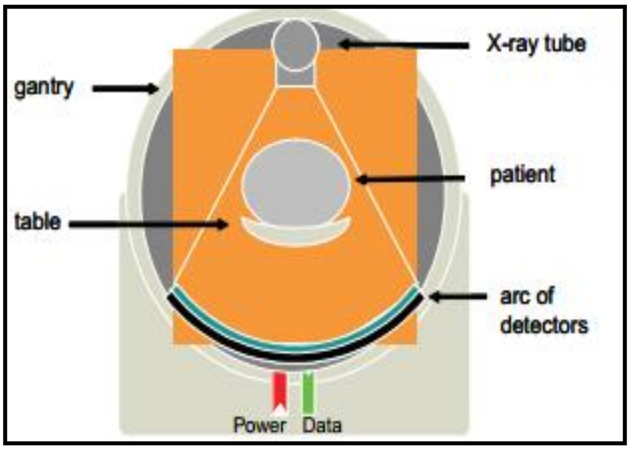

Figure 2.3 Schematic diagram of the CT scanner [9].

The gantry is the backbone of a CT system. The rotating side of the gantry typically contains the x-ray tube, detector, high-voltage device, tube-cooling tank, slip ring, and other supporting devices, as shown in Figure 2.4. With such a large load, the gantry still needs to maintain angular and position accuracy. Angular accuracy requires the gantry to rotate at highly constant speeds. Position accuracy requires the gantry to be free of significant vibrations in all directions and the clinical applications in which sub millimeter slice thickness is required. Since the width of the x-ray beam is less than a millimeter, the position of the x-ray beam should not vary more than a small fraction of the beam width during gantry rotation to ensure true sub millimeter imaging. Consequently, the gantry must be stable within a fraction of a millimeter for all projection angles. With increased demanding scan speeds, the requirements of gantry performance have also increased significantly. These requirements place large design constraints on the components mounted on the gantry.

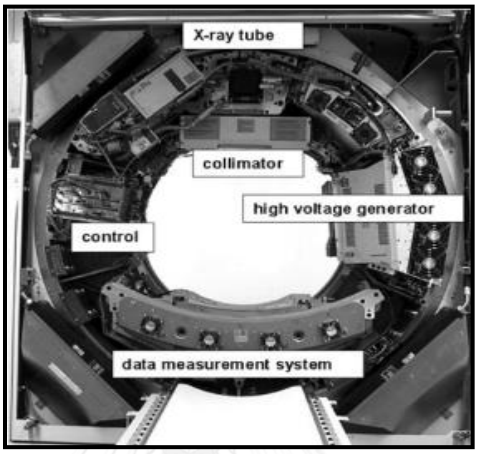

Figure 2.4 Basic system components of a third-generation CT system [2].

One of the components of the CT system is the slip ring which allows the gantry components to be coupled without cables. The x-ray tube rotates continuously around the gantry without hanging up the electronic mechanisms. The technology eliminates the time-consuming, start-and-stop process of earlier CT scanners and permits data acquisition to begin very quickly. Faster scan times led to the development of continuous acquisition exams such as computed tomography angiography. Slip-ring technology made helical CT scanning a reality.

Slip rings compose of electrical conductive rings and brushes. The slip ring transmits an electrical current across the rotating surface and supplies the electrical power to the x-ray tube and helps transfer the signals from the detectors to the computer for image reconstruction. High-voltage slip rings provide greater voltage capacity, typically more than 600 volts, as shown in Figure 2.5. [2, 4]

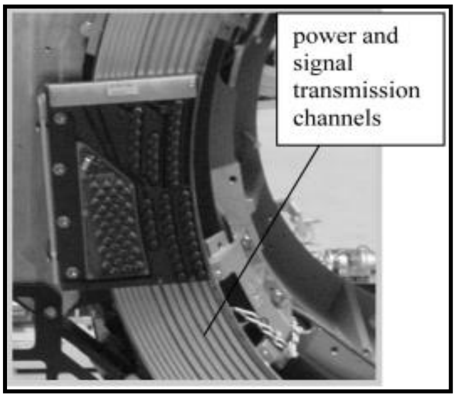

Figure 2.5 Photograph of a slip ring used for power and data transmission [2].

The patient table, patient couch, is made of a material that will absorb the least amount of radiation possible while still supporting the weight of the patient. Carbon fiber is the most common material used in CT tables. The table does much more than simply transport the patient into the scanner; its movement determine which part of a patient's anatomy is scanned and the thickness of the image sections [9].

The x-ray tube is mounted inside the gantry and rotates continuously around the patient. The tube consists of two major components: a cathode and an anode. The electron beam travels from the cathode and strikes a target on the anode. The tube then generates high-energy photons from the anode. The cathode contains compact tungsten filaments that set the current of the electrons flowing to the anode. The rotating anode usually is composed of an alloy of tungsten, and the target area of the anode is made of tungsten. Tungsten is an ideal metal for use in multislice CT scanners because of its high heat tolerance and high melting point of 3,400° C. Tungsten also dissipates heat quickly so that the target area can cool rapidly and be ready for the next bombardment of electrons. The target is fixed at an angle of approximately 11° to 12°. The cathode and anode are enclosed in a metal tube as shown in Figure 2.6.

The CT tube voltage (kV), and tube current, (mA), move the electron beams from the cathode to the anode. Changing the mA changes the cathode filament temperature so that the cathode produces the desired number of electrons. The energy level of these electrons can be controlled by adjusting the kV affects the penetrating power of the electrons that pass through the patient's body.

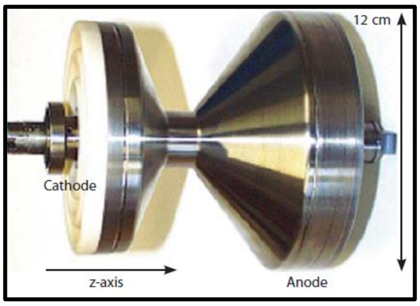

Figure 2.6 A rotating-envelope X-ray tube [10].

The generator is responsible for the high voltage needed to create x-rays. It produces voltages from 90 to 140 kV, with a typical CT scan using 120 kV. Generators convert the low-voltage alternating current to a high-voltage direct current that powers the x-ray tube with constant energy. The incoming power supply of 60 hertz (Hz) is transformed into a high-voltage, high-frequency current of 500 to 25,000 Hz. The power demands on a multislice CT unit are enormous, typically 20 to 100 kilowatts (kW). A 60-kW generator produces enough voltage to provide 80 to 120 kV and 20 to 500 mA.

The detectors, which measure the patient's x-ray attenuation data, are located opposite the x-ray tube. Detectors are very sensitive. They recognize the ionizing radiation that has passed through the patient, capture the signal and then transport the signal to the digitizer. X-rays produce an analog signal that must be converted into a digital signal so that the computer can read the information and produce the final CT image. The detector geometry is the relationship of the tube, the beam shape and the detectors. Current CT scanners use hundreds of detectors that are arranged in a curved array and aligned with the x-ray tube. (Figure2.7)

Detector efficiency determines how accurately the CT image is reproduced every time and with every patient. Different terms describe the detector efficiency. Capture efficiency is the measurement of how efficiently the detectors gather the photons coming from the patient. Absorption efficiency describes how efficiently the photons are captured by the detectors. Stability is the measurement of how consistently the detectors respond. The response time is how fast the detectors record the photons and how quickly they recover for the next event. Dynamic range refers to the accuracy of the detector's response to both high-energy and low-energy radiations. Finally, reproducibility describes how consistently the detectors respond to similar transmitted radiation events.

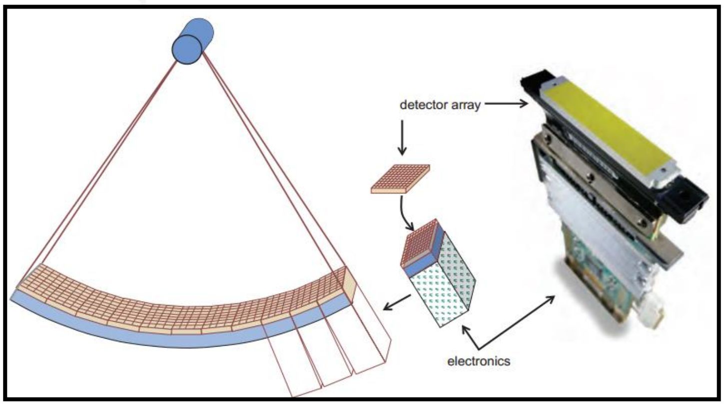

Figure 2.7 Detector array of modern CT [4].

In CT scanner the collimators is to provide a consistent beam width, which is defined by slice thickness. The beam width is measured in the z-axis at the center of the rotation for a single-row detector array. Collimation limits the amount of x-ray exposure to the patient by reducing scatter radiation and improves image contrast. CT scanners contain both pre-patient and post-patient collimators. Pre-patient collimators are located just outside the x-ray tube where the beam leaves the tube. These collimators, which are made of thick metal plates, define beam width and restrict the shape of the x-ray beam before it ever reaches the patient. In single-slice CT scanning, the collimators define the thickness of the cross-sectional slice. Pre-patient collimators also define the thickness of the x-ray beam in multislice CT scanning, which spreads the beam over the entire detector array, or multiple rows of detectors. In multidetector CT scanning, however, image reconstruction rather than pre-patient collimation determines the slice thickness. Post-patient collimators are positioned just above the detector array. These collimators improve image quality and axial resolution. Post-patient collimation also works in conjunction with pre-patient collimation to help define slice thickness. If post-patient collimation is reduced, the slice thickness decreases. Thin collimation results in better resolution, but it take longer to scan a particular area of anatomy. Wider collimation results in lower resolution, but it provide better volume coverage speed. [2, 4, 8, 9]

The x-ray photons emitted from an x-ray tube represent a wide spectrum. Many soft (low-energy) x-rays are present. The low-energy x rays are primarily absorbed by the patient and contribute little to the detected signal. Therefore, it is necessary to remove these soft x- rays to reduce the patient dose. To achieve this objective, most CT manufacturers employ additional x-ray filtration to improve beam quality. The most commonly used filters are the flat filter and the bowtie filter. The flat filter is typically made of copper or aluminum and is placed between the x-ray source and the patient. The flat filter modifies the x-ray spectrum uniformly across the entire FOV. Since the cross section of a patient is mostly oval-shaped, some manufacturers employ a bowtie filter to modify the x-ray beam intensity inside the FOV to further reduce the patient dose (Figure2.8). [2]

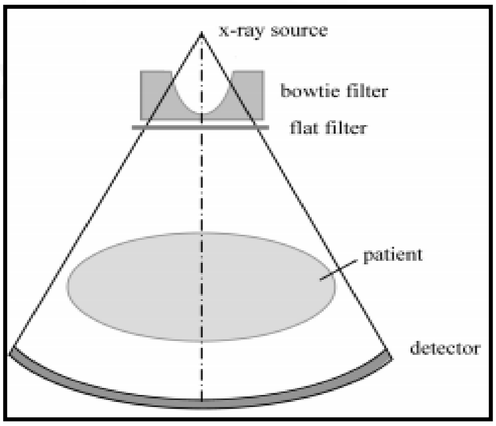

Figure 2. 8 Schematic diagram of a bowtie filter and a flat filter [2].

2.1.4 The principle of Multislice/ Multidetector Computed Tomography

Rapid acquisition of data, both for improved volume coverage and to minimize patient movement, is a major goal in CT and, as a means to this end, faster rotation times and spiral CT has already been discussed. The development of scanners in the mid1990s which allowed the simultaneous acquisition of more than one slice presented a further significant advance in CT technology

The principle of multi-slice CT is relatively straightforward. In a third generate on single slice design, up to 900 detector elements were arranged in an arc that was concentric with the *z*-axis but the detectors were only one element deep (typically 10 mm) in the *z* direction. To achieve slices less than 10 mm thick the beam width was restricted using physical collimators, often both between the x-ray tube and the patient and between the patient and the detectors. In multi-slice systems the detectors are physically and electronically separated along the *z*-axis and thus form a matrix of elements (Figure 2.9). Several designs of detector array have been developed by different manufacturers. Two basic designs have been used filed array detectors, in which all elements have the same width, and adaptive array detectors, in which the outer detectors are wider than those nearer the center.

An example of each is shown in Figure 2.9. Figure 2.9(a) shows a filed array detector with 64 detector rows and a collimated detector of 0.625 mm giving a maximum coverage of 40 mm along the *z*-axis. Thicker *z* values may be obtained by combining the detectors in groups. Figure 2.9(b) shows an adaptive array detector with 24 detector rows. In the middle there are 16 detectors with a width of 0.75 at the center of rotation. These are flanked by eight outer detector rows 1.5 mm wide. This array may operate as a 16 × 0.75 mm array covering 12 mm or as a 16 × 1.5 mm array covering 24 mm.

The development of multi-slice CT allowed imaging time to be significantly reduced. For example, an early multi-slice scanner offering four 5 mm slices per rotation allowed a volume of data to be acquired in a quarter of the time that a single-slice scanner would have taken to acquire 5 mm images through the same volume. However, the scanner could alternatively be used to acquire thinner slices, and hence achieve better *z*-axis resolution. The development of CT has been to acquire images with isotropic resolution, in the *z* direction matches that in the *x-y* plane. Once this is achieved, high quality images can be reconstructed in the coronal and sagittal planes, and various 3-D visualization techniques can be applied.[2, 4]

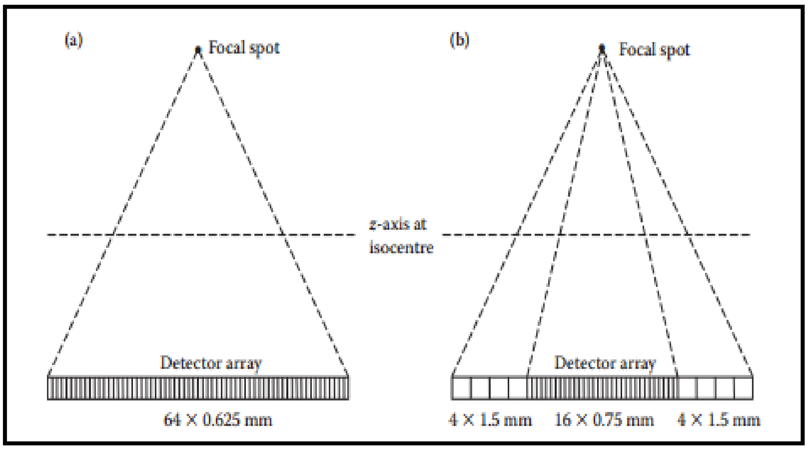

Figure 2.9 Multi-detector arrangements; (a) A filed array detector with 64 × 0.625 mm detectors, (b) an adaptive array with 16 × 0.75 mm detectors at the center and 4 × 1.5 mm detectors on each side [2].

2.1.5 Image reconstruction of CT

Each registered beam is just a projection of attenuation characteristics of the irradiated tissue. The aim of the reconstruction algorithm is to estimate how the tissue absorptions are distributed along the x-ray path. This goal is not achievable using a single projection profile. Instead it needs a large number of projections for many different angles. The acquired projection profile can be displayed as a sinogram (Figure 2.10). Sinograms are not used for clinical routine, but they are relevant for understanding tomographic principles. The horizontal axis of the sinogram represents the different projection profiles. The vertical axis in the sinograms corresponds to each angle of projections. Objects closer to the center of the field of view produce small sinusoid amplitudes in the sinogram, and objects closer to the edge produce heightened sinusoidal amplitudes.

Reconstructing an image from the projection profiles is a classical inverse problem. Early attempts at CT reconstruction used an iterative approach called algebraic reconstruction algorithm. This algorithm starts with an assumed image, computes projections from the image, compares the original projection data, and updates the image based on errors between projections that would be obtained from the current pixels, values, and actual projection. This method was very time-consuming and computationally intensive.

A faster CT reconstruction approach has been developed called filtered back-projection. It became widely accepted because reconstruction of the images is completed as soon as the CT examination is finished.

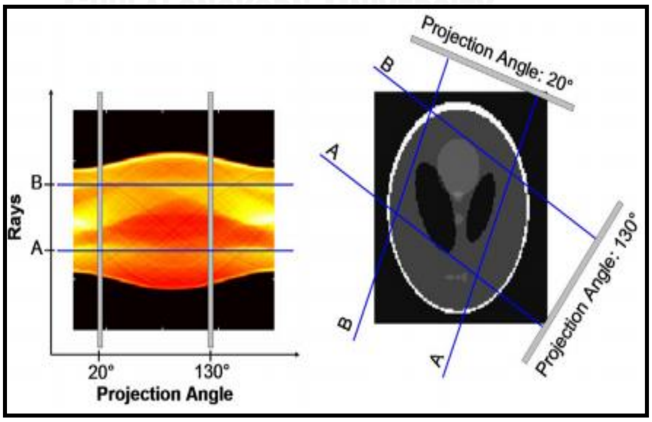

Figure 2.10 The sinogram contains the raw data of a CT acquisition [11].

Today, faster computer processors are allowing for the use of iterative reconstruction algorithms. These algorithms begin to replace filtered back-projection algorithms because they permit reduced image noise with low milli-Ampere/peak kilovolt settings. The algorithms use approximations of voxel attenuation to calculate projection data; these approximations of voxel attenuation are iteratively adjusted to decrease the difference between the measured data and the estimated data. The signal-to-noise ratios obtained by iterative reconstruction techniques are better compared with filtered back-projection while simultaneously conserving spatial resolution. [4, 9]

2.1.6 The dosimetry in computed tomography

For a single CT scan taken with a step-and-shoot mode, nearly all of the primary radiation is confined to a thin cross-section of the nominal slice thickness *T*. Because of the beam divergence, the penumbra of the beam, and the scattered radiation, dose is also delivered to tissues outside the nominal imaging section. This results in a dose profile in *z* (perpendicular to the cross-section) with long tails, as illustrated in Figure 2.11 for the dose profile of a 10-mm scan.

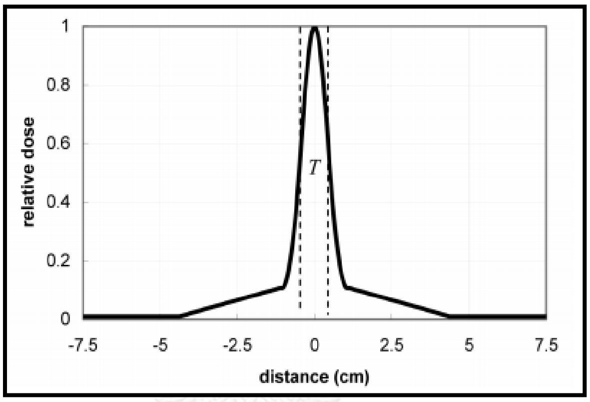

Figure 2.11 The single-scan dose profile for 10-mm slice thickness [8].

When multiple scans are performed in the adjacent region, x-ray dose from nearby scans also contributes to the dose to the current location, due to the long tails of the dose profile. If we combine the x-ray dose from all scans, we obtain a composite dose profile, as shown in Figure 2.12. This figure illustrates the composite dose profile of seven scans acquired with 10-mm collimation at 10-mm increments (the table travels 10 mm between adjacent scans). The dose at the center section is significantly higher than the single-slice dose profile. In this particular example, the average composite dose within the center region of width *T* is roughly 85% higher than the average dose of a single scan. Although this example is obtained with scans taken with step-and-shoot mode, similar conclusions can be obtained for the helical/spiral scan mode as well. In fact, the multiple-scan dose profiles for the helical mode are very similar to those of the step-and-shoot scans with the exception of inhomogeneities following the spiral pattern.

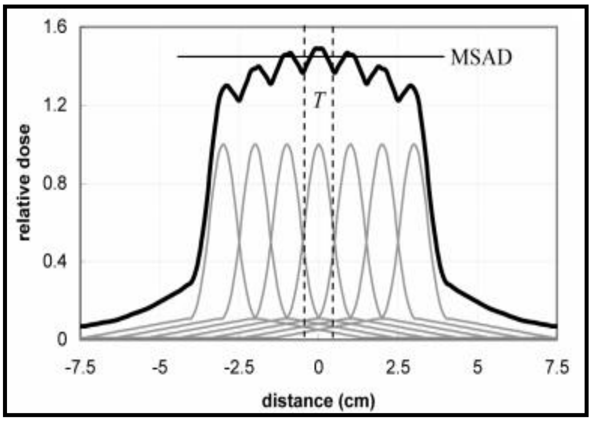

Figure 2.12 Multiple-scan dose contributions for 10-mm slice thickness at 10-mm increments [8].

To account for the fact that the majority of CT scans performed in a clinical environment consist of multiple scans, Computed Tomography Dose Index (CTDI) was proposed. The most commonly used index is $CTDI_{100}$, which refers to the dose absorbed in air, although it is measured in the standard polymethylmethacrylate (PMMA) phantoms as shown in Figure 2.13. For this index, the dose is integrated over a fixed length of 100 mm,

$$CTDI_{100} = \frac{1}{nT}\int_{-50mm}^{50mm} D_a(Z)dz$$

Where $D_a(z)$ is the dose absorption distribution in *z* for a single axial scan, *n* is the number of detector rows used during the scan, and *T* is the nominal thickness of each row. The quantity nT, therefore, is the nominal x-ray beam width during the data acquisition.

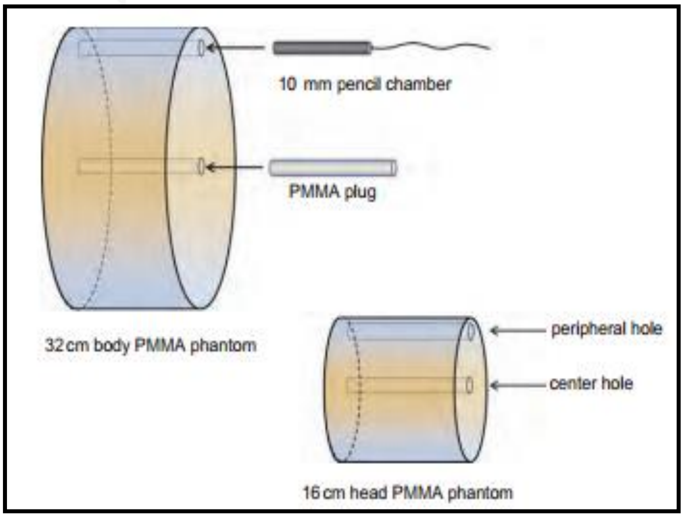

Figure 2.13 The computed tomography dose index (CTDI) is measured using either a 16-cm or 32-cmdiameter polymethyl methacrylate (PMMA) phantom [4].

CT scanners expose patients to x-rays over 360 degrees, the x-ray dose is significantly more homogeneous than in conventional x-ray. In CT scans, the portion of the phantom that directly faces the x-ray source changes constantly as the x-ray tube rotates about the patient. As a result, doses are distributed more evenly across the entire phantom, as shown by Figure 2.14. A closer inspection of Figure 2.14 shows that variation in dose still exists between the periphery of the phantom and the center of the phantom. The degree of dose non-uniformity depends highly on the size, shape, and composition of the object. For CT head scans, for example, the center of the patient receives nearly as much radiation dose as the periphery. For body scans, the dose uniformity decreases with the patient size increase. For a 35-cm diameter body, the central dose is roughly one fifth to one third of the peripheral dose. To account for the spatial variation of the dose, a weighted dose index, $CTDI_w$, which combines dose information at different locations, was proposed, and is calculated based on the formula:

$$CTDI_w = \left(\frac{1}{3}\right) CTDI_{100(center)} + \left(\frac{2}{3}\right) CTDI_{100(peripheral)}$$

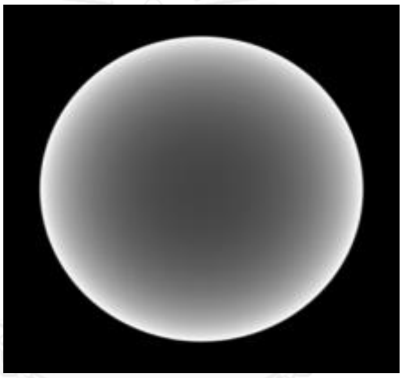

Figure 2.14 CT dose distribution when the gantry rotates 360 deg [8].

The most commonly used phantoms for dosimetry are the PMMA phantoms with a diameter of 16 cm for head and 32 cm for body. Figure 2.15 shows the CT dose measurement setup with a 32-cm body phantom. The peripheral dose is based on the dose measurements of the ion chamber in the four predrilled peripheral holes near the rim of the phantom that is highlighted by the dotted circles. The center dose is based on the measurement of the ion chamber in the center hole of the phantom that is highlighted by the solid circle.

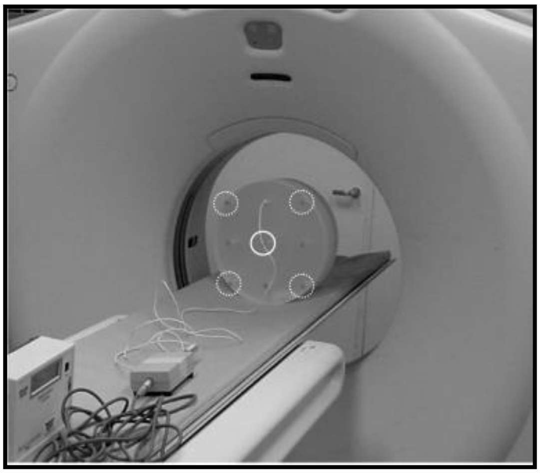

Figure 2.15 Dose measurement setup with CTDI body phantom (32-cm diameter) and ion chamber (100-mm length) [8].

The definition of $CTDI_w$ considers only the x-ray exposure for a step-and shoot scan, and does not take into account the x-ray dose received when a helical scan is performed. In helical or spiral scans, the patient table travels at a constant speed while data collection takes place. One parameter that describes how fast the patient table travels is the helical pitch, defined as the ratio of the table traveling distance in one gantry rotation over the nominal beam width. As the helical pitch increases (assuming all other parameters are kept constant), the same amount of x-ray radiation is distributed over a longer *z*. Since CTDI is defined as the dose per unit length in *z*, its value should reduce with the increase in helical pitch. This led to the introduction of $CTDI_{vol}$.

Most scanners have the ability to display the $CTDI_{vol}$ on the CT scanner console prior to the actual scan. The value can be displayed because the CT manufacturer has measured $CTDI_{vol}$ in the factory over the range of kV values for that model of scanner, and then that stored value, scaled appropriately by the mAs and pitch, is displayed on the console. [18]

$$CTDI_{vol} = \frac{CTDI_w}{Pitch}$$

This value is expressed in mGy and is displayed on most of the CT consoles during the scan prescription. In a clinical environment, however, the scan range in *z* can vary significantly depending on the clinical indications.

The CTDI is the phantom used in the dose measurement. The dose measurements of the two CTDI phantoms (16 and 32 cm) are used to provide the basis for the patient dose calculation. However, patients come in different shapes and sizes, and two round phantoms are an oversimplification of the patient population. In addition, patient organs consist of different tissue types and are not uniform across the entire FOV. This leads to a non-uniform dose distribution inside the patient, which is in sharp contrast to the uniform CTDI phantoms. [4, 12]

$$DLP = CTDI_{vol} \times scan\ length$$

The product of the $CTDI_{vol}$ and the length of the CT scan along the z-axis of the patient, *L*, is the dose length product (DLP) with the unit in mGy.cm

Limitations of $CTDI_{vol}$, the most important limitation of $CTDI_{vol}$ is that it is a dose index, and was not initially meant to be a measurement of dose per se. CTDI concepts were meant to enable medical physicists to compare the output between different CT scanners and were not originally intended to provide patient-specific dosimetry information. The body $CTDI_{vol}$ as reported by the CT scanner, or as measured on a CT scanner, is a dose index that results from air kerma measurements at two locations to a very large (32-cm diameter) cylinder of PMMA plastic with a density of 1.19 g/cm^3. In terms of human dimensions, the 32-cm-diameter PMMA body phantom corresponds to a person with a 119 cm waistline—a large individual, indeed. For smaller patients, the actual doses are larger than the $CTDI_{vol}$ for the same technique factors—thus, the $CTDI_{vol}$ tends to underestimate dose to most patients.

In light of this limitation, researchers have recently shown that patient size conversion factors can be used with the $CTDI_{vol}$ reported on a given CT scanner to produce size specific dose estimates (SSDEs). These conversion factors for the $CTDI_{vol}$ measured on a 32-cm-diameter phantom. The conversion factors described in AAPM Report 204 may be used to more accurately estimate size-corrected doses from the $CTDI_{vol}$, and these conversion factors are independent of scanner manufacturer and tube voltage. However, some CT scanner models use the $CTDI_{vol}$ value measured using the 16-cm-diameter PMMA phantom, and caution is needed to ensure that the correction factors specific to the appropriate reference phantom are used. [4, 8]

2.1.7 Thoracic computed tomography

Computerized tomography of the chest has revolutionized thoracic imaging. It can provide important information in the diagnosis and management of pulmonary masses and malignancy, mediastinal disease, bronchiectasis, interstitial lung disease and pleural abnormalities. However, it is a relatively expensive technique and carries a risk of inducing malignant disease due to radiation exposure. To improve current practice, requesting doctors need a greater understanding of the indications for computerzed tomography scanning and its different forms (conventional vs high resolution).

By altering the processing algorithms, two sets of images can be obtained – lung windows (Figure 2.16a) and mediastinal windows (Figure 2.16 b). In the mediastinal windows the lungs are overexposed and simply appear black. This algorithm is used to assess chest wall and mediastinal structures, usually with intravenous contrast so that vascular structures in the mediastinum can be distinguished from enlarged lymph nodes or other masses. These mediastinal windows are also appropriate to look at the chest wall and pleura and in particular for pleural plaques such as calcium containing asbestos pleural plaques. In the lung windows the mediastinal and chest wall structures are essentially whited out and the lung tissue can be seen in detail including areas of consolidation, and pulmonary vascular structures.

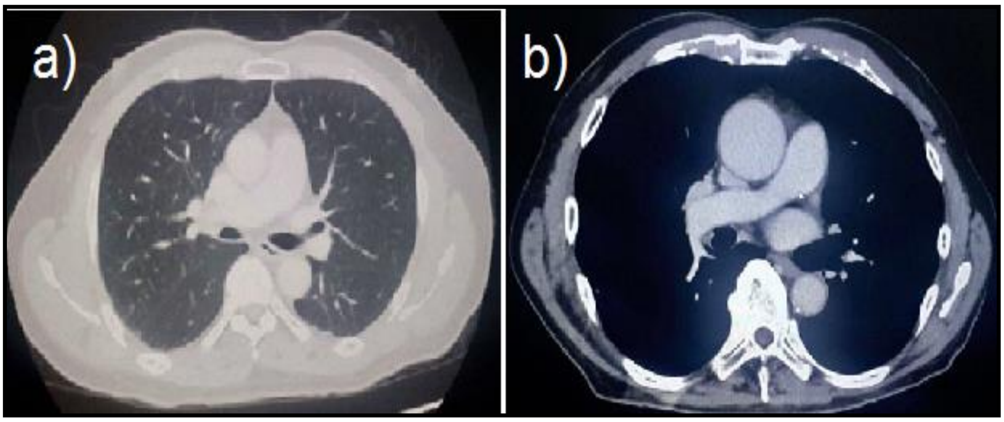

Figure 2.16 Processing algorithms of thoracic images (a) Lung windows and (b) mediastinal windows.

In staging of lung cancer a contrast CT is needed and should include the upper abdomen to assess the liver and adrenal glands. Usually detectable on plain chest radiographs) is very reassuring and implies that the lesion is both chronic and benign. However, a specialist referral is almost always indicated and CT scanning is unlikely to alter this requirement.[12, 13]

2.2 Review of related literature

American Association of Physicists in Medicine (AAPM) Report no.204 [5] described the use of a size metric that involved the physical dimensions of the patient (anteroposterior [AP], lateral, AP+ lateral, or effective diameter), in combination with scanner output ($CTDI_{vol}$), to determine size specific dose estimates (SSDE) from CT scanning. The electronic measurement tools can be used to measure physical dimensions from either the CT localizer radiograph or an axial CT image on the monitor. The conversion factors used to calculate SSDE from $CTDI_{vol}$ were derived from four different methods: measurements in anthropomorphic phantoms or polymethy-methacrylate cylindrical phantoms and Monte Carlo simulations in cylinders or voxelized phantoms and normalized to patient size. The specific formula to estimate patient dose for a specific patient size is given by:

$$SSDE = f_{size} \times CTDI_{vol}$$

Where f_{size} is the correction factor that takes into account the patient size (anteroposterior [AP], lateral, AP+ lateral, or effective diameter).

American Association of Physicists in Medicine (AAPM) Report no.220 [6] introduced SSDE to allow estimation of patient dose based on $CTDI_{vol}$ and water equivalent diameter (Dw). This task group was to develop a robust and scientifically sound metric for automatically estimating patient size in CT that would account for patient attenuation and allow routine determination of SSDE for all patients, with little or no user intervention. AAPM report 220 had a specific goal of developing a practical, standardized approach to estimating patient size that could be implemented by CT scanner manufacturers and others using CT localizer radiographs, axial CT images reconstructed using a full FOV, or other data derived from the scanning process (e.g., projection data). The specific formula to estimate patient dose for a specific patient size is given by:

$$SSDE = f_{Dw} \times CTDI_{vol}$$

Where f_{Dw} represents the SSDE conversion factor as a function of patient size (D_w).

Determination of water-equivalent diameter (D_w) from the CT Image was computed from the attenuation-area product of each image. The attenuation values, or CT numbers, in the axial CT image are expressed using a special unit known as Hounsfield Units (HU):

$$CT_{(x,y)} = \frac{\mu(x,y) - \mu_{water}}{\mu_{water}} \times 1000 \quad (1)$$

Where μ(x,y) is the linear attenuation coefficient for a voxel in an axial CT image at position(x,y). Because μ(x,y) is normalized to the attenuation of water in the definition of CT number, water equivalent area (Aw) can be represented in terms of CT numbers, as shown in Equation 2,

$$A_w = \sum \left[\frac{\mu(x,y)}{\mu_{water}} \right]^{\alpha} \times A_{pixel} \quad (2a)$$

$$A_w = \sum \left[\frac{\mu(x,y)}{1000} + 1 \right]^{\alpha} \times A_{pixel} \quad (2b)$$

Where A_{pixel} is the area of a pixel in the CT image and CT(x,y) is the CT number of a voxel. The parameter α determines the weighting of the linear attenuation coefficients relative to water. Linear dependence (α = 1) was assumed. A_w can be calculated using the mean CT number within a region of interest (ROI). The ROI must be large enough to include the entire patient cross section, but should not include irrelevant objects such as the patient table, since it is only the dose to the patient that is of interest. Equation 2b can then be expanded as,

$$A_w = \sum \left[\frac{\mu(x,y)}{1000} + 1 \right] \times A_{pixel} \quad (3a)$$

$$A_w = \sum \frac{CT(x,y)}{1000} \times A_{pixel} + \sum A_{pixel} \quad (3b)$$

$$A_w = \sum \frac{1}{1000} \times \frac{\sum CT(x,y)}{N_{pixel}} \times \left(N_{pixel} \times A_{pixel} \right) + \left(N_{pixel} \times A_{pixel} \right) \quad (3c)$$

$$A_w = \frac{1}{1000}\overline{CT(x,y)_{ROI}}A_{ROI} + A_{ROI} \quad (3d)$$

Where the mean CT number in the ROI, N_{pixel} is the number of pixels in the region of interest, and, which is the total area of the ROI. The ROI may include the air surrounding the patient, since voxels that have an attenuation coefficient of nearly zero negligibly change the value of the sum in Equation 2b.

D_w is calculated from the CT images as Equation:

$$D_w = 2\sqrt{A_w / \pi}$$

$$Dw = 2 \times \sqrt{\left(\frac{\overline{CT(x,y)_{ROI}}}{1000} + 1\right) \times A_{ROI} / \pi}$$

Thus, D_w of an object can be calculated from the mean CT number in an ROI containing that object. The mean CT number can be evaluated using tools readily available on most CT operator consoles or workstations. Alternatively, automatic segmentation algorithms could be used.

Christner JAet al [14] studied on: size-specific dose estimates for adult patients at CT of the torso.The purpose of the study was to determine the relationships among patient size, scanner radiation output, and size-specific dose estimates (SSDEs) for adults who underwent CT of torso. 545 adult patients (322 men, 223 women) were included in the study. $CTDI_{vol}$ was used with measurements of patient size (AP+LAT) and the conversion factors from the AAPM Report 204 to determine SSDE. Linear regression models were used to assess the dependence of $CTDI_{vol}$ and SSDE on patient size.

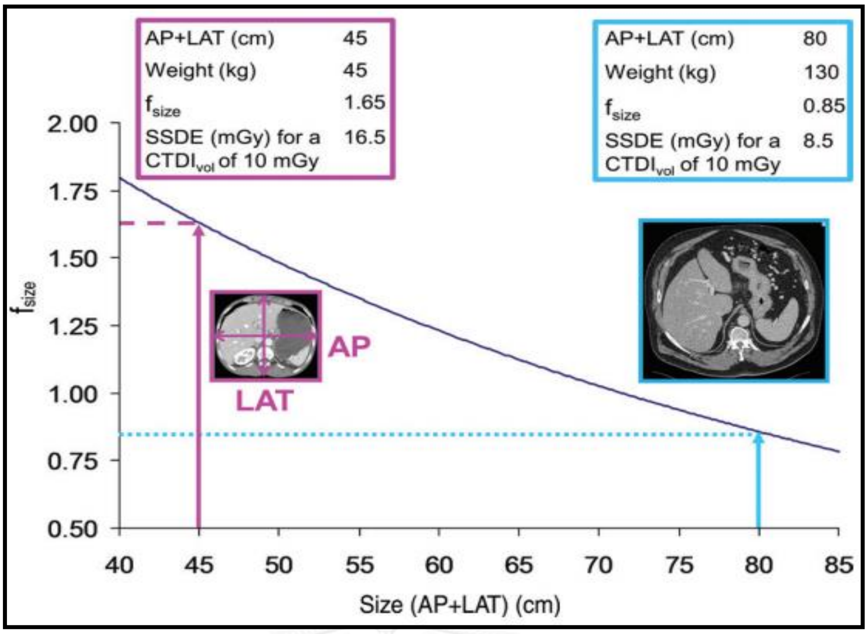

Figure 2.17 Graph shows how f_{size} was used to convert $CTDI_{vol}$ to SSDE, according to method in AAPM Report 204 [14].

The result showed patient sizes ranged from 42 to 84 cm. In this range, $CTDI_{vol}$ was significantly correlated with size (slope = 0.34 mGy/cm; 95% confidence interval [CI]: 0.31, 0.37 mGy/cm; $R^2 = 0.48$; $P < .001$), but SSDE was independent of size (slope = 0.02 mGy/cm; 95% CI: -0.02, 0.07 mGy/cm; $R^2 = 0.003$; $P = 0.3$). These R^2 values indicated that patient size explained 48% of the observed variability in $CTDI_{vol}$ but less than 1% of the observed variability in SSDE. The regression of $CTDI_{vol}$ versus patient size demonstrated that, in the 42-84 cm range, $CTDI_{vol}$ varied from 12 to 26 mGy. However, use of the evaluated automatic exposure control system to adjust scanner output for patient size resulted in SSDE values that were independent of size.

It can be concluded that for the evaluated automatic exposure control, $CTDI_{vol}$ (scanner output) increased linearly with patient size; however, patient dose (as indicated by SSDE) was independent of patient size.

Imai R et al [15] studied on: Local diagnostic reference level based on size-specific dose estimates: assessment of pediatric abdominal/pelvic computed tomography at a Japanese national children's hospital. The purpose of the study was to calculate the SSDE of abdominal/pelvic CT, compare the SSDE with $CTDI_{vol}$ and calculate the DRLs of $CTDI_{vol}$ and SSDE. The results showed the $CTDI_{vol}$ and DLP of 117 children who underwent abdominal/pelvic CT examinations. The SSDE was calculated from the sum of the LAT and AP diameters. The relationship between body weight and effective diameter and between effective diameter and $CTDI_{vol}$/SSDE were compared. Further, the local DRL was compared with the DRLs of other countries. The result showed the body weight and effective diameter and effective diameter and SSDE were positively correlated.

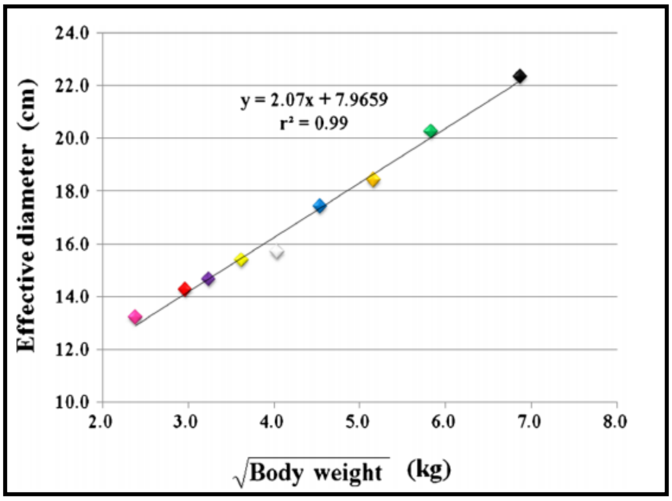

Figure 2.18 The relationship between the mean body weight of each color code and effective diameter [15].

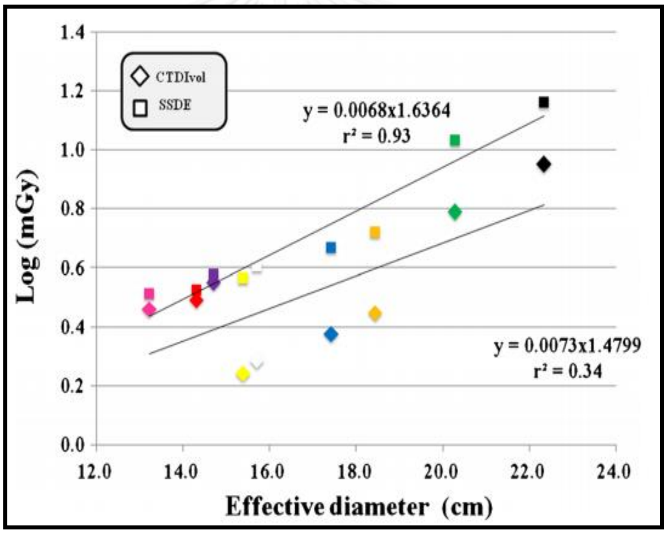

Figure 2. 19 The relationship between SSDE or $CTDI_{vol}$ and effective diameter [15].

In children age of 1, 5 and 10 years, the SSDE is closer to the exposure dose of $CTDI_{vol}$ for the 16-cm cylindrical phantom. The local DRL was lower than those of other countries. The conclusion was that with SSDE, the radiation dose increased with increasing body weight. Since SSDE takes body size into account, it proved to be a useful indicator for estimating the exposure dose.

Leng S et al [16] studied on: size-specific dose estimates for chest, abdominal, and pelvic CT: Effect of intrapatient variability in water-equivalent diameter. The purpose of the study was to develop software to automatically calculate size SSDE and to assess the impact of variations in water equivalent diameter (Dw) along the z axis on SSDE for CT examinations of the torso. This study used Matlab program to calculate Dw at each image position from 102 consecutive CT exams of the combined chest, abdomen and pelvis (CAP). SSDE was calculated by multiplying the size-dependent conversion factor and $CTDI_{vol}$ at each image position. The variations in Dw along the z axis were determined for 6 hypothetical scan ranges: chest alone; abdomen alone; pelvis alone; chest and abdomen; abdomen and pelvis; and CAP. Mean SSDE was calculated in two ways: (A) from the SSDE at each position; (B) from mean $CTDI_{vol}$ over each scan range and the conversion factor corresponding to Dw at the middle of the scan range. The result showed the scan ranges 1 to 6, the average across patients of the difference between maximal and minimal Dw within a given patient was 5.2, 4.9, 2.5, 6.0, 5.6, and 6.5 cm. The mean SSDE values calculated using methods A and B were in close agreement, with root mean square differences of 0.9, 0.5, 0.5, 1.4, 1.0, and 1.1 mGy or 6%, 3%, 2%, 9%, 4%, and 6%. In conclusions, using the mean $CTDI_{vol}$ from over the whole scan range and D_W from the image at the center of the scan range provided an easily obtained estimate of SSDE for the whole scan range that agreed well with an image by image approach, having a root mean square difference below 1.4 mGy (9%).

Khawaja RD et al [17] studied on: Simplifying SSDE in pediatric CT. The purpose of the study was to determine whether body weight can be used as a surrogate for measuring diameter in children. D_{AP} and D_{LAT} were measured in 522 consecutive CT examinations (chest, 187 and abdomen-pelvis, 335). Effective diameter (D_{E1}) was calculated as the square root of the product of D_{AP} and D_{LAT}. A second measurement of effective diameter (D_{E2}) was obtained using automated software. Correlation coefficients between patient body weight, age, and diameter were measured in addition to 95% prediction interval analysis for diameters corresponding to body weight. The result showed median body weight was 51 kg, and mean D_{AP}, D_{LAT}, D_{E1}, and D_{E2} were 207.1 ± 50.8 mm, 289.8 ± 72.6 mm, 243.3 ± 62.0 mm, and 233.6 ± 55.4 mm, respectively. Overall body weight had a strong correlation with diameter (0.88, 0.85, 0.86, and 0.93 respectively; all $p < 0.0001$). SSDE measured using body weight was statistically not different than SSDE measured using effective diameters ($p = 0.9$). Children weighing less than 27 kg and between 46 and 100 kg had statistically significant correlations with torso diameters, whereas only anteroposterior and effective diameters were correlated with children weighing between 27 and 45 kg. Children less than 4 years old had strong correlation with all diameters. Adolescents (15-18 years) did not have statistically significant correlation with any of the diameters. In conclusions, body weight, instead of body diameter, can be used as a surrogate to estimate size-specific dose in children, making dose estimation clinically simpler and more rapid.

CHAPTER III

RESEARCH METHODOLOGY

3.1 Research Design

This study is an observational descriptive research design in type of retrospective study.

3.2 Conceptual framework

Effective dose from SSDE is affected by sum of anterior-posterior and lateral dimension (AP+LAT), body weight, body mass index (BMI), gender, anterior-posterior dimension (AP, lateral dimension (LAT), water-equivalent diameter (Dw) and $CTDI_{vol}$.

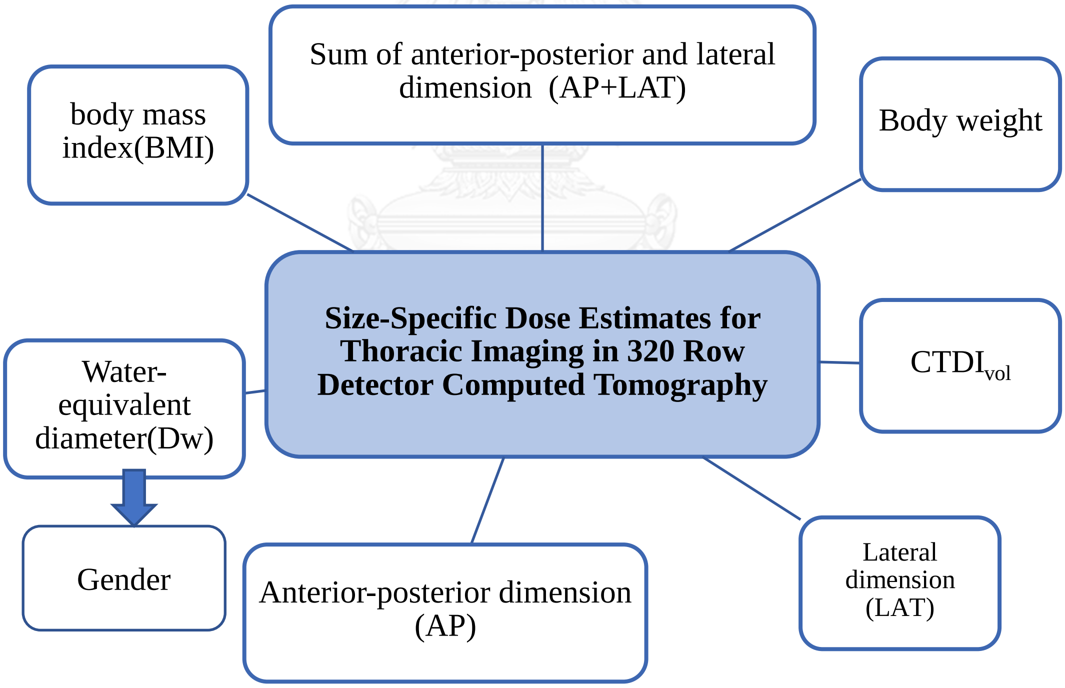

Figure 3.1 Conceptual framework

In this study, we focus on sum of anterior-posterior and lateral dimension (AP+LAT), body weight, body mass index (BMI), gender and water-equivalent diameter (Dw).

3.3 Research design model

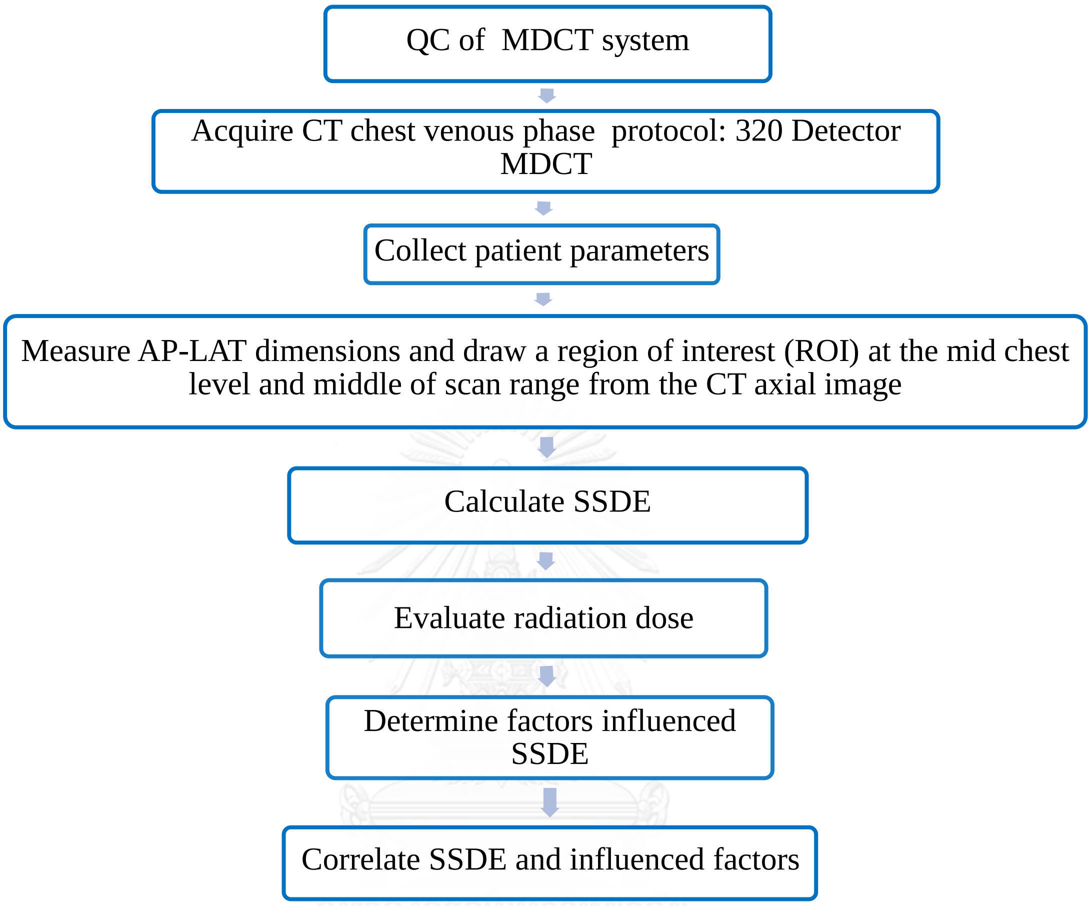

3.4 Research questions and research objectives

3.4.1 Research questions

3.4.1.1 What is the radiation dose to patient, SSDE, from thoracic CT examination?

3.4.1.2 Which parameters influence SSDE?

3.4.2 Research objectives

3.4.2.1 To determine the patient dose using SSDE for thoracic imaging in 320 row detector computed tomography.

3.4.2.2 To determine parameters influence SSDE.

3.5 Key words

Multi-detector computed tomography, Size-specific dose estimates, Thoracic CT examination, Patient size, MDCT 320

3.6 Material

3.6.1 Computed Tomography scanner

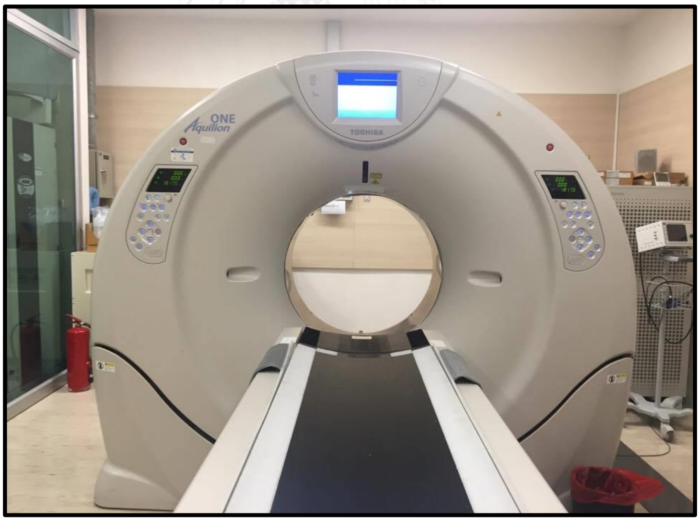

Figure 3.2 CT Toshiba Aquilion ONE, 320-row detector.

In this study, Toshiba Aquilion ONE, 320-row detector CT scanner at 2nd Floor of Bhumisiri Mangkalanusorn Building, Department of Radiology, King Chulalongkorn Memorial Hospital was used. CT scanner has been installed in January 2011. Computer software unit was used for the WindowNT® operating system and the application software coneXact™ was used for acquisition and processing.

3.6.2 Patients information

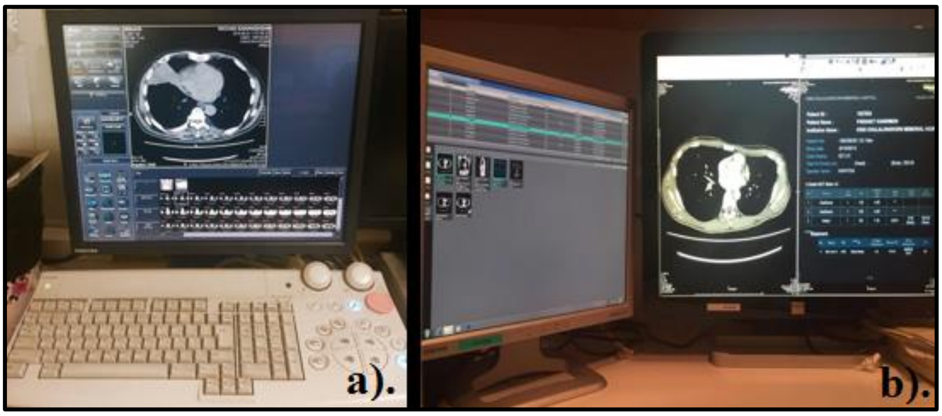

Figure 3.3 Image DICOM header (a) and workstation of CT scanner (b).

Patient data with thoracic MDCT scan from the synapse workstation version 4.3.221 were extracted from DICOM header and workstation of CT scanner at King Chulalongkorn Memorial Hospital as shown in the Figure 3.3.

3.6.3 QC equipment for MDCT

3.6.3.1 The cylindrical PMMA phantom of 16 and 32 cm diameters

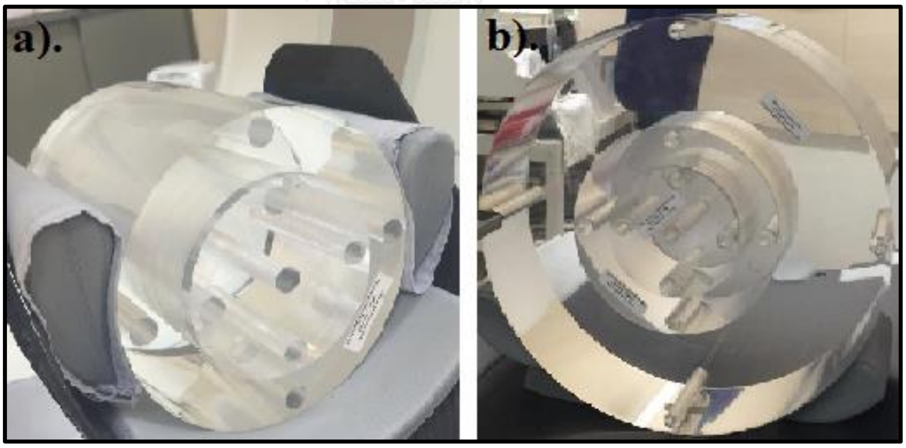

Figure 3.4 PMMA head phantom 16 cm (a) and body phantom 32 cm diameters (b).

The CT phantoms were used to perform CT dosimetry verification in terms CT Dose Index (CTDI) for CT scanner. The phantoms are made by polymethyl methacrylate (PMMA). There are two standard PMMA dosimetry phantoms; the body phantom is 32 cm in diameter and the head phantom is 16 cm in diameter and 15 cm in length as shown in figure 3.4. The PMMA phantoms consist of 5 holes (one hole at the center and four holes at the peripheral at the 3, 6, 9, 12 o'clock position) to insert the ion chamber.

3.6.3.2 Catphan® 600 phantom

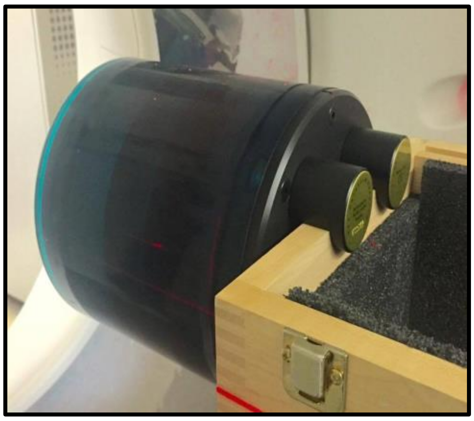

Figure 3.5 Catphan® 600 phantom.

Catphan® 600 phantom was used for performance of CT scanner study in part of the image quality evaluation. The Catphan® phantom was positioned in the CT gantry as shown in figure 3.5.

The Catphan® 600 phantoms are designed so all test sections can be located by precisely indexing the table from the center of section 1 (CTP404) to the center of each subsequent test module.

Catphan® 600 phantoms test module location:

Module		Distance from section 1 center	
CTP404	Slice width, sensitometry and pixel size		
CTP591	Bead geometry	32.5	mm
CTP528	21 line pair high resolution	70	mm
CTP528	Point source	80	mm
CTP515	Sub-slice and supra-slice low contrast	110	mm
CTP486	Solid image uniformity module	150	mm

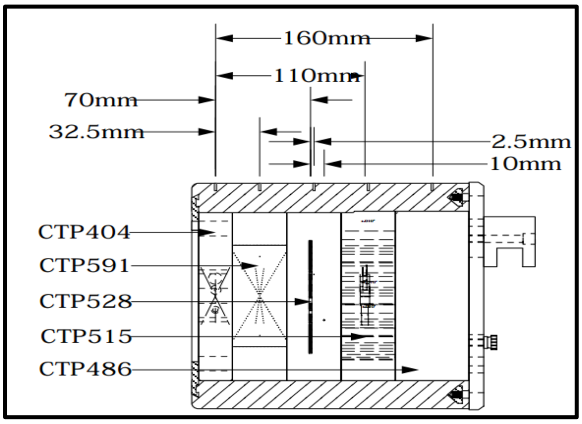

Figure 3.6 Catphan® 600 phantom with internal dimension and details on various Modules

3.6.3.3 The pencil type ionization chamber

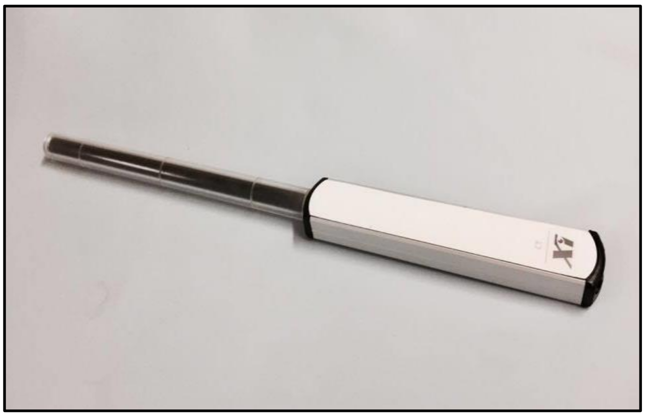

Figure 3.7 Pencil-type ionization Unfors Xi CT Detector.

The ionization pencil chamber utilized for CT dosimetry as illustrated in figure 3.7 is a non-sealed cylindrical chamber with sensitive length 10 cm. One typical characteristic of this chamber is uniform response to incident radiations in every angle around its axis. In this study, the RaySafe Xi CT detector has been used. It is a hybrid ion chamber designed by Unfors RaySafe. The ion chamber and electronics are combined into one unit making it possible to measure both temperature and pressure to actively compensate for this dependency. The temperature is actually measured inside the ion chamber giving very precise compensations both with and without a CT phantom. With no baseline drift, this carbon fiber ion chamber is ready to use within one minute.

Usually the reading by this chamber is expressed in dose or exposure units x scan length (mGy.cm or R.cm), so as to provide the computed tomography dose index (CTDI). The dosimetric quantity was reported by digital display of dosimeter.

Figure 3.8 Unfors model Xi platinum dosimeter.

3.7 Sample

3.7.1 Target population

Adult patients' weight between 40-70 kilograms underwent CT thoracic contrast enhancement with venous phase protocol examined in September 2015 to December 2016 at King Chulalongkorn Memorial Hospital.

3.7.2 Eligible criteria

3.7.2.1 Inclusion criteria

- Patient data analyzed from CT Toshiba's Aquilion ONE, 320 MDCT.
- Adult patients' weight between 40-70 kilograms underwent thoracic contrast enhancement with venous phase protocol
- CT scanner automatic exposure control systems (AEC)
- Same levels of CT image noise setting (targeted SD) for patients of various sizes.

3.7.2.2 Exclusion criteria

- Patients underwent thoracic CT with non-contrast or arterial phase protocol
- Non AEC or low dose technique
- Patients with breast prosthesis implant
- Patient with Implantable cardioverter defibrillator (ICD) and pacemaker.
- The contour skin of chest level not visible on the FOV reconstruction.

3.8 Methods

3.8.1 Perform the quality control of CT Toshiba Aquilion ONE, 320-row detector

The quality control of CT scanner was performed following the IAEA Human Health Series No.19 [18]. The quality control in acceptance test consists of mechanical accuracy, radiation output to determine $CTDI_{air}$, $CTDI_{vol}$ using PMMA phantoms and image quality evaluation using Catphan ®600 phantom.

3.8.2 Patient study

3.8.2.1 Select patients in accordance with inclusion and exclusion criteria as mentioned above. The data of the patients who have already been performed thoracic CT examination using contrast enhancement with venous phase CT routine protocol in September 2015 to December 2016 at King Chulalongkorn Memorial Hospital were collected.

3.8.2.2 Collect the patients' data for thoracic CT examination in terms of body weight, body mass index (BMI), height, gender and age.

3.8.2.3 Measure AP-LAT dimensions at mid chest level and middle of the scan range from the CT axial image by using ruler on image tools.

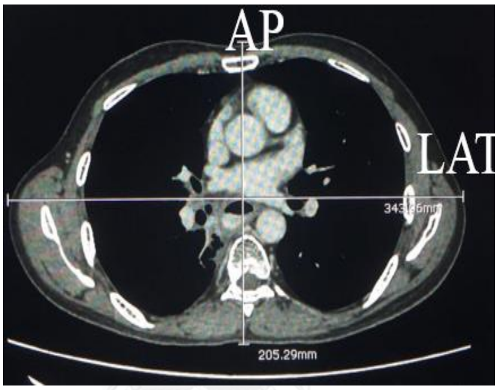

Figure 3.9 AP-LAT dimensions measurement at the midline from transverse CT image at thorax.

3.8.2.4 Draw region of interest (ROI) at the mid chest level and middle of scan range from the CT axial image, include the whole patient cross section (full FOV) by using free hand ROI on image tools and record the mean CT number (HU) and the area of the ROI.

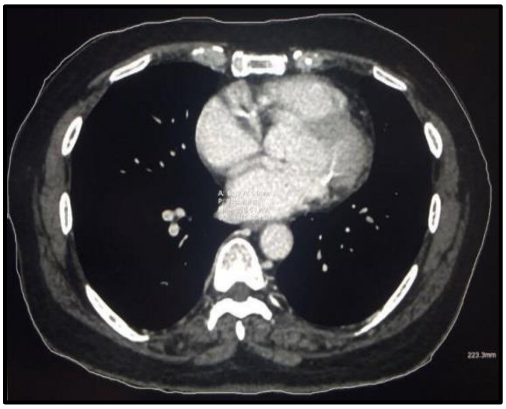

Figure 3.10 Region of interest (ROI) contouring from the CT chest transaxial slice.

3.8.2.5 Record $CTDI_{vol}$ from CT monitor or PACS system.

3.8.2.6 Apply the conversion factors (f_{size}) from the AAPM Report no.204 and no. 220 [5, 6] to determine SSDE in terms of sum AP and LAT (AP+LAT) dimension, effective diameter and water equivalent diameter (Dw).

3.8.2.7 Calculate SSDE by equation: SSDE = f_{size} (size-dependent conversion factor) x $CTDI_{vol}$.

3.8.2.8 Analyze the data.

3.8.2.9 Determine parameters affected SSDE.

3.9 Sample size determination

The sample population is retrospective data, determined by this equation:

$$N = \left(\frac{2Z_{\alpha/2}}{Z_U - Z_L} \right)^2 + 3$$

$$Z_U = \frac{1}{2} In \left(\frac{1+\rho_U}{1-\rho_U} \right)$$

$$Z_L = \frac{1}{2} In \left(\frac{1+\rho_L}{1-\rho_L} \right)$$

Define*:* N/group

Reference from literature review*:* Correlation coefficient (*r*) = 0.96

Where α = 0.05, $Z_{\alpha/2}$ = 1.96

ρ = Population correlation coefficient

ρ_L = Lower limit of population correlation; 0.95

ρ_U = Upper limit of population correlation; 0.97

$$Z_U = \frac{1}{2} In \left(\frac{1+0.97}{1-0.97} \right) = 2.09$$

$$Z_L = \frac{1}{2} In \left(\frac{1+0.95}{1-0.95} \right) = 1.83$$

Define from formula*:*

$$N = \left(\frac{2 \times 1.96}{2.09 - 1.83} \right)^2 + 3$$

= 230.3

N= 230 sample size

3.10 Measurement variable

- Independent variable: AP+LAT dimensions, effective diameter, body weight, body mass index (BMI), water-equivalent diameter and $CTDI_{vol}$
- Dependent variable: SSDE

3.11 Data analysis

- Descriptive statistics: SSDE and $CTDI_{vol}$ presented by mean, median, percentage and range (min–max). Data were analyzed using SPSS version 22.0 and Microsoft excel version.2013
- Correlation coefficient between SSDE and related factors.
- Presentation format in scatter plot and tables.

3.12 Data collection

In this study, the data were collected from Toshiba Aquilion ONE, 320-row detector CT scanner at 2nd Floor of Bhumisiri Mangkhalanusorn Building, Department of Radiology, King Chulalongkorn Memorial Hospital.

3.12.1 Patient information: body weight, height, body mass index (BMI), gender and age from DICOM header.

3.11.2 $CTDI_{vol}$ had been recorded from CT monitor or PACS system.

3.13 Expected benefits

SSDE to apply for the patients of different sizes (AP+LAT dimensions, effective diameter and water equivalent diameter (Dw)) with higher accuracy is expected for this study. The location for determination SSDE, middle of scan range and middle of organ (chest) that suitable for measurement the dimension from CT image is also expected.

3.14 Ethic consideration

This research involves the determination of patient dose in Computed Tomographic. The patient data collection during the period from September 2015 to December 2016 had been extracted from the image DICOM header. The research proposal was submitted for approval by Ethical Committee of Faculty of Medicine, Chulalongkorn University.

The researcher was ethical conduct research follow in Belmont Report Principles, consists of 3 basic principles.

- Respect for person by consent from patients to participate in research. But this study, using data collected radiation dose a patient receives from a DICOM header, for this reason, are exceptions to the consent of the patient. However, researcher will conceal the information, it's cannot identify to patient.

-Beneficence (Maximize benefits/minimize risks) patients will not receive benefits and risk because of this study using data collected radiation dose a patient receives from a retrospective tool. The data is not identify the patient.

- Justice is a clear inclusion and exclusion criteria. Researcher used the data of adult patients weight between 40-70 kilograms underwent thoracic contrast enhancement with venous phase protocol examined in September 2015 to December 2016 at King Chulalongkorn Memorial Hospital.

CHAPTER IV

RESULTS

4.1 Quality control of the Multidetector Computed Tomography scanner: Toshiba Aquilion ONE

The quality control of CT scanner was performed following IAEA report No.19 [24]. It includes the test of electromechanical component, image quality and radiation dose. The details of quality control of CT scanner are shown with the summarized report of CT scanner performance test in Appendix B.

4.2 Patient data and radiation dose determined from thoracic CT examination

Patient information of 230 cases that underwent thoracic contrast enhancement with venous phase protocol scanned by CT Toshiba Aquilion ONE, 320-row detector from September 2015 to December 2016 was collected. Patient data from the image DICOM header or CT control with thoracic MDCT is scanned at King Chulalongkorn Memorial Hospital.

4.2.1 Patient characteristics of thoracic CT examination

The patient characteristics of 230 adult patients (115 males and 115 females) of the mean age were 60.36 ± 15.11 (range 18-93) years old. The mean ± SD of patient body weight was 55.42 ± 7.75(range 40-70) kg. The mean ± SD of patient height was 160.26 ± 8.04(range 140-186) cm. The mean ± SD of patient BMI was 21.58 ± 2.71 (range 15.62-29.08) kg/m^2. The results are shown in Table 4.1-4.3.

Table 4.1 Patient characteristics of thoracic CT examination

Statistics	Mean ± SD	Minimum	Maximum
Age (year)	60.36 ± 15.11	18	93
Body weight (kg)	55.42 ± 7.75	40	70
Height (cm)	160.26 ± 8.04	140	186
BMI (kg/m^2)	21.58 ± 2.71	15.62	29.08

Table 4.2 Patient characteristics of 115 male patients

Statistics	Mean ± SD	Minimum	Maximum
Age (year)	61.62 ± 14.99	20	93
Body weight (kg)	58.35 ± 7.39	40	70

Height (cm)	165.21 ± 6.46	142	186
BMI (kg/m^2)	21.39 ± 2.65	15.77	27.34

Table 4.3 Patient characteristics of 115 female patients

Statistics	Mean ± SD	Minimum	Maximum
Age (year)	59.09 ± 15.19	18	87
Body weight (kg)	52.49 ± 6.98	40	70
Height (cm)	155.31 ± 6.23	140	175
BMI (kg/m^2)	21.78 ± 2.76	15.62	29.08

4.2.2 Patient data and radiation dose determined from middle slice of organ (chest).

SSDE estimated from middle slice of organ (chest) of 230 adult patients (115 males and 115 females). The middle slice of organ (chest) located at center of chest (7th thoracic vertebrae). $CTDI_{vol}$ was recorded from PACS system or CT monitor. The results are shown in Table 4.4.

Table 4.4 Patient data and radiation dose determined from middle slice of organ (chest).

Statistics	Mean ± SD	Minimum	Maximum
AP length(cm)	20.08 ± 1.81	15.88	25.91
LAT length(cm)	31.40 ± 2.58	25.11	39.23
AP+LAT(cm)	51. 49 ± 3.78	41.52	63.14
Effective diameter (cm)	25. 09 ± 1.85	20.17	30.62
Mean CT number (HU)	-285.70 ± 60.53	-422.53	-100.59
Area of ROI (cm^2)	544.63 ± 75.77	356.10	808.34
Water equivalent diameter (D_w)(cm)	22.19 ± 1.97	17.28	30.42
Conversion factor based on AP+LAT (f_{AP+LAT})	1.48 ± 0.10	1.19	1.76
Conversion factor based on effective diameter (f_{EFF})	1.47 ± 0.10	1.20	1.76
Conversion factor based on D_w (f_{Dw})	1.64 ± 0.11	1.21	1.96
$CTDI_{vol}$ (mGy)	12.40 ± 2.55	6.00	19.20
$SSDE_{AP+LAT}$ (mGy)	18. 13 ± 2.75	10.50	24.45

$SSDE_{EFF}$ (mGy)	18. 09 ± 2.75	10.43	24.25
$SSDE_{Dw}$ (mGy)	20.12 ± 2.93	11.66	26.83

4.2.3 Patient data and radiation dose determined from middle slice of scan range.

SSDE estimated from middle slice of scan range of 230 adult patients (115 males and 115 females). The middle slice of scan range located at center of scan volume. $CTDI_{vol}$ were recorded from PACS system or CT monitor. The results are shown in Table 4.5.

Table 4.5 Patient data and radiation dose determined from slice middle of scan range.

Statistic	Mean ± SD	Minimum	Maximum
AP length(cm)	20.42 ± 2.09	16.01	31.62
LAT length(cm)	30.67± 2.83	19.17	38.76
AP+LAT(cm)	51.09 ± 3.89	38.17	63.11
Effective diameter (cm)	24.98 ± 1.91	19.08	30.72
Mean CT number (HU)	-274.83 ± 62.74	-410.98	-100.02
Area of ROI (cm^2)	541.50± 75.26	352.53	798.70
Water equivalent diameter (D_w)(cm)	22.29 ± 1.96	18.23	30.11
Conversion factor based on AP+LAT (f_{AP+LAT})	1.49 ± 0.10	1.19	1.87
Conversion factor based on effective diameter (f_{EFF})	1.48 ± 0.10	1.19	1.83
Conversion factor based on D_w (f_{Dw})	1.63 ± 0.11	1.22	1.89
$CTDI_{vol}$ (mGy)	12.40 ± 2.55	6.00	19.20
$SSDE_{AP+LAT}$ (mGy)	18.26 ± 2.77	10.83	24.85
$SSDE_{EFF}$ (mGy)	18.16 ± 2.74	10.70	24.70
$SSDE_{Dw}$ (mGy)	20.04 ± 2.92	11.33	27.13

4.2.4 $SSDE_{AP+LAT}$, $SSDE_{EFF}$ and $SSDE_{Dw}$ determined from middle slice of organ (chest).

The $SSDE_{AP+LAT}$ and $SSDE_{EFF}$ related to patient geometry, mean $SSDE_{AP+LAT}$ ± SD was 18.13 ± 2.75 mGy and mean $SSDE_{EFF}$ ± SD was 18.09 ± 2.75 mGy respectively. The $SSDE_{Dw}$ related to body composition, mean $SSDE_{Dw}$ ± SD was 20.12

± 2.93 mGy. Statistical different between 3 methods ($SSDE_{AP+LAT}$, $SSDE_{EFF}$ and $SSDE_{Dw}$ are significant (p-value < 0.001). The results are shown in Table 4.6.

Table 4.6 SSDE measured from middle slide of organ (chest).

	Mean ± SD	***p-value***
$SSDE_{AP+LAT}$ (mGy)	18. 13 ± 2.75	
$SSDE_{EFF}$ (mGy)	18. 09 ± 2.75	*< 0.001*
$SSDE_{AP+LAT}$ (mGy)	18. 13 ± 2.75	
$SSDE_{Dw}$ (mGy)	20.12 ± 2.93	*< 0.001*
$SSDE_{EFF}$ (mGy)	18. 09 ± 2.75	
$SSDE_{Dw}$ (mGy)	20.12 ± 2.93	*< 0.001*

*Correlation is significant at the 0.05 (p-value < 0.05) level (2 tailed)

The $SSDE_{AP+LAT}$, $SSDE_{EFF}$ and $SSDE_{Dw}$ displayed as box plots are shown in Figure1. Box plots show the distribution of SSDE for the 230 patients. The bar indicates the range of SSDE in each calculation method. Each box contains the values of SSDE within 25th and 75th percentiles, error bar, and thick black lines represent the median.

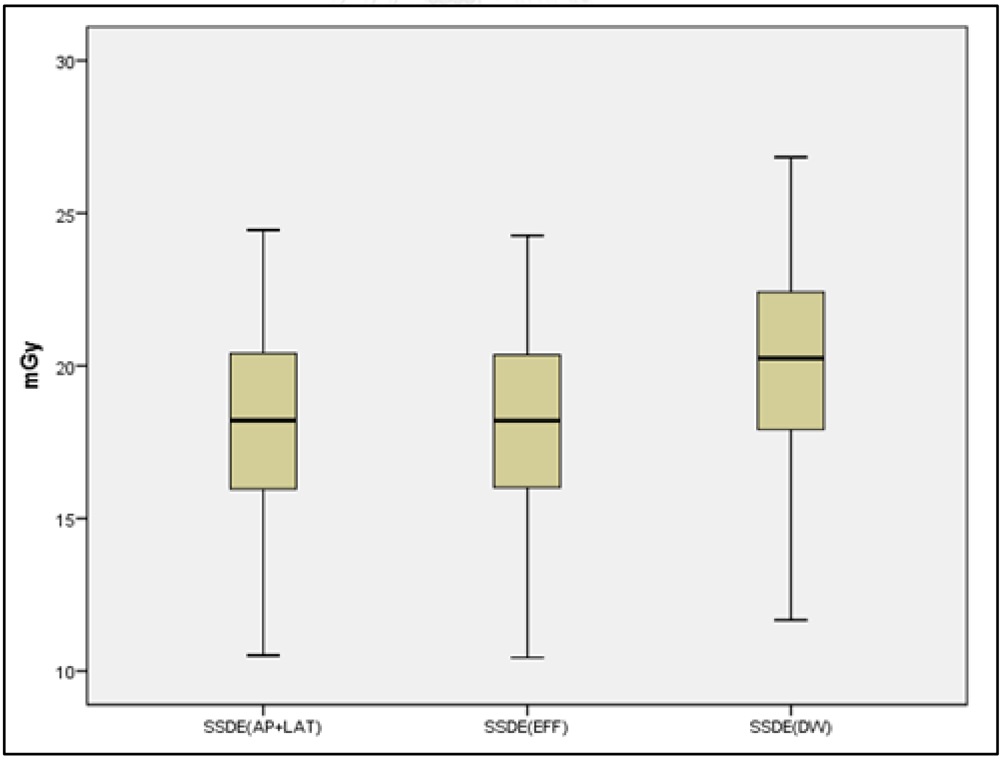

Figure 4.1 Box plots of $SSDE_{AP+LAT}$, $SSDE_{EFF}$ and $SSDE_{Dw}$ determined from middle slice of organ (chest).

4.2.5 Comparison between $SSDE_{AP+LAT}$, $SSDE_{EFF}$ and $SSDE_{Dw}$ determined from middle slice of scan range.

The $SSDE_{AP+LAT}$ and $SSDE_{EFF}$ related to patient geometry, mean $SSDE_{AP+LAT} \pm$ SD was 18.26 ± 2.77 mGy and mean $SSDE_{EFF} \pm$ SD was 18.16 ± 2.74mGy respectively. The $SSDE_{Dw}$ related to body composition, mean $SSDE_{Dw} \pm$ SD was 20.04 ± 2.92 mGy. Statistical different between 3 $SSDE_{AP+LAT}$, $SSDE_{EFF}$ and $SSDE_{Dw}$ are significant (p-value < 0.001). The results are shown in Table 4.7.

Table 4.7 SSDE measured from middle slice of scan range.

	Mean ± SD	***p-value***
$SSDE_{AP+LAT}$(mGy)	18.26 ± 2.77	
$SSDE_{EFF}$ (mGy)	18.16 ± 2.74	*< 0.001*
$SSDE_{AP+LAT}$(mGy)	18.26 ± 2.77	
$SSDE_{Dw}$ (mGy)	20.04 ± 2.92	*< 0.001*
$SSDE_{EFF}$ (mGy)	18.16 ± 2.74	
$SSDE_{Dw}$ (mGy)	20.04 ± 2.92	*< 0.001*

*Correlation is significant at the 0.05 (p-value < 0.05) level (2 tailed)

The $SSDE_{AP+LAT}$, $SSDE_{EFF}$ and $SSDE_{Dw}$ displayed as box plots are shown in Figure 2. Box plots show the distribution of SSDE for the 230 patients. The bar indicates the range of SSDE, boxes contain the values of SSDE within 25^{th} and 75^{th} percentiles and thick black lines represent the median.

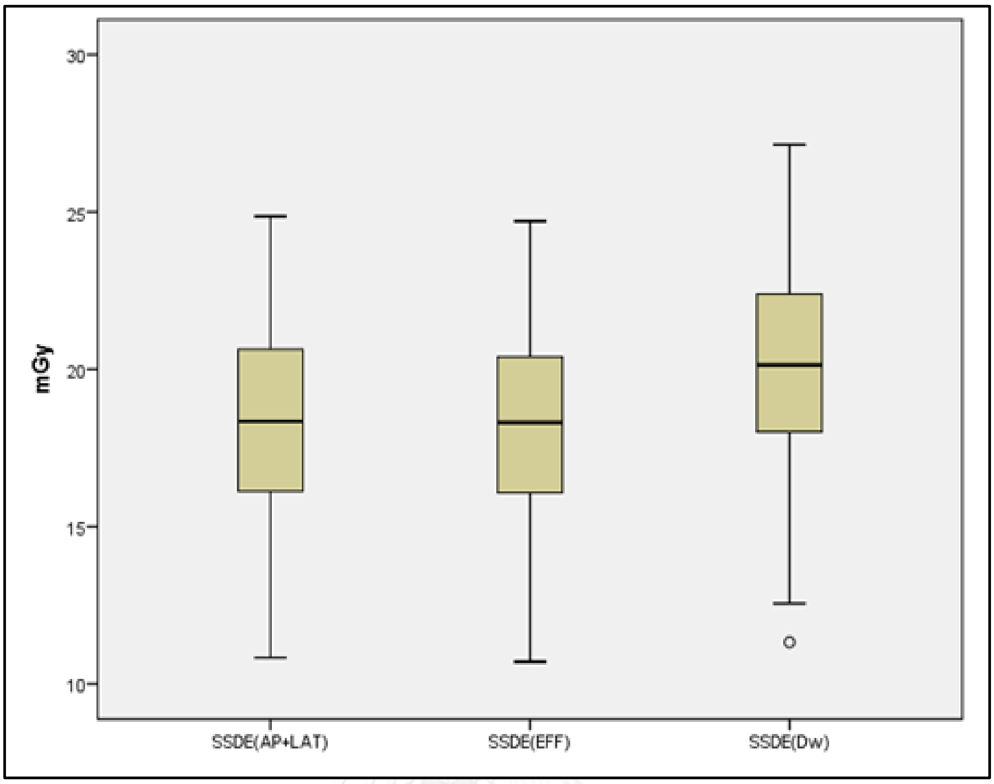

Figure 4.2 Box plots of $SSDE_{AP+LAT}$, $SSDE_{EFF}$ and $SSDE_{Dw}$ determined from middle slice of scan range.

4.3 The slice locations used to estimate SSDE

SSDE estimated from two locations, at the middle slice of scan range and at the middle slice of the organ (chest).

The $SSDE_{AP+LAT}$, $SSDE_{EFF}$ and $SSDE_{Dw}$ were estimated from the middle slice of the organ (chest), mean $SSDE_{AP+LAT}$ was 18.13 (range 10.50-24.45) mGy and mean $SSDE_{EFF}$ 18.09 (range 10.43 – 24.25) mGy. The mean $SSDE_{Dw}$ was 20.12 (range 11.66 – 26.83) mGy.

The $SSDE_{AP+LAT}$, $SSDE_{EFF}$ and $SSDE_{Dw}$ were estimated from the middle slice of scan range, mean $SSDE_{AP+LAT}$ was 18.26 (range 10.83-24.85) mGy and mean $SSDE_{EFF}$ 18.16 (range 10.70 – 24.70) mGy. The mean $SSDE_{Dw}$ was 20.04 (range 11.33 – 27.13) mGy.

The correlation of SSDEs was estimated between the middle slice of the organ (chest) and the middle slice of scan range as shown in Table 4.8.

- The correlation of $SSDE_{AP+LAT}$ between the middle slice of the organ (chest) and the middle slice of scan range were perfectly correlated, R^2 = 0.9820

- The correlation of $SSDE_{EFF}$ between the middle slice of the organ (chest) and the middle slice of scan range were perfectly correlated, R^2 = 0.9864

- The correlation of $SSDE_{Dw}$ between the middle slice of the organ (chest) and the middle slice of scan range were perfectly correlated, $R^2 = 0.9933$.

Table 4.8 SSDE were determined from mid organ (chest) and middle of scan ranges.

	Mid organ (chest) range Mean ± SD	**Middle of scan range Mean ± SD**	**R^2**
$SSDE_{AP+LAT}$(mGy)	18. 13 ± 2.75	18.26 ± 2.77	0.9820
$SSDE_{EFF}$ (mGy)	18. 09 ± 2.75	18.16 ± 2.74	0.9864
$SSDE_{Dw}$ (mGy)	20.12 ± 2.93	20.04 ± 2.92	0.9933

The correlation of $SSDE_{AP+LAT,}$ $SSDE_{EFF}$ and $SSDE_{Dw}$ between the middle slice of the organ (chest) and the middle slice of scan range were perfectly correlated. Therefore, the middle slice of the organ (chest) has been used to determine parameters affecting SSDE.

4.4 The correlation

4.4.1 The correlation between SSDE and $CTDI_{vol}$

The correlation between $SSDE_{AP+LAT}$, $SSDE_{EFF}$ or $SSDE_{Dw}$ and $CTDI_{vol}$ of thoracic CT examination has been investigated. The results are shown in Table 4.9.

- Very strong linear relationship between the $SSDE_{AP+LAT}$ and $CTDI_{vol}$ was significant at R^2 equal 0.9433 and p-value < 0.001.
- Very strong linear relationship between the $SSDE_{EFF}$ and $CTDI_{vol}$was significant at R^2 equal 0.9420 and p-value < 0.001.
- The strongest linear relationship between the $SSDE_{Dw}$ and $CTDI_{vol}$ was significant at R^2 equal0.9529 and p-value < 0.001.

Table 4. 9 SSDE and $CTDI_{vol}$

	$SSDE_{AP+LAT}$ (mGy)	**$CTDI_{vol}$ (mGy)**	**R^2**	*p-value< 0.001*
Mean ± SD	18.13 ± 2.75	12.40 ± 2.55	0.9489	
	$SSDE_{EFF}$ (mGy)	**$CTDI_{vol}$ (mGy)**		*p-value< 0.001*
Mean ± SD	18.09 ± 2.75	12.40 ± 2.55	0.9495	
	$SSDE_{Dw}$ (mGy)	**$CTDI_{vol}$ (mGy)**		*p-value< 0.001*
Mean ± SD	20.12 ± 2.93	12.40 ± 2.55	0.9529	

- Correlation is significant at the 0.05 (p-value < 0.05) level (2 tailed)

The correlation of $CTDI_{vol}$ and SSDE of thoracic CT examination are plotted as shown in figure 4.3.

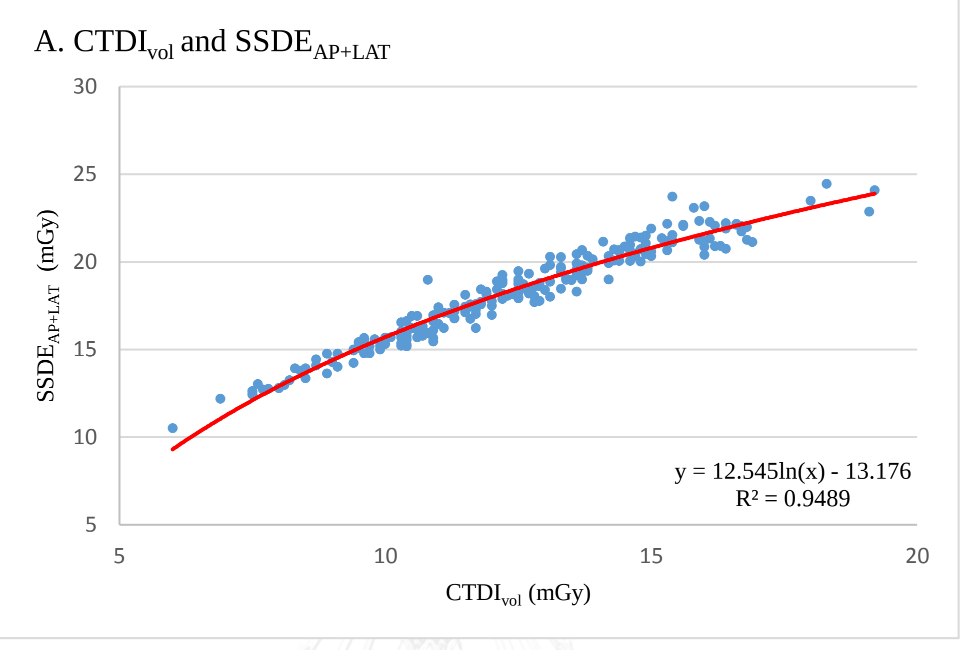

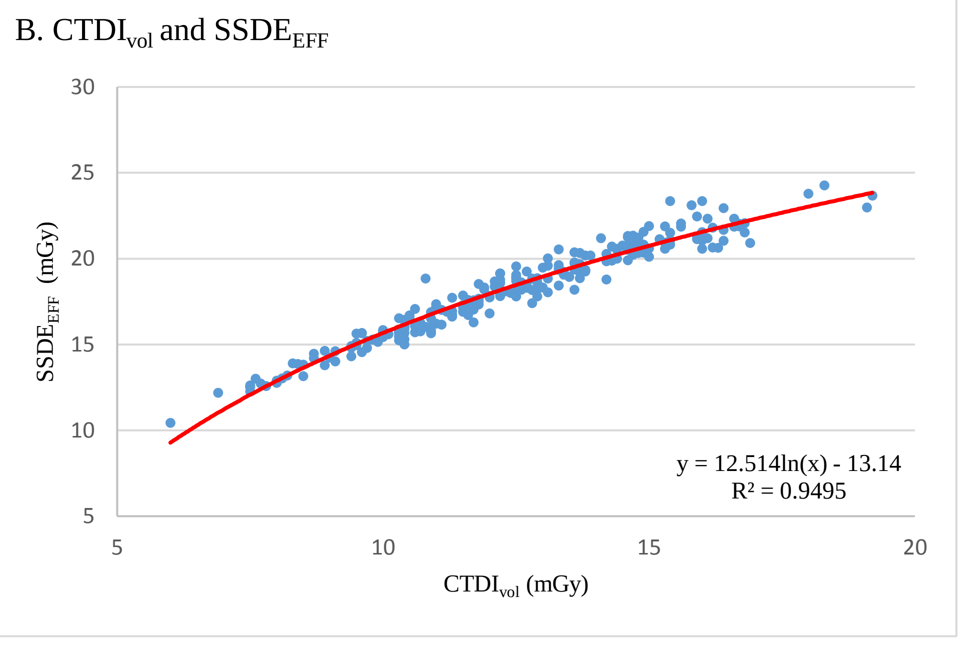

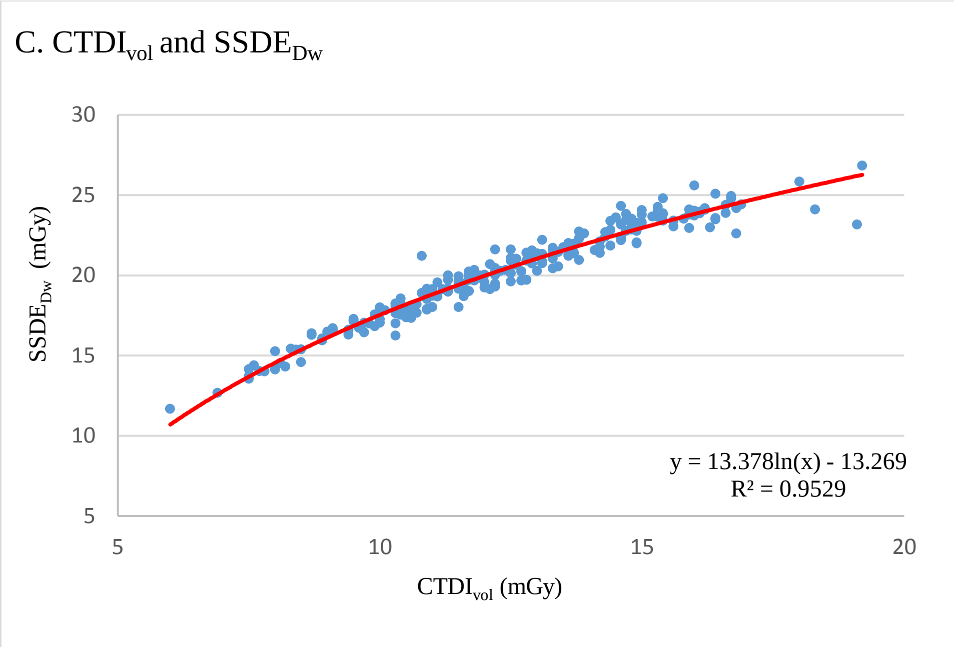

Figure 4.3 A-C The correlation of $CTDI_{vol}$ and SSDE; A. $CTDI_{vol}$ and $SSDE_{AP+LAT}$, B. $CTDI_{vol}$ and $SSDE_{EFF}$ and C. $CTDI_{vol}$ and $SSDE_{Dw}$.

The correlation of $SSDE_{Dw}$ and $CTDI_{vol}$ were perfectly correlated with R^2 = 0.9529. The exponential equation for using as the prediction function for $SSDE_{Dw}$ in chest CT study was y= 13.378ln(x) – 13.269. This function can be used to calcuate $SSDE_{Dw}$ based on $CTDI_{vol}$ as shown in Table 4.10. The calculation of SSDE is as the following equation:

$$y = 13.378\ln(x) - 13.269$$

where, x is the $CTDI_{vol}$ (mGy) displayed on CT monitor.

Table 4.10 Determination of $SSDE_{Dw}$ from $CTDI_{vol}$ displayed on the CT monitor

$CTDI_{vol}$ (mGy)	**$SSDE_{Dw}$ (mGy)**
5	8.26
6	10.70
7	12.76
8	14.55
9	16.13
10	17.53
11	18.81
12	19.97

13	21.04
14	22.04
15	22.96
16	23.82
17	24.63
18	25.40
19	26.12
20	26.81

4.4.2 Body weight and SSDE

4.4.2.1 Data on body weight and $SSDE_{AP+LAT}$

230 Adult patient weight between 40-70 kilograms underwent thoracic contrast enhancement with venous phase protocol examined in September 2015 to December 2016 at King Chulalongkorn Memorial Hospital. The results are shown in Table 4.11.

Body weight from 40-50 kg, mean $SSDE_{AP+LAT}$ ± SD was 16.06 ± 2.42 mGy (range 10.50 – 21.50 mGy).

Body weight from 51-60 kg, mean $SSDE_{AP+LAT}$ ± SD was 18.33 ± 2.09 mGy (range 12.61-23.18 mGy).

Body weight from 61-70 kg, mean $SSDE_{AP+LAT}$ ± SD was 20.06 ± 1.81 mGy (range 14.94-24.45 mGy).

Table 4.11 Data are presented of body weight and $SSDE_{AP+LAT}$.

Body weight (kg)	**$SSDE_{AP+LAT}$ (mGy)**		
	Mean ± SD	**Minimum**	**Maximum**
40-50 (n=78)	16.06 ± 2.42	10.50	21.50
51-60 (n=94)	18.33 ± 2.09	12.61	23.18
61-70 (n=58)	20.06 ± 1.81	14.94	24.45

4.4.2.2 The correlation between body weight and $SSDE_{AP+LAT}$.

The correlation between body weight and $SSDE_{AP+LAT}$ for thoracic CT examination has been investigated. The results are shown in Figure 4.4.

- The moderate linear relationship between the body weight and $SSDE_{AP+LAT}$, R^2 was 0.473.

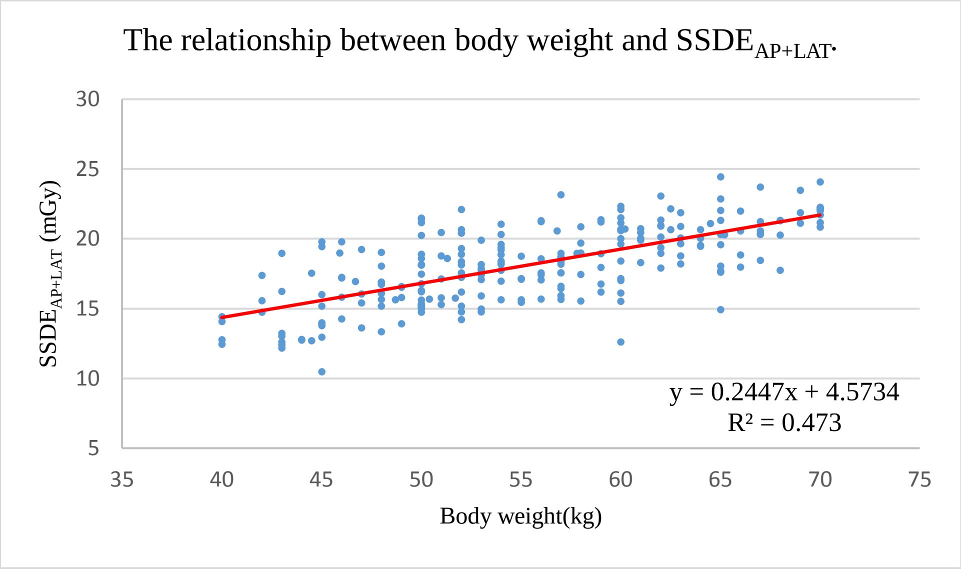

Figure 4.4 The correlation of body weight and $SSDE_{AP+LAT}$.

4.4.3 Body weight and $SSDE_{EFF}$

4.4.3.1 Data on body weight and $SSDE_{EFF}$.

230 Adult patient weight between 40-70 kilograms underwent thoracic contrast enhancement with venous phase protocol from September 2015 to December 2016 at King Chulalongkorn Memorial Hospital. The results are shown in Table 4.12.

Body weight from 40-50 kg, mean $SSDE_{EFF} \pm SD$ was 16.03 ± 2.42 mGy (range 10.50 – 21.50 mGy).

Body weight from 51-60 kg, mean $SSDE_{EFF} \pm SD$ was 18.29 ± 2.10 mGy (range 12.61-23.34 mGy).

Body weight from 61-70 kg, mean $SSDE_{EFF} \pm SD$ was 20.53 ± 1.80 mGy (range 14.81-24.25 mGy).

Table 4.12 Data on body weight and $SSDE_{EFF}$.

Body weight (kg)	**$SSDE_{EFF}$(mGy)**		
	Mean ± SD	**Minimum**	**Maximum**
40-50 (n=78)	16.03 ± 2.42	10.50	21.50
51-60 (n=94)	18.29 ± 2.10	12.61	23.34
61-70 (n=58)	20.53 ± 1.80	14.81	24.25

4.4.3.2 The correlation between body weight and $SSDE_{EFF}$.

The correlation between body weight and $SSDE_{EFF}$ for thoracic CT examination has been investigated. The results are shown in Figure 4.5.

- The moderate linear relationship between the body weight and $SSDE_{EFF}$, R^2 was 0.4724.

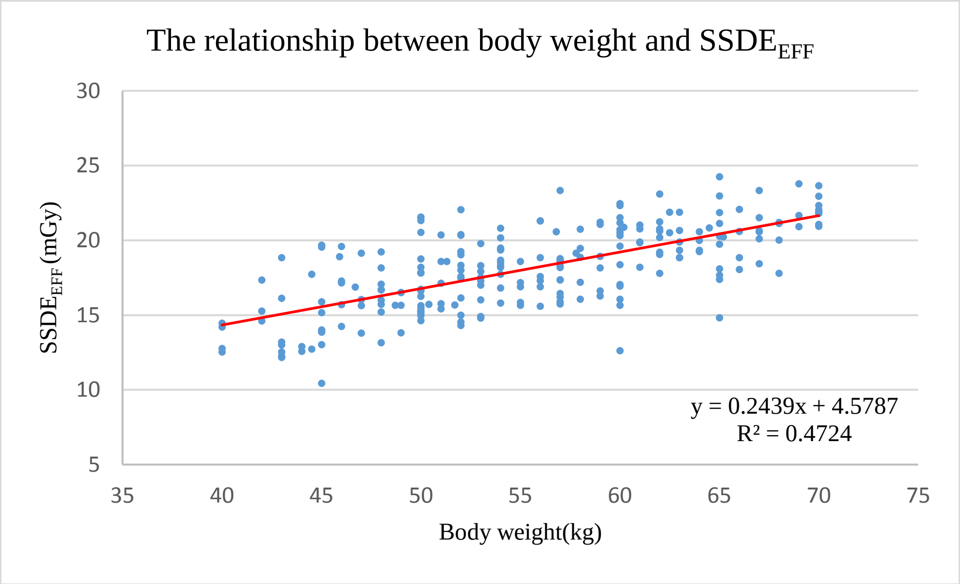

Figure 4.5 The correlation of body weight and $SSDE_{EFF}$.

4.4.4 Body weight and $SSDE_{Dw}$

4.4.4.1 Data on body weight and $SSDE_{Dw}$.

230 Adult patients weight between 40-70 kilograms underwent thoracic contrast enhancement with venous phase protocol between September 2015 to December 2016 at King Chulalongkorn Memorial Hospital. The results are shown in Table 4.13.

Body weight from 40-50 kg, mean $SSDE_{Dw}$ ± SD was 17.70 ± 2.49 mGy (range 11.66-23.81 mGy).

Body weight from 51-60 kg, mean $SSDE_{Dw}$ ± SD was 20.37 ± 2.09 mGy (range 13.54-25.58 mGy).

Body weight from 61-70 kg, mean $SSDE_{Dw}$ ± SD was 22.96 ± 1.64 mGy (range 16.55-26.83 mGy).

Table 4.13 Data on body weight and $SSDE_{Dw}$.

Body weight (kg)	$SSDE_{Dw}$ (mGy)		
	Mean ± SD	Minimum	Maximum
40-50 (n=78)	17.70 ± 2.49	11.66	23.81
51-60 (n=94)	20.37 ± 2.09	13.54	25.58
61-70 (n=58)	22.96 ± 1.64	16.55	26.83

4.4.4.2 The correlation between body weight and $SSDE_{Dw}$.

The correlation between body weight and $SSDE_{Dw}$ for thoracic CT examination has been investigated. The results are shown in Figure 4.6.

- The moderate linear relationship between the body weight and $SSDE_{Dw}$, R^2 was 0.5571.

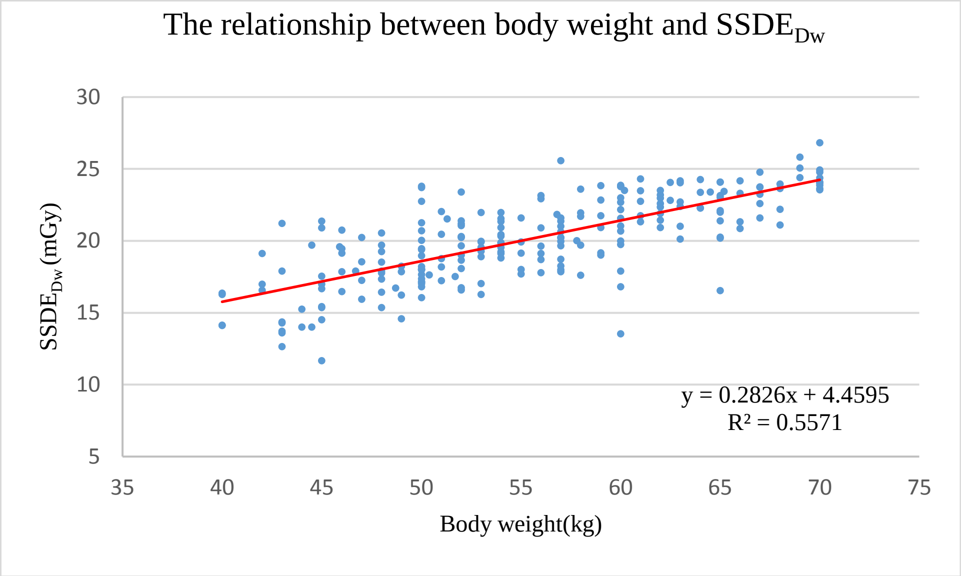

Figure 4.6 The correlation of body weight and SSDE$_{Dw}$.

4.4.5 Body mass index (BMI) and SSDE

4.4.5.1 Data on BMI and SSDE$_{AP+LAT}$.

At BMI less than 18.5 kg/m^2, mean SSDE$_{AP+LAT}$ ± SD was 15.45 ± 2.38 mGy (range 12.19-21.43 mGy).

At BMI from 18.5-22.9 kg/m^2, mean SSDE$_{AP+LAT}$ ± SD was 17.41 ± 2.27 mGy (range 10.43-23. 34mGy).

BMI greater than or equal to 23 kg/m^2, mean SSDE$_{AP+LAT}$ ± SD was 20.44 ± 1.97 mGy (range 14.94-24.45 mGy).

The results are shown in Table 4.14

Table 4.14 Data are presented of BMI and SSDE$_{AP+LAT}$.

BMI (kg/m^2)	**SSDE$_{AP+LAT}$ (mGy)**		
	Mean ± SD	**Minimum**	**Maximum**
< 18.5 (n=27)	15.45 ± 2.38	12.19	21.43
18.5-22.9 (n=131)	17.41 ± 2.27	10.43	23.34
≥23 (n=72)	20.44 ± 1.97	14.94	24.45

4.4.5.2 The correlation between BMI and SSDE$_{AP+LAT}$.

The correlation between BMI and SSDE$_{AP+LAT}$ for thoracic CT examination has been investigated. The results are shown in Figure 4.7.

- The moderate linear relationship between the BMI and $SSDE_{AP+LAT}$, R^2 was 0.4728.

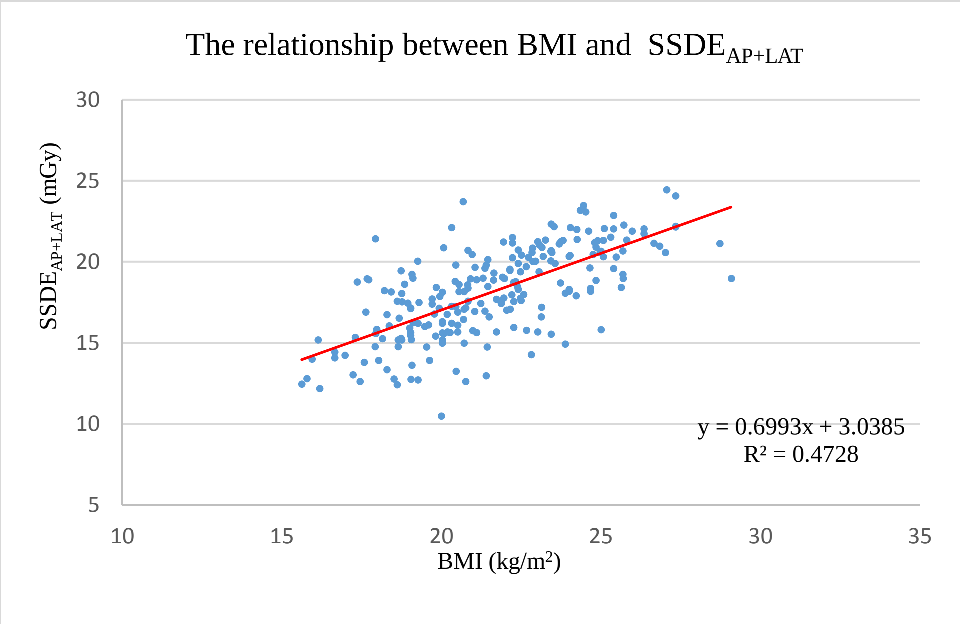

Figure 4.7 The correlation of body mass index (BMI) and $SSDE_{AP+LAT}$.

4.4.6 BMI and $SSDE_{EFF}$

4.4.6.1 Data on BMI and $SSDE_{EFF}$

At BMI less than 18.5 kg/m^2, mean $SSDE_{EFF}$± SD was 15.43 ± 2.37 mGy (range 12.17-21.32mGy).

At BMI from 18.5-22.9 kg/m^2, mean $SSDE_{EFF}$ ± SD was 17.38 ± 2.27 mGy (range 10.43-23.34 mGy).

At BMI greater than or equal to 23 kg/m^2, mean $SSDE_{EFF}$ ± SD was 20.38 ± 1.98 mGy (range 14.81-24.25 mGy). The results are shown in Table 4.15

Table 4.15 Data are presented of body mass index (BMI) and $SSDE_{EFF}$.

BMI (kg/m^2)	**$SSDE_{EFF}$ (mGy)**		
	Mean ± SD	**Minimum**	**Maximum**
< 18.5 (n=27)	15.43 ± 2.37	12.17	21.32
18.5-22.9 (n=131)	17.38 ± 2.27	10.43	23.34
≥ 23 (n=72)	20.38 ± 1.98	14.81	24.25

4.4.6.2 The correlation between BMI and $SSDE_{EFF}$

The correlation between BMI and $SSDE_{EFF}$ for thoracic CT examination has been investigated. The results are shown in Figure 4.8.

- The moderate linear relationship between the BMI and $SSDE_{EFF}$, R^2 was 0.4698.

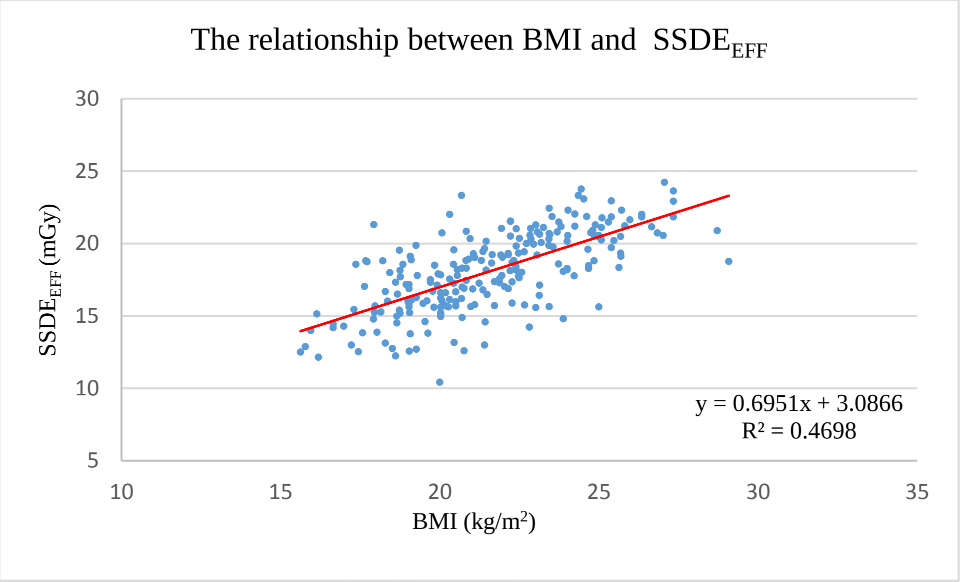

Figure 4.8 The correlation of body mass index (BMI) and $SSDE_{EFF}$.

4.4.7 BMI and $SSDE_{Dw}$

4.4.7.1 Data on BMI and $SSDE_{Dw}$

At BMI less than 18.5 kg/m^2, mean $SSDE_{Dw}$± SD was 17.41 ± 2.60 mGy (range 12.66-23.81 mGy).

At BMI from 18.5-22.9 kg/m^2, mean $SSDE_{Dw}$ ± SD was 19.41 ± 2.53 mGy (range 11.66- 24.79 mGy).

At BMI greater than or equal to 23 kg/m^2, mean $SSDE_{Dw}$ ± SD was 22.41 ± 2.12 mGy (range 16.24-26.83 mGy). The results are shown in Table 4.16

Table 4.16 Data on body mass index (BMI) and $SSDE_{Dw}$.

BMI (kg/m^2)	**$SSDE_{Dw}$(mGy)**		
	Mean ± SD	**Minimum**	**Maximum**
< 18.5 (n=27)	17.41 ± 2.60	12.66	23.81
18.5-22.9 (n=131)	19.41 ± 2.53	11.66	24.79

≥ 23 (n=72)	22.41 ± 2.12	16.24	26.83

4.4.7.2 The correlation between BMI and $SSDE_{Dw}$

The correlation between BMI and $SSDE_{Dw}$ for thoracic CT examination has been investigated. The results are shown in Figure 4.9.

- The moderate linear relationship between the BMI and $SSDE_{Dw}$, R^2 was 0.4347.

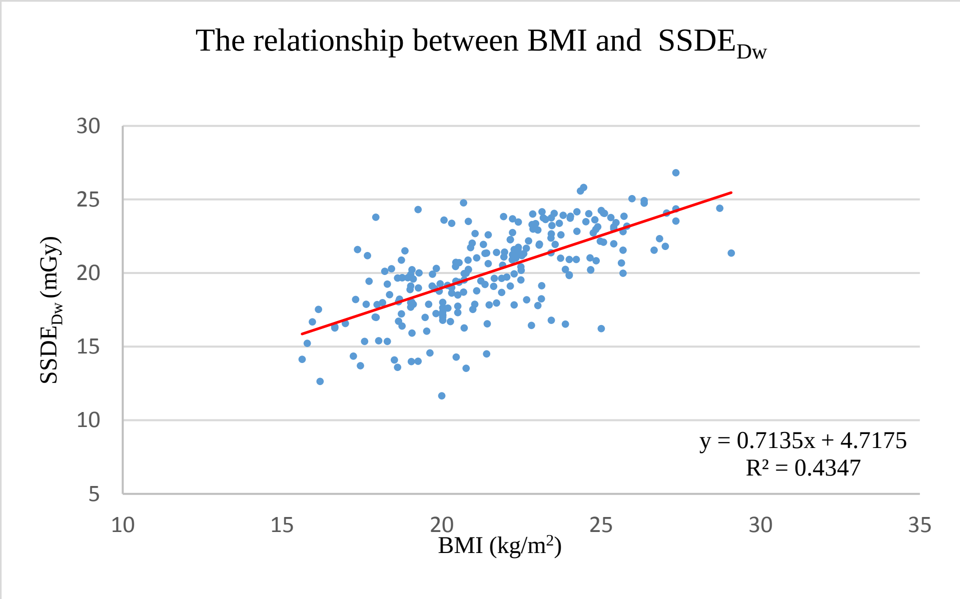

Figure 4.9 The correlation of body mass index (BMI) and $SSDE_{Dw}$.

4.4.8 AP+LAT dimension and $SSDE_{AP+LAT}$

4.4.8.1 Data on AP+LAT dimension and $SSDE_{AP+LAT}$

At AP+LAT dimension less than 50 cm, mean $SSDE_{AP+LAT}$ ± SD was 15.97 ± 2.32 mGy (range 10.50-23.71 mGy).

At AP+LAT dimension from 50- 53 cm, mean $SSDE_{AP+LAT}$ ± SD was 18.58 ± 2.05 mGy (range 14.23-23.18 mGy).

At AP+LAT dimension greater than or equal to 54 cm, mean $SSDE_{AP+LAT}$ ± SD was 20.73 ± 1.59 mGy (range 16.21-24.45 mGy). The results are shown in Table 4.17

Table 4.17 Data are presented of patient size in terms of AP+LAT dimension and $SSDE_{AP+LAT}$.

AP+LAT (cm)	**$SSDE_{AP+LAT}$ (mGy)**		
	Mean ± SD	**Minimum**	**Maximum**
< 50	15.97 ± 2.32	10.50	23.71

(n=84)			
50-53 (n=91)	18. 58 ± 2.05	14.23	23.18
≥ 54 (n=55)	20. 73 ± 1.59	16.21	24.45

4.4.8.2 The correlation between AP+LAT dimension and $SSDE_{AP+LAT}$.

The correlation between $SSDE_{AP+LAT}$ or $CTDI_{vol}$ and AP+LAT dimension for thoracic CT examination has been investigated. The results are shown in Figure 4.10.

- The moderate linear relationship between the $SSDE_{AP+LAT}$ and AP+LAT dimension , R^2 was 0.5642.
- The strong linear relationship between the $CTDI_{vol}$ and AP+LAT dimension, R^2 was 0.7763.

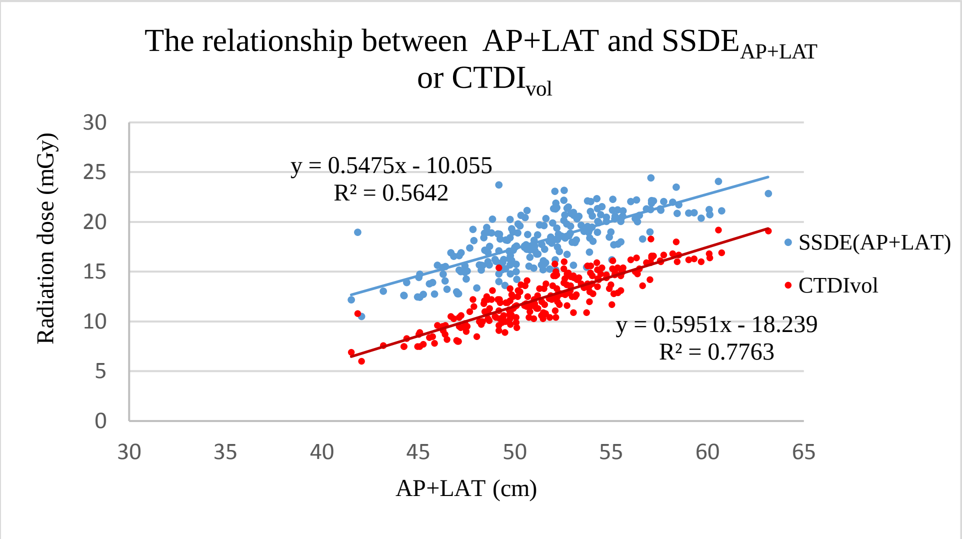

Figure 4.10 The correlation of AP+LAT dimension and $CTDI_{vol}$ or $SSDE_{AP+LAT}$.

4.4.9 Effective diameter (EFF) and $SSDE_{EFF}$

4.4.9.1 Data on effective diameter (EFF) and $SSDE_{EFF}$

At effective diameter (EFF) less than 23 cm, mean $SSDE_{EFF}$ ± SD was 13.90 ± 1.81mGy (range 10.43-18.82 mGy).

At effective diameter (EFF) from 23- 25 cm, mean $SSDE_{EFF}$ ± SD was 17.69 ± 2.12 mGy (range 13.15-23.34 mGy).

At effective diameter (EFF) greater than or equal to 26 cm, mean $SSDE_{EFF}$ ± SD was 20.44 ± 1.65 mGy (range 16.27-24.25 mGy). The results are shown in Table 4.18.

Table 4.18 Data are presented of patient size in terms of effective diameter and $SSDE_{EFF}$.

Effective diameter(cm)	$SSDE_{EFF}$(mGy)		
	Mean ± SD	Minimum	Maximum
< 23 (n=26)	13.90 ± 1.81	10.43	18.82
23-25 (n=134)	17.69 ± 2.12	13.15	23.34
≥ 26 (n=70)	20.40 ± 1.65	16.27	24.25

4.4.9.2 The correlation between effective diameter (EFF) and $SSDE_{EFF}$

The correlation between $SSDE_{EFF}$ or $CTDI_{vol}$ and effective diameter for thoracic CT examination has been investigated. The results are shown in Figure 4.11.

- The moderate linear relationship between the $SSDE_{EFF}$ and effective diameter, R^2 was 0.5696.
- The strong linear relationship between the $CTDI_{vol}$ and effective diameter, R^2 was 0.7789.

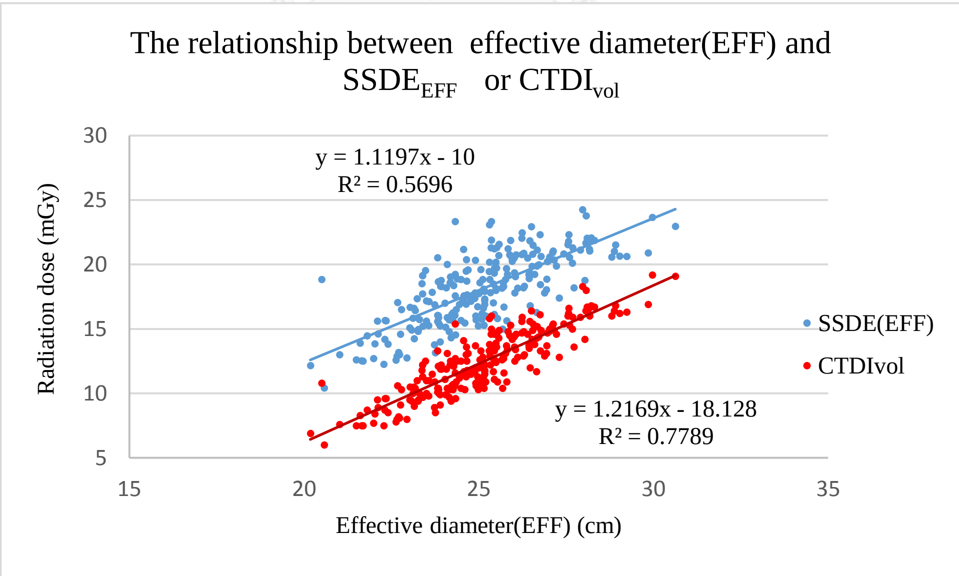

Figure 4.11 The correlation of effective diameter and $CTDI_{vol}$ and $SSDE_{EFF}$.

4.4.10 Water equivalent diameter (Dw) and $SSDE_{Dw}$

4.4.10.1 Data on water equivalent diameter (Dw) and $SSDE_{Dw}$ of male adult patients.

At water equivalent diameter (Dw) less than 20 cm, mean $SSDE_{Dw}$ ± SD was 16.36 ± 1.45mGy (range 13.54-18.55 mGy).

At water equivalent diameter (Dw) from 20-23 cm, mean $SSDE_{Dw}$ ± SD was 20.77 ± 2.14 mGy (range 16.55-25.58 mGy).

At water equivalent diameter (Dw) greater than or equal to 24 cm, mean $SSDE_{Dw}$ ± SD was 24.25 ± 1.14 mGy (range 21.76-26.83 mGy).

4.4.10.2 Data on water equivalent diameter (Dw) and $SSDE_{Dw}$ of female adult patients.

At water equivalent diameter (Dw) less than 20 cm, mean $SSDE_{Dw}$ ± SD was 15.23 ± 2.15 mGy (range 11.66-21.21 mGy).

At water equivalent diameter (Dw) from 20-23 cm, mean $SSDE_{Dw}$ ± SD was 19.19 ± 2.10 mGy (range 14.11-23.80 mGy).

At water equivalent diameter (Dw) greater than or equal to 24 cm, mean $SSDE_{Dw}$ ± SD was 22.80 ± 1.06 mGy (range 20.55-24.42 mGy). The results are shown in Table 4.19

Table 4.19 Data on patient size in terms of water equivalent diameter and $SSDE_{Dw}$.

Gender	D_w (cm)	$SSDE_{Dw}$ (mGy)		
		Mean ± SD	Minimum	Maximum
Male	<20 (n= 9)	16.36 ±1.45	13.54	18.55
	20-23 (n= 90)	20.77 ±2.14	16.55	25.58
	≥ 24 (n= 16)	24.25 ±1.14	21.76	26.83
Female	<20 (n= 18)	15.23 ±2.15	11.66	21.21
	20-23 (n= 73)	19.19 ±2.10	14.11	23.80
	≥ 24 (n= 24)	22.80 ±1.06	20.55	24.41

4.4.10.3 The correlation between water equivalent diameter (Dw) and $SSDE_{Dw}$

The correlation between water equivalent diameter (Dw) and $SSDE_{Dw}$ of male and female for thoracic CT examination has been investigated. The results are shown in Figure 4.12.

- The strong linear relationship between the water equivalent diameter (Dw) and $SSDE_{Dw}$ of male, R^2 was 0.7307.
- The moderate linear relationship between the water equivalent diameter (Dw) and $SSDE_{Dw}$ of female, R^2 was 0.6679.

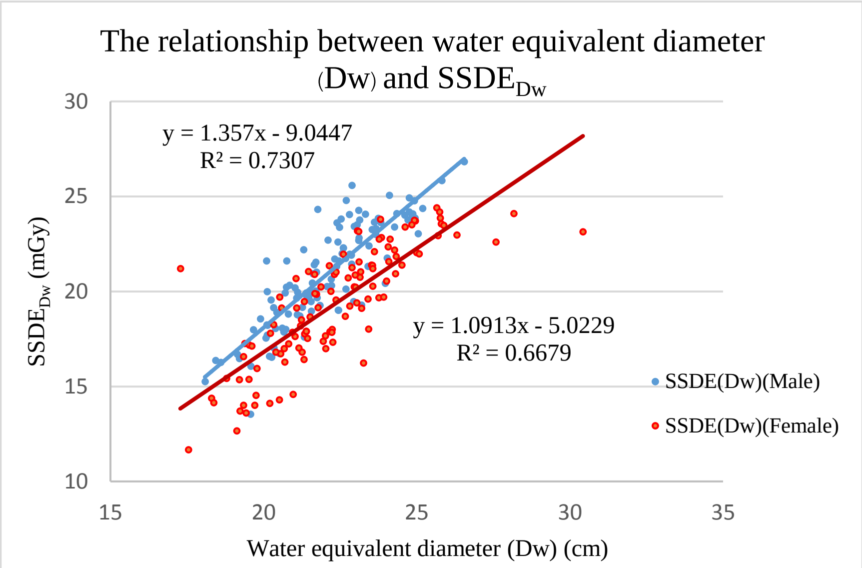

Figure 4.12 The correlation of water equivalent diameter (Dw) of male and female patients.

CHAPTER V

DISCUSSION AND CONCLUSIONS

5.1 Discussion

The modern CT scanners can display the patient dose in terms of the volume computed tomography dose index ($CTDI_{vol}$) and the dose length product (DLP) [1]. The dose received by patient from CT scan is dependent on both patient size and scanner radiation output. However, $CTDI_{vol}$ provides information regarding only the scanner output. It does not address patient size, and hence does not estimate patient dose accurately.

AAPM Report no.204 [5] was introduced in 2011 and AAPM Report no.220 [6] was also introduced in 2014 on the size-specific dose estimates (SSDEs) for CT examination in order to provide more accurate on radiation dose estimation to the patients. The conversion factors that take into account the patient size, and can be applied to the displayed $CTDI_{vol}$ to estimate patient dose were developed and available in the reports.

In this study, the conversion factors (f_{size}) from the AAPM Reports were applied to determine SSDE for thoracic imaging in 320 row detector computed tomography. The parameters affecting SSDE were also evaluated.

5.1.1 SSDE for thoracic imaging in 320 row detector computed tomography

In this study, 230 adult patients of the age range from 18-93 years old, the weight range from 40 – 70 kg were included to determine SSDEs. The patient radiation dose was calculated in terms of SSDE, product of conversion factor (f_{size}) and the $CTDI_{vol}$. The f_{size} was shown in AAPM Reports [5, 6] based on patient size sum of anterior-posterior, lateral dimension, effective diameter and water equivalent diameter (Dw). Patient sizes were measured at the middle of organ (chest) and from the slice at the middle of scan range by using digital caliper on image tools from PACS system.

5.1.1.1 The slice locations used to estimate SSDE

At our institute, CT chest is routinely used the scan range from apex of the lung to adrenal gland or include liver so the slice at the middle of scan range located at lower lung zone but mid organ (chest) range is located at center of chest (7^{th} thoracic vertebrae). $SSDE_{AP+LAT,}$ $SSDE_{EFF}$ and $SSDE_{Dw}$ had been estimated from two locations, at the middle slice of scan range and the middle slice of the organ (chest).

In this study, according to Figure 4.2, the outlier of $SSDE_{Dw}$ at the middle slice of scan range caused by large size of the mass in the lung as shown in Figure5.1. When Dw increased, the mean CT number increased. On the other word, the conversion factor (f_{Dw}) to calculate $SSDE_{DW}$ will decrease, so $SSDE_{Dw}$ was also decreased.

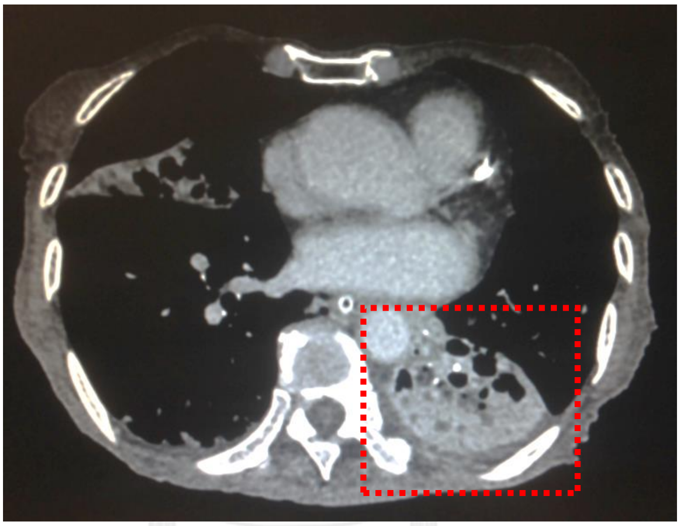

Figure 5.1 Example of CT chest transaxial image at the middle slice of scan with mass in lung region which is largely affected the CT number for $SSDE_{Dw}$ calculation.

In previous study, Leng S et al [16] reported on SSDE for chest, abdominal and pelvic CT: effect of intra-patient variability in Dw. The results showed D_w from the image at the center of the scan range provided an easily obtained estimate of SSDE for the whole scan range that agreed well with values from an image-by-image approach, with a root mean square difference of less than 9%. $SSDE_{mid}$ and $\overline{SSDE}$ were almost perfectly correlated (R^2 was 0.9914) for chest as shown in Figure5.2.

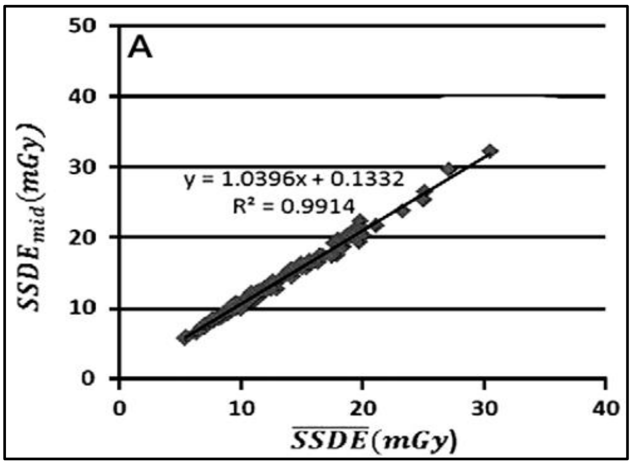

Figure 5.2 Scatterplots for $SSDE_{mid}$ in relative to $\overline{SSDE}$ for chest CT. The correlation coefficient (R^2) as determined from the linear regression is also shown [16].

In our study, SSDE calculated from the middle slice at scan range is a little higher than SSDE calculated from slice at middle of organ. The correlation of $SSDE_{AP+LAT}$, $SSDE_{EFF}$ and $SSDE_{Dw}$ between the middle slice of the organ (chest) and the middle slice of scan range were perfectly correlated, R^2 of 0.9820, 0.9864 and 0.9933 respectively(Figure5.3), root mean square difference were 0.003%, 0.001% and 0.001% respectively.

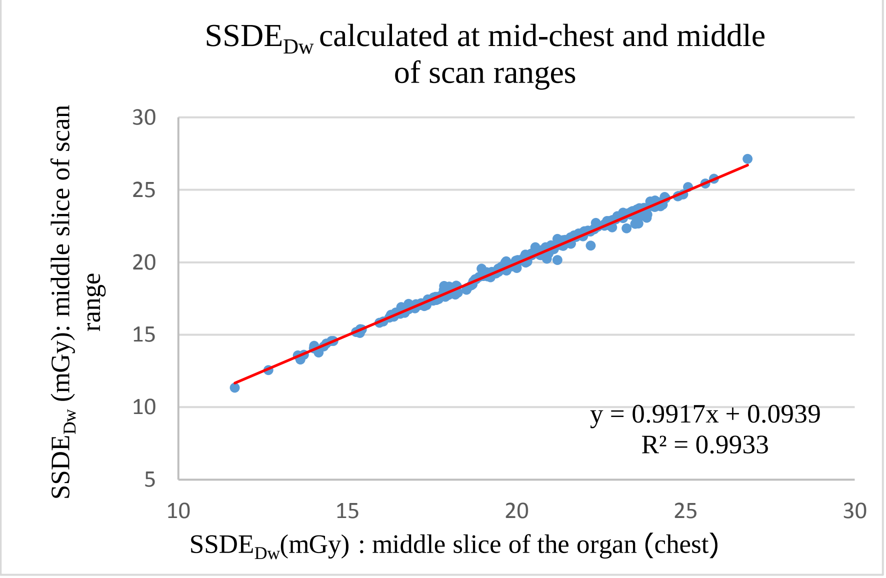

Figure 5.3 The correlation of $SSDE_{Dw}$ between the middle slice of the organ (chest) and the middle slice of scan range were perfectly correlated.

Both locations can be used to determine SSDE but in clinical, slice at middle of the scan range is recommended which is more convenient than at the slice at center of chest (7th thoracic vertebrae) and similar to Leng S et al for estimation of SSDE.

5.1.1.2 Determination of SSDE from middle slice of the chest.

230 adult patients weight range from 40 – 70 kg were included. They underwent thoracic contrast enhancement with venous phase protocol scanned by CT Toshiba Aquilion ONE, 320-row. The CT scanner was operated with automatic exposure control systems (AEC). The $CTDI_{vol}$ was displayed on CT monitor and determined from the 32-cm cylindrical phantom. The patient radiation dose (SSDE) was taken into a function of patient size (AP+LAT dimension, effective diameter (EFF) and water-equivalent diameter (Dw)).

The $SSDE_{AP+LAT}$ and $SSDE_{EFF}$ related to patient geometry, mean $SSDE_{AP+LAT}$ ± SD was 18.13 ± 2.75 mGy and mean $SSDE_{EFF}$ ± SD was 18.09 ± 2.75 mGy respectively .The $SSDE_{Dw}$ related to body composition, the mean $SSDE_{Dw}$ ± SD was 20.12 ± 2.93 mGy. $SSDE_{Dw}$ was considered to water equivalent diameter, therefore it needs to be applied to estimate the patient radiation dose in the thorax which consists of air, tissue and lung of different x-ray attenuations. Statistical difference between 3 methods, $SSDE_{AP+LAT}$, $SSDE_{EFF}$ and $SSDE_{Dw,}$ are significant (p-value < 0.001).

The mean $CTDI_{vol}$ ± SD was 12.40 ± 2.55 mGy which was less than $SSDE_{AP+LAT}$, $SSDE_{EFF}$ and $SSDE_{Dw}$ as shown in Table5.1. $CTDI_{vol}$ is used for the patient radiation dose estimation but it is not realistic and inaccurate as it was determined from 32 cm diameter PMMA cylindrical and homogeneous phantom, on the contrary thoracic region is not in the cylindrical shape, non-uniform in size and density.

Table 5. 1 Data on $CTDI_{vol}$, $SSDE_{AP+LAT}$, $SSDE_{EFF}$ and $SSDE_{Dw}$

Radiation dose (mGy)	**Mean ± SD**	**Minimum**	**Maximum**
$CTDI_{vol}$ (mGy)	12.40 ± 2.55	6.00	19.20
$SSDE_{AP+LAT}$ (mGy)	18. 13 ± 2.75	10.50	24.45
$SSDE_{EFF}$ (mGy)	18. 09 ± 2.75	10.43	24.25
$SSDE_{Dw}$ (mGy)	20.12 ± 2.93	11.66	26.83

As the recommendations and guidance published by the International Commission on Radiological Protection (ICRP publication 87) , European Commission Guidelines (EUR 16262) [19] and national diagnostic refence levels (Japan 2015), stated that diagnostic refence levels (DRL) are the important tools for optimization of image quality and the radiation dose delivered to patients . The internatonal and national DRL data were shown in table 5.2.

Table 5.2 Diagnostic reference level for CT chest in adult patients

Diagnostic reference level for CT chest in adult patients	
	$CTDI_{vol}$ (mGy)
EUR 16262	30
ICRP publication 87	30
Japan (2015)	15

*The application of this concept is in line with the reference dose values for a standard sized patient (70kg) indicated in the European Guidelines.
* ICRP publication 87 relate to body phantom (PMMA, 32 cm diameter)

In our study, the result of the mean $CTDI_{vol}$ was lower than the European Commission Guidelines (EUR 16262), ICRP publication 87 and Japan (2015) dose reference level for chest as shown in Figure5.4.

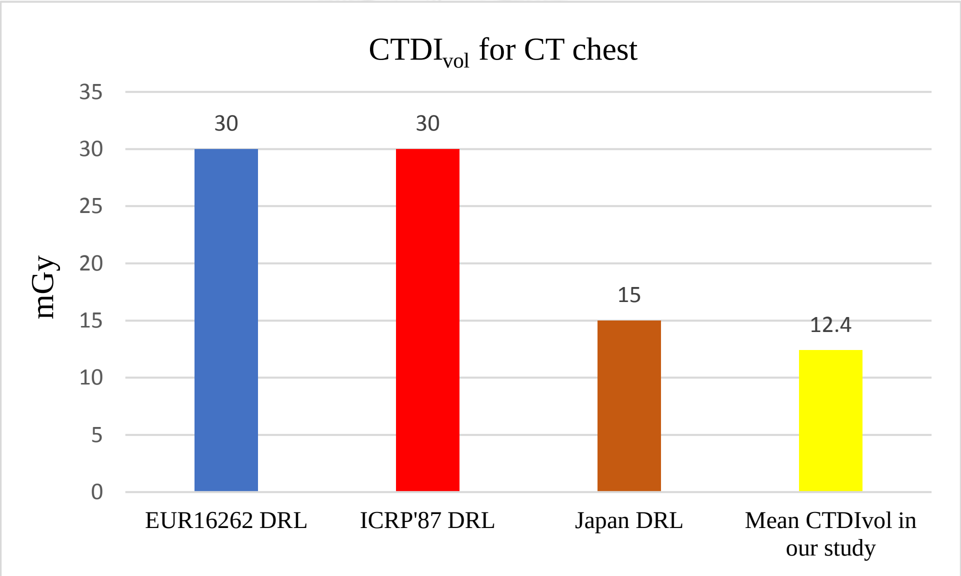

Figure 5.4 $CTDI_{vol}$ in comparison to Diagnostic Reference Levels and our study for chest CT.

According to patient information of 230 cases in this study, the weight ranges from 40 – 70 kg were included to determine SSDEs. They underwent thoracic contrast enhancement with venous phase protocol scanned by CT Toshiba Aquilion ONE, 320-row detector**.** The 75th percentiles in the distribution of $SSDE_{Dw}$ was 22.45 mGy as shown in Figure 5.5. This value could be used as the guidance level for $SSDE_{Dw}$ at our institution.

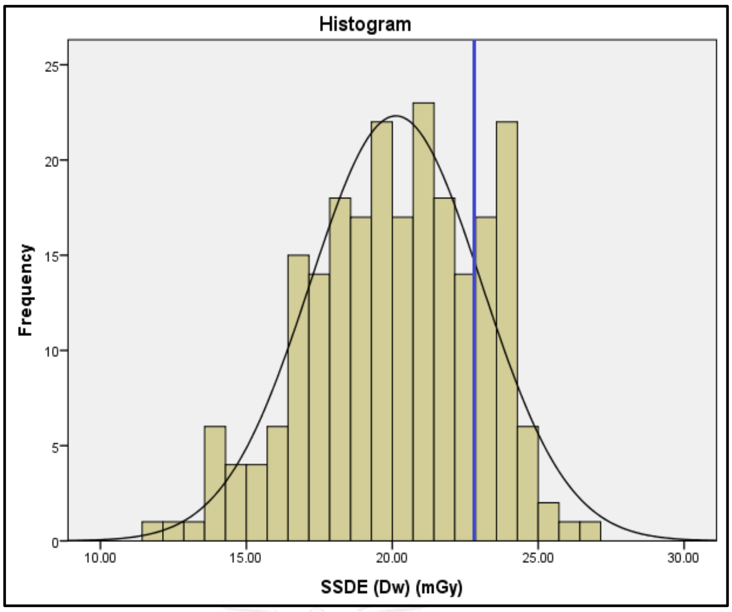

Figure 5.5 The distribution of $SSDE_{Dw}$, the weight range from 40 – 70 kg.

As the guidance level in this study was investigated from only one manufacturer, it should be therefore investigated for several CT scanners to represent the guidance level of institution for the future study.

5.1.2 The parameters influence SSDE

5.1.2.1 $CTDI_{vol}$ and SSDE

The correlation of $SSDE_{Dw}$ and $CTDI_{vol}$ was perfectly correlated, $R^2 = 0.9529$. $SSDE_{Dw}$ can be determined from $CTDI_{vol}$ displayed on the CT monitor for adult patients weight range from 40 – 70 kg and underwent thoracic CT examination by this function: $y = 13.378 \ln(x) - 13.269$, x is the $CTDI_{vol}$ (mGy). However, the limitation of this function is specific for 320 row MDCT in thoracic examination.

5.1.2.2 Body weight and SSDE

Imai R et al [15] studied on: Local diagnostic reference level based on size-specific dose estimates: assessment of pediatric abdominal/pelvic computed tomography at a Japanese national children's hospital. This is a result of the switch in the SFOV from the 16-cm phantom to the 32-cm phantom, leading to a massive drop in the exposure dose. In contrast, SSDE is adjusted for body size, the dose gradually increased with increasing body weight. The difference between $CTDI_{vol}$ and SSDE was greatest in the yellow section (11.5–14.5 kg), corresponding to the switch from the 16-cm to the 32-cm phantom, where $CTDI_{vol}$ was estimated to be half of SSDE as shown in Figure 5.6.

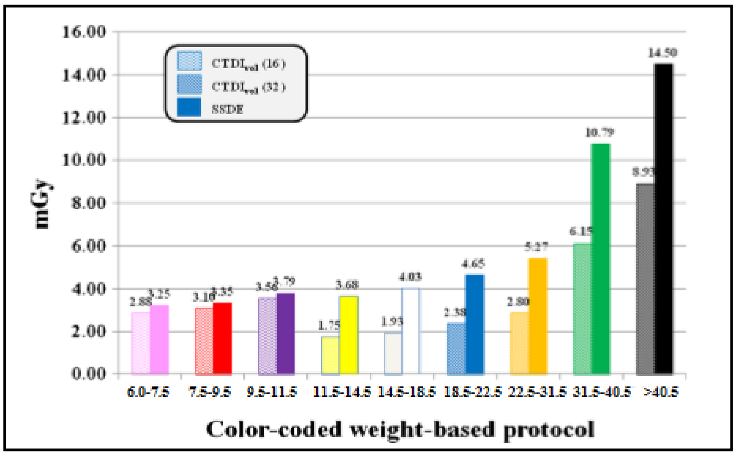

Figure 5.6 The relationship between SSDE and $CTDI_{vol}$ on the basis of the body weight.

In our study with 230 adult patients, the weight range from 40 – 70 kg was included in the study. When body weight increased, the pateint size (AP+LAT dimension, effective diameter(EFF), water equivalent diameter(Dw)) increased, so $SSDE_{AP+LAT}$, $SSDE_{EFF}$ and $SSDE_{Dw}$ also increased. The result similar to Imai R et al for the dose increased with increasing body weight when corresponding to 32-cm cylindrical phantom and SSDE was higher than $CTDI_{vol}$ as shown in Figure 5.7.

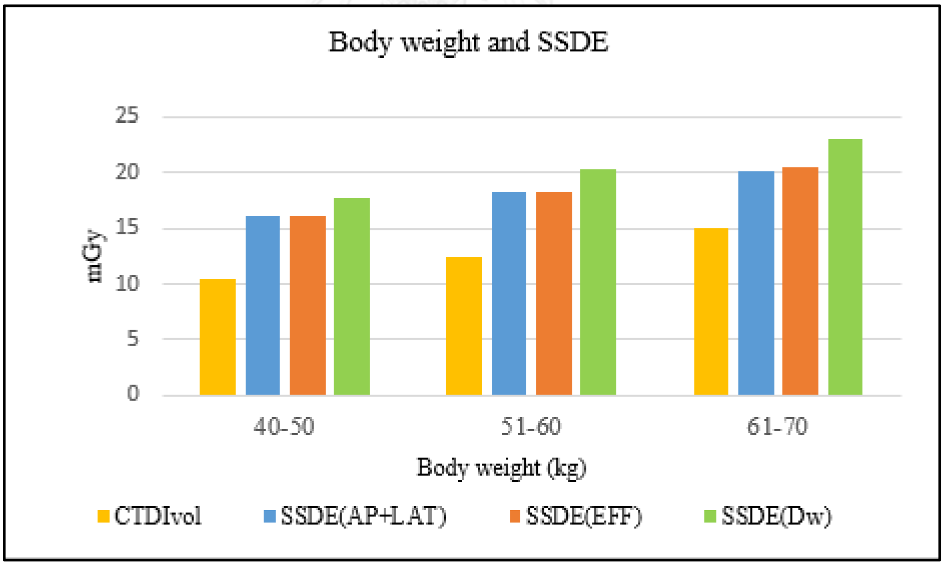

Figure 5. 7 SSDE and $CTDI_{vol}$ based on body weight.

The correlation of body weight and $SSDE_{AP+LAT}$, $SSDE_{EFF}$ and $SSDE_{Dw}$ for thoracic CT examination was moderate linear relationship (R^2 were 0.4730, 0.4724 and 0.5571 respectively). However, body weight is one of factors affected SSDE.

5.1.2.3 AP+LAT dimension and $SSDE_{AP+LAT}$

Christner JA , Braun N. et al [14] studied on: size-specific dose estimates for adult patients at CT of the torso.The data were obtained from Siemens Healthcare, Forchheim, Germany.The result showed, for the evaluated automatic exposure control, $CTDI_{vol}$ (scanner output) increased linearly with patient size; however, patient dose (as indicated by $SSDE_{AP+LAT}$) was independent of patient size. The results were shown in Figure5.8.

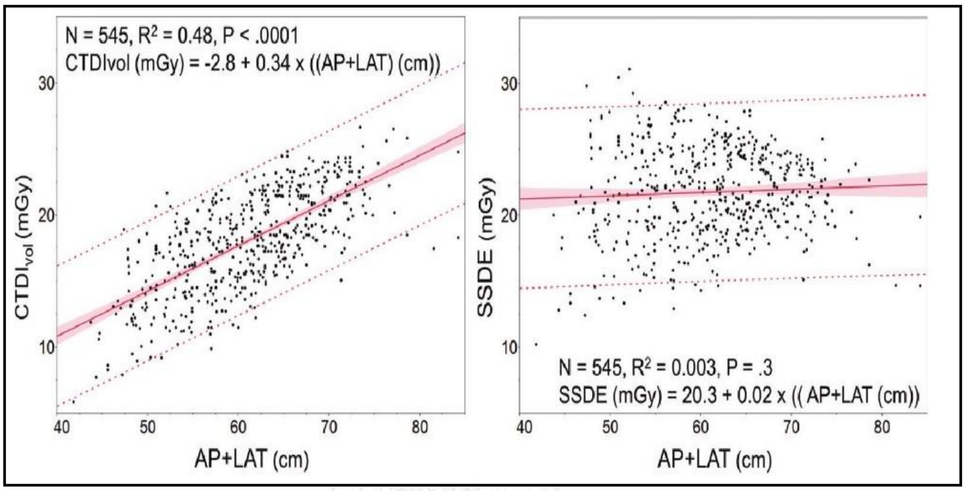

Figure 5.8 Data on $CTDI_{vol}$ or SSDE and AP+LAT.

Table 5. 3 Data are presented from Christner JA and our study

	CT scanner	Patient size (AP+LAT) (cm) Mean ± SD	Conversion factor based on AP+LAT (f_{size})	$CTDI_{vol}$ (mGy) Mean ± SD	$SSDE_{AP+LAT}$ (mGy) Mean ± SD
Christner JA et al	Siemens Healthcare, Forchheim, Germany.	61.2 ± 7.4 (41.8-84.2)	Range 0.80-1.74	18.10 ± 3.7 (5.90-26.70)	21.8 ± 3.4 (10.20-31.10)
In this study	CT Toshiba Aquilion ONE	51.49 ± 3.78 (41.52-63.14)	Range 1.19-1.76	12.40 ± 2.55 (6.00-19.20)	18. 13 ± 2.75 (10.5-24.45)

Our study, the data obtained from CT Toshiba Aquilion ONE, AEC system with standard strength was used. $CTDI_{vol}$ and SSDE increased when patient size increased, the moderate linear relationship between the $SSDE_{AP+LAT}$ and AP+LAT dimension, R^2 was 0.5642 and strong linear relationship between the $CTDI_{vol}$ and AP+LAT dimension, R^2 was 0.7763. The conversion factor of our study was 1.19-1.76 and sum of AP and LAT was 41.52-63.14 cm while Christner JA et al reported, the relationship between $SSDE_{AP+LAT}$ and AP+LAT dimension, R^2 was 0.003. This is because of the conversion factor range from 0.80-1.74 and sum of AP and LAT was 41.8-84.2 cm.

When the sum of AP and LAT dimension length was greater than 72cm, the conversion factor was less than 1. So, the result was decreasing in $SSDE_{AP+LAT}$. In the opposite way, the AP and LAT dimension lengths of less than 72cm, the conversion factor was greater than 1, result in increasing $SSDE_{AP+LAT}$.

In our study, sum of AP and LAT at less than 72cm were collected. The conversion factor according to AAPM no.204 was greater than 1. The result showed that when patient size (AP and LAT dimension) increased, the $SSDE_{AP+LAT}$ increased.

The result showed (Figure4.10) that correlation of $SSDE_{AP+LAT}$ and AP+LAT dimension for thoracic CT examination was moderated linear relationship (R^2 was 0.5642). However, AP+LAT dimension is one of the factors affected SSDE.

5.1.2.4 Effective diameter (D_{EFF}) and $SSDE_{EFF}$

In the result, mean effective diameter ± SD was 25.09 ± 1.85 cm, range was 20.17-30.62 cm, and the conversion factor range from 1.20-1.76. Mean $SSDE_{EFF}$ ± SD was 18. 09 ± 2.75 (10.43 -24.25) mGy and $CTDI_{vol}$ 12.40 ± 2.55 (6.00-19.20) mGy, $CTDI_{vol}$ was lower than $SSDE_{EFF}$.

When the effective diameter was less than 35.2 cm, the conversion factor was greater than 1, the result was increasing in $SSDE_{EFF}$ in comparison to $CTDI_{vol}$.

The correlation between $SSDE_{EFF}$ and effective diameter for thoracic CT examination, the results showed the moderate linear relationship between the $SSDE_{EFF}$ and effective diameter, R^2 was 0.5696. However, effective diameter is one of the factors affected SSDE.

5.1.2.5 Water equivalent diameter and $SSDE_{EFF}$

In our study, the patient size in terms of water equivalent diameter was measured by manual contour at the middle slice of chest. The benefit of manual measuring is suitable for clinical users (physician and radiological technologist) and save the cost instead of purchasing commercial software.

Mean water equivalent diameter (Dw) ± SD was 22.19 ± 1.97 cm (range 17.28-30.42 cm), mean $SSDE_{Dw}$ ± SD was 20.19 ± 1.97 mGy (range 17.28-30.42 mGy). The correlation between water equivalent diameter (Dw) and $SSDE_{Dw}$, R^2 was 0.6096. When water equivalent diameter decreased, resulting in a decrease in the value of $SSDE_{Dw}$.

The relationship between the water equivalent diameter (Dw) and $SSDE_{Dw}$ of male is higher than female, R^2 was 0.7307 and 0.6679 in male and female respectively. For male patients, the thoracic cavity size is bigger than female of larger lungs. When Dw decreased, the mean CT number decreased. On the other hand, the conversion factor (f_{Dw}) to calculate $SSDE_{DW}$ will increase, so $SSDE_{Dw}$ was also increased, therefore $SSDE_{Dw}$ of male is higher than female.

The result showed (Figure 4.12) that correlation between $SSDE_{Dw}$ and water equivalent diameter (Dw) for thoracic CT, R^2 was 0.6096. Therefore, water equivalent diameter (Dw) is one of the factors affected SSDE.

5.2 Conclusions

This study revealed the SSDE for 320 detector row MDCT in thoracic examination at King Chulalongkorn Memorial Hospital. The SSDE had been estimated by 3 methods, i**.**e**.** $SSDE_{AP+LAT}$, $SSDE_{EFF}$ and $SSDE_{Dw}$ of patient configurations in CT dosimetry**.** The results indicated that mean $SSDE_{AP+LAT}$, $SSDE_{EFF}$ and $SSDE_{Dw}$ were 18.13, 18.09 and 20.12 mGy while mean $CTDI_{vol}$ was 12**.**39 mGy and statistical difference between 3 methods, were significant *(p-value* < 0.001). For the location to determine SSDE, at the middle of scan range and middle of organ (chest) are both suitable for measuring the patient size from CT images for all 3 methods. When using the automatic mA modulation technique, the patient AP+LAT dimension, effective diameter, body weight, and body attenuation are the factors affecting SSDE. The strong correlation was found between SSDE and water equivalent diameter.

5.3 Recommendations

1. SSDEs should be applied as the CT patient dose indicator further from $CTDI_{vol}$ and provide higher accuracy especially in patients of different sizes and body composition.

2. $SSDE_{Dw}$ is considered to patient size and composition, so $SSDE_{Dw}$ should be reported in patients of different attenuations especially in thorax region.

3. The in-vivo measurement is a gold standard to determine patient radiation dose that takes into account for both output radiation dose and the patient characteristics. However, such method is difficult to use in clinical situation. So, the concepts of the size-specific dose estimates (SSDEs) is more appropriate to be used as in clinical studies for patient dose estimation.

REFERENCES

1. Kak, A.C. and M. Slaney, *Principles of Computerized Tomographic Imaging*. 1988, New York: IEEE Press.
2. Hsieh, J., *Computed Tomography: Principles, Design, Artifacts, and Recent Advances*. 2009, Bellingham, WA, USA: SPIE Press.
3. ICRP., *1990 Recommendations of the International Commission on Radiological Protection.* Ann ICRP, 1991. **21**(1-3): p. 1-201.
4. Bushberg, J.T., et al., *The Essential Physics of Medical Imaging*. second edition. 2001, Philadelphia, PA, USA: Lippincott Williams & Wilkins.
5. *American Association of Physicists in Medicine. Size-specific dose estimates (SSDE) in Pediatric and adult body CT examinations (task group 204)*. 2011.
6. McCollough, C., et al., *Use of Water Equivalent Diameter for Calculating Patient Size and Size-Specific Dose Estimates (SSDE) in CT: The Report of AAPM Task Group 220.* AAPM Rep, 2014. **2014**: p. 6-23.
7. *Diagnostic radiology physics : a handbook for teachers and students*. 2014, Vienna: International Atomic Energy Agency.
8. Buzug, T.M., *Computed Tomography: From Photon Statistics to Modern Cone-Beam CT*. 2008, Berlin-Heidelberg, Germany: Springer-Verlag.
9. *Multi-slice CT scanners CEP08007*. 2009 [cited 2009; Available from: impactscan.org.
10. Ohnesorge, B.M., et al., *Multi-slice and Dual-source CT in Cardiac Imaging*. second edition. 2008, Berlin, Heidelberg, New York: Springer.
11. Heverhagen, J.T., *Physics of Computed Tomography Scanning,Handbook of Neuro-Oncology Neuroimaging*. 2016: Academic Press.
12. Cho, Z.H., J.P. Jones, and M. Singh, *Foundations of Medical Imaging*. first edition. 1993, New York: Wiley-Interscience.
13. Simpson, G., *Thoracic computed tomography: principles and practice.* Australian Prescriber, 2009:105-7. **32**(4).
14. Christner, J.A., et al., *Size-specific dose estimates for adult patients at CT of the torso.* Radiology, 2012. **265**(3): p. 841-7.
15. Imai, R., et al., *Local diagnostic reference level based on size-specific dose estimates: assessment of pediatric abdominal/pelvic computed tomography at a Japanese national children's hospital.* Pediatr Radiol, 2015. **45**(3): p. 345-53.
16. Leng, S., et al., *Size-specific Dose Estimates for Chest, Abdominal, and Pelvic CT: Effect of Intrapatient Variability in Water-equivalent Diameter.* Radiology, 2015. **277**(1): p. 308-9.
17. Khawaja, R.D., et al., *Simplifying size-specific radiation dose estimates in pediatric CT.* AJR Am J Roentgenol, 2015. **204**(1): p. 167-76.
18. *Quality assurance programme for computed tomography: diagnostic and therapy applications*. Vol. IAEA human health series no. 19. 2012, Vienna, Austria: International Atomic Energy Agency.
19. *European Guidelines on Quality Criteria for Computed Tomography (EUR 16262 EN, May 1999);*. 2002.

APPENDIX

Appendix A

Table A 1 Case Record Form

No.	Age (Yr)	Gender	BW (kg)	Height (cm)	BMI (kg/m^2)	AP+ LAT (cm)	Effective diameter (cm)	A_{ROI} (cm^2)	CT number (HU)	D_W (cm)	f_{AP_LAT}	f_{EFF}	f_{D_W}	$CTDI_{vol}$ mGy	SSDE (AP+LAT) mGy	SSDE (EFF) mGy	SSDE (D_W) mGy
1																	
2																	
3																	
4																	
5																	
6																	
7																	
8																	
9																	
10																	
11																	
12																	
13																	
14																	
15																	
16																	
17																	
18																	
19																	
20																	

Table A 2 Patient data and radiation dose determined from middle slice of organ (chest)

No.	Age (Yr)	Gender	BW (kg)	HT (cm)	BMI (kg/m^2)	AP+ LAT (cm)	Effective diameter (cm)	A_{ROI} (cm^2)	CT number (HU)	Dw (cm)	f_{AP+LAT}	f_{EFF}	f_{Dw}	CTDIvol mGy	SSDE (AP+LAT) mGy	SSDE (EFF) mGy	SSDE (Dw) mGy
1	55	Male	60	165	22.04	52.3	25.41	555.13	-351.47	21.41	1.46	1.46	1.69	11.7	17.03	17.04	19.75
2	33	Female	53	160	20.70	47.19	23.08	474.20	-291.17	20.69	1.60	1.59	1.73	9.4	15.00	14.91	16.29
3	73	Man	45	167	16.14	49.33	24.05	486.07	-349.06	20.07	1.54	1.53	1.77	9.9	15.20	15.15	17.55
4	69	Woman	54	159	21.36	53.87	26.46	592.76	-310.68	22.81	1.41	1.40	1.60	12.0	16.98	16.81	19.24
5	62	Man	65	173	21.72	55.12	27.30	618.84	-404.92	21.65	1.38	1.36	1.67	12.8	17.71	17.39	21.41
6	47	Man	66	171	22.57	55.49	26.93	582.08	-323.95	22.38	1.37	1.38	1.63	13.1	18.00	18.04	21.33
7	41	Man	67	173	22.39	54.9	26.76	579.95	-317.38	22.45	1.39	1.39	1.62	13.3	18.47	18.43	21.61
8	64	Woman	54	145	25.68	53.87	26.02	590.72	-290.12	23.11	1.41	1.42	1.59	13.6	19.24	19.37	21.57
9	57	Man	52	160	20.31	51.54	24.57	519.46	-239.47	22.43	1.48	1.50	1.63	11.7	17.26	17.57	19.02
10	75	Woman	51	150	22.67	51.53	25.08	507.53	-304.31	21.20	1.48	1.47	1.70	10.7	15.79	15.77	18.20
11	55	Woman	56	156	23.01	48.66	23.81	482.24	-334.00	20.22	1.55	1.54	1.76	10.1	15.69	15.59	17.81
12	65	Man	64	167	22.95	54.75	26.72	606.96	-346.59	22.47	1.39	1.39	1.62	14.4	20.05	19.99	23.38
13	79	Man	65	161	25.08	56.82	27.91	646.84	-280.70	24.34	1.34	1.33	1.52	15.9	21.33	21.12	24.10
14	76	Woman	40	147	18.51	47.07	22.94	429.97	-255.21	20.19	1.60	1.59	1.76	8.0	12.79	12.76	14.12
15	24	Man	58	170	20.07	50.72	23.81	477.20	-251.85	21.32	1.50	1.54	1.69	10.4	15.57	16.06	17.61
16	75	Man	63	165	23.14	59.01	29.03	696.65	-309.25	24.75	1.29	1.27	1.49	16.2	20.89	20.65	24.18
17	77	Man	47	160	18.36	49.02	23.84	466.33	-333.39	19.90	1.54	1.54	1.78	10.4	16.06	16.04	18.56
18	71	Man	65	160	25.39	53.93	26.46	589.72	-164.40	25.05	1.41	1.40	1.48	15.6	22.05	21.86	23.04
19	63	Man	70	163	26.35	58.5	28.30	661.62	-273.00	24.75	1.30	1.31	1.49	16.7	21.74	21.87	24.94
20	57	Man	60	160	23.44	54.25	26.24	596.24	-195.70	24.71	1.41	1.41	1.50	15.9	22.34	22.46	23.77
21	68	Woman	54	150	24.00	49.54	24.07	520.39	-287.99	21.72	1.53	1.53	1.67	11.9	18.20	18.20	19.86
22	79	Woman	42	146	19.70	47.65	23.23	446.25	-254.40	20.58	1.58	1.58	1.74	11.0	17.41	17.35	19.14
23	31	Man	63	186	18.21	52.2	24.48	527.76	-234.30	22.68	1.46	1.51	1.61	12.5	18.22	18.83	20.13
24	93	Man	40	155	16.65	45.01	21.80	415.31	-345.72	18.60	1.66	1.66	1.87	8.7	14.44	14.46	16.28
25	72	Woman	57	152	24.67	53.18	25.71	578.04	-284.14	22.95	1.43	1.44	1.59	12.7	18.19	18.29	20.25

No.	Age (Yr)	Gender	BW (kg)	HT (cm)	BMI (kg/m^2)	AP+ LAT (cm)	Effective diameter (cm)	A_{ROI} (cm^2)	CT number (HU)	Dw (cm)	f_{AP+LAT}	f_{EFF}	f_{Dw}	CTDIvol mGy	SSDE (AP+LAT) mGy	SSDE (EFF) mGy	SSDE (Dw) mGy
26	81	Man	68	173	22.72	48.83	24.09	513.27	-305.64	21.30	1.55	1.53	1.69	13.1	20.29	20.02	22.20
27	62	Man	67	180	20.68	49.16	24.32	530.73	-237.69	22.70	1.54	1.52	1.61	15.4	23.72	23.34	24.79
28	55	Woman	48	148	21.91	53.59	25.81	588.55	-230.60	24.01	1.42	1.43	1.53	13.4	19.05	19.23	20.56
29	60	Man	68	171	23.26	54.28	26.67	608.94	-280.70	23.62	1.40	1.39	1.56	15.2	21.35	21.13	23.66
30	54	Man	50	166	18.14	51.8	25.15	528.06	-361.77	20.72	1.47	1.47	1.73	10.4	15.27	15.29	18.01
31	74	Man	60.2	170	20.83	54.44	26.29	601.55	-306.50	23.05	1.40	1.41	1.59	14.8	20.73	20.87	23.52
32	84	Woman	57	140	29.08	57.01	28.03	585.38	-193.90	24.51	1.34	1.32	1.51	14.2	18.99	18.78	21.39
33	65	Woman	62	152	26.84	53.03	26.06	590.44	-229.60	24.07	1.44	1.42	1.53	14.6	20.97	20.76	22.35
34	62	Woman	54	158	21.63	48.42	23.84	552.15	-234.60	23.20	1.56	1.54	1.58	12.1	18.88	18.66	19.13
35	67	Woman	52	158	20.83	53.89	26.30	598.48	-271.80	23.56	1.41	1.41	1.56	13.0	18.39	18.32	20.28
36	61	Woman	51	165	18.73	49.52	23.85	509.29	-331.80	20.82	1.53	1.54	1.73	10.0	15.30	15.42	17.25
37	84	Woman	51	156	20.96	55.53	27.15	598.77	-180.50	25.00	1.37	1.37	1.48	14.9	20.46	20.35	22.05
38	69	Woman	50	150	22.22	57.56	27.55	641.65	-237.90	24.95	1.32	1.35	1.48	16.0	21.18	21.54	23.71
39	61	Woman	48	153	20.50	51.47	25.19	508.28	-303.80	21.23	1.48	1.47	1.70	10.9	16.10	16.00	18.52
40	62	Woman	62	155	25.81	52.01	25.44	558.46	-252.30	23.06	1.46	1.45	1.59	14.6	21.36	21.24	23.20
41	69	Man	49	162	18.67	46.83	22.78	457.35	-306.11	20.10	1.61	1.60	1.77	10.3	16.54	16.52	18.24
42	49	Woman	43	152	18.61	45.07	22.28	451.34	-343.60	19.42	1.66	1.63	1.82	7.5	12.43	12.25	13.62
43	65	Man	57	160	22.27	50.56	24.88	531.65	-342.04	21.10	1.50	1.48	1.71	11.7	17.57	17.37	19.97
44	75	Man	53	164	19.71	50.58	24.88	550.29	-347.32	21.38	1.50	1.48	1.69	11.8	17.71	17.52	19.93
45	59	Woman	43	145	20.45	46.47	22.70	461.10	-283.10	20.52	1.62	1.61	1.74	8.2	13.25	13.19	14.30
46	68	Man	58	170	20.07	52.9	25.88	557.04	-293.30	22.39	1.44	1.43	1.63	14.5	20.88	20.75	23.61
47	64	Woman	46	150	20.44	50.16	24.69	566.92	-258.21	23.14	1.51	1.50	1.58	13.1	19.81	19.59	20.75
48	62	Woman	70	160	27.34	56.31	26.50	671.68	-221.90	25.80	1.35	1.40	1.44	16.4	22.21	22.95	23.56
49	69	Woman	46	141	23.14	50.77	24.77	516.78	-279.40	21.78	1.50	1.49	1.67	11.5	17.20	17.14	19.15
50	62	Man	52	158	20.83	50.5	24.73	538.06	-371.99	20.74	1.50	1.49	1.73	11.7	17.59	17.47	20.24

No.	Age (Yr)	Gender	BW (kg)	HT (cm)	BMI (kg/m^2)	AP+ LAT (cm)	Effective diameter (cm)	A_{ROI} (cm^2)	CT number (HU)	Dw (cm)	f_{AP+LAT}	f_{EFF}	f_{Dw}	CTDIvol mGy	SSDE (AP+LAT) mGy	SSDE (EFF) mGy	SSDE (Dw) mGy
51	87	Woman	49	140	25.00	49.29	24.26	487.98	-129.80	23.25	1.54	1.52	1.58	10.3	15.82	15.65	16.25
52	66	Woman	54	150	24.00	51.6	25.30	534.50	-132.16	24.30	1.47	1.46	1.52	13.8	20.34	20.18	20.94
53	58	Woman	59	156	24.24	52.7	25.84	599.61	-255.43	23.84	1.44	1.43	1.54	14.8	21.38	21.22	22.85
54	78	Woman	69	155	28.72	60.72	29.84	701.77	-264.00	25.64	1.25	1.24	1.44	16.9	21.14	20.91	24.42
55	53	Woman	66	163	24.84	52.87	25.76	565.32	-265.82	22.99	1.44	1.44	1.59	13.1	18.87	18.83	20.87
56	60	Man	64.5	165	23.69	55.61	27.43	650.00	-288.27	24.27	1.37	1.35	1.52	15.4	21.12	20.82	23.40
57	69	Man	57	166	20.69	50.78	25.09	534.75	-340.89	21.18	1.50	1.47	1.70	11.0	16.45	16.21	18.72
58	54	Woman	46.7	149	21.04	48.6	23.73	505.42	-237.00	22.16	1.56	1.55	1.64	10.9	16.96	16.88	17.90
59	86	Woman	50	150	22.22	49.75	23.82	529.87	-223.60	22.89	1.52	1.54	1.60	13.3	20.27	20.53	21.26
60	50	Woman	60	175	19.59	49.83	24.31	516.71	-304.37	21.39	1.52	1.52	1.69	10.6	16.13	16.07	17.90
61	61	Man	70	168	24.80	55.06	27.11	636.27	-299.80	23.82	1.38	1.37	1.55	15.3	21.19	20.93	23.64
62	67	Woman	60	153	25.63	49.75	24.28	510.63	-318.40	21.05	1.52	1.52	1.71	12.1	18.44	18.37	20.69
63	53	Woman	52	157	21.10	50.15	24.18	541.31	-331.90	21.46	1.51	1.52	1.68	12.5	18.91	19.04	21.06
64	75	Woman	56	156	23.01	57.03	27.68	678.38	-236.10	25.69	1.34	1.34	1.44	15.9	21.25	21.30	22.94
65	71	Woman	56.8	145	27.02	53.32	25.94	578.70	-197.40	24.32	1.43	1.43	1.52	14.4	20.58	20.57	21.84
66	29	Man	50	170	17.30	50.97	24.59	493.26	-355.10	20.13	1.49	1.50	1.77	10.3	15.35	15.45	18.22
67	70	Woman	60	150	26.66	50.63	24.56	532.18	-144.10	24.08	1.50	1.50	1.53	14.1	21.15	21.18	21.57
68	56	Man	57	175	18.61	51.02	25.17	555.62	-331.63	21.74	1.49	1.47	1.67	11.8	17.57	17.34	19.67
69	63	Woman	60	158	24.03	57.19	27.57	653.55	-202.21	25.77	1.33	1.34	1.44	16.6	22.12	22.33	23.88
70	42	Woman	47	154	19.82	46.24	22.09	432.15	-317.13	19.38	1.62	1.64	1.82	9.5	15.42	15.62	17.27
71	74	Woman	56	160	21.88	50.08	24.32	537.95	-250.47	22.66	1.51	1.52	1.61	11.6	17.57	17.58	18.70
72	64	Man	59	171	20.18	51.19	25.13	544.18	-347.27	21.27	1.48	1.47	1.70	11.3	16.78	16.62	19.17
73	75	Woman	56	164	20.82	52.42	25.11	546.61	-285.30	22.30	1.45	1.47	1.63	12.8	18.59	18.84	20.91
74	52	Man	58	165	21.30	54.98	26.94	589.40	-306.67	22.81	1.39	1.38	1.60	13.7	19.00	18.86	21.96
75	56	Woman	67	168	23.74	60.08	28.91	695.46	-140.97	27.58	1.27	1.28	1.35	16.8	21.25	21.51	22.61

No.	Age (Yr)	Gender	BW (kg)	HT (cm)	BMI (kg/m^2)	AP+ LAT (cm)	Effective diameter (cm)	A_{ROI} (cm^2)	CT number (HU)	Dw (cm)	f_{AP+LAT}	f_{EFF}	f_{Dw}	CTDIvol mGy	SSDE (AP+LAT) mGy	SSDE (EFF) mGy	SSDE (Dw) mGy
76	60	Woman	66	165	24.24	58.18	28.22	710.08	-266.94	25.74	1.31	1.31	1.44	16.8	21.99	22.07	24.18
77	58	Woman	62	158	24.84	59.29	29.24	720.89	-246.10	26.31	1.28	1.27	1.41	16.3	20.92	20.63	22.98
78	69	Man	59	164	21.94	55.32	27.12	608.78	-272.79	23.74	1.38	1.37	1.55	15.4	21.23	21.06	23.86
79	54	Man	59	175	19.27	55.02	26.65	619.30	-361.17	22.44	1.39	1.39	1.62	11.7	16.21	16.28	19.01
80	26	Woman	55	170	19.03	48.44	23.50	550.39	-294.71	22.23	1.56	1.56	1.64	11.0	17.16	17.18	18.01
81	50	Man	61	165	22.41	56.63	27.72	612.75	-297.76	23.41	1.35	1.34	1.57	13.6	18.31	18.19	21.33
82	65	Woman	65	155	27.06	57.05	27.97	715.70	-129.34	28.17	1.34	1.33	1.32	18.3	24.45	24.26	24.10
83	55	Woman	48	162	18.29	48.02	23.76	476.02	-371.57	19.52	1.57	1.55	1.81	8.5	13.36	13.15	15.38
84	60	Man	63	173	21.05	53.44	26.48	583.77	-343.23	22.09	1.43	1.40	1.65	13.8	19.68	19.32	22.71
85	58	Man	53	160	20.70	49.62	23.90	513.08	-289.40	21.55	1.53	1.54	1.68	11.9	18.17	18.32	19.99
86	63	Woman	43	158	17.22	43.17	21.02	400.42	-343.27	18.30	1.72	1.71	1.89	7.6	13.04	13.00	14.38
87	61	Man	51	160	19.92	48.48	23.57	489.14	-285.42	21.10	1.56	1.56	1.71	11.0	17.15	17.14	18.78
88	56	Woman	45	160	17.58	45.56	22.02	424.28	-317.01	19.21	1.64	1.65	1.83	8.4	13.80	13.85	15.37
89	51	Man	63	160	24.61	52.13	25.36	569.87	-283.65	22.80	1.46	1.46	1.60	15.0	21.90	21.88	24.06
90	59	Woman	48	153	20.50	46.67	23.03	491.13	-271.80	21.34	1.61	1.59	1.69	10.5	16.91	16.69	17.77
91	37	Woman	43	156	17.67	41.85	20.50	387.30	-394.46	17.28	1.76	1.74	1.96	10.8	18.97	18.83	21.21
92	71	Man	51.3	165	18.84	52.75	25.70	534.38	-307.63	21.70	1.44	1.44	1.67	12.9	18.62	18.59	21.54
93	50	Man	68	176	21.95	55.35	26.88	599.78	-351.54	22.25	1.38	1.38	1.64	12.9	17.77	17.80	21.11
94	68	Man	70	160	27.34	57.09	28.15	681.94	-268.98	25.19	1.34	1.32	1.47	16.6	22.16	21.86	24.38
95	52	Woman	56	150	24.89	52.11	25.35	569.96	-264.61	23.10	1.46	1.46	1.59	14.6	21.32	21.31	23.16
96	70	Woman	60	155	24.97	54.02	26.39	609.38	-240.76	24.27	1.41	1.40	1.52	14.6	20.60	20.51	22.18
97	57	Man	55	170	19.03	53.72	25.80	559.43	-420.30	20.32	1.42	1.44	1.76	10.9	15.46	15.65	19.15
98	72	Woman	54	159	21.36	50.27	24.63	545.83	-294.89	22.14	1.51	1.50	1.64	13.0	19.62	19.48	21.36
99	19	Woman	43	163	16.18	41.52	20.18	374.96	-234.03	19.12	1.77	1.76	1.84	6.9	12.19	12.17	12.67
100	68	Woman	57	157	23.12	47.11	23.18	459.12	-293.42	20.32	1.60	1.58	1.76	10.4	16.62	16.44	18.27

No.	Age (Yr)	Gender	BW (kg)	HT (cm)	BMI (kg/m^2)	AP+ LAT (cm)	Effective diameter (cm)	A_{ROI} (cm^2)	CT number (HU)	Dw (cm)	f_{AP+LAT}	f_{EFF}	f_{Dw}	CTDIvol mGy	SSDE (AP+LAT) mGy	SSDE (EFF) mGy	SSDE (Dw) mGy
101	40	Man	65	165	23.88	51.77	25.14	527.72	-275.41	22.07	1.47	1.47	1.65	12.3	18.07	18.09	20.27
102	55	Woman	63	168	22.32	52.25	25.31	563.69	-303.57	22.36	1.46	1.46	1.63	12.9	18.79	18.85	21.03
103	88	Man	43	150	19.11	49.41	24.22	492.35	-270.49	21.39	1.53	1.52	1.69	10.6	16.25	16.12	17.91
104	77	Woman	42	140	21.43	46.27	22.76	410.53	-284.19	19.34	1.62	1.61	1.82	9.1	14.76	14.61	16.57
105	69	Man	57	160	22.27	50.66	24.65	534.64	-367.14	20.76	1.50	1.50	1.73	12.5	18.74	18.71	21.61
106	20	Man	62	160	24.22	53.12	26.02	546.47	-328.99	21.61	1.43	1.42	1.68	12.5	17.93	17.80	20.95
107	61	Man	62	170	21.45	52.54	25.49	585.07	-325.42	22.42	1.45	1.45	1.63	13.9	20.14	20.18	22.61
108	30	Woman	48.7	155	20.27	45.98	22.34	482.66	-312.81	20.55	1.63	1.63	1.74	9.6	15.65	15.65	16.72
109	60	Woman	54	153	23.07	53.92	26.54	584.76	-155.45	25.08	1.41	1.40	1.48	14.9	21.06	20.81	21.98
110	52	Man	52	167	18.65	52.12	25.67	544.51	-387.73	20.60	1.46	1.44	1.74	10.4	15.18	15.00	18.08
111	48	Woman	65	161	25.08	53.22	25.96	616.79	-290.30	23.61	1.43	1.43	1.56	14.2	20.33	20.27	22.11
112	56	Man	62.5	163	23.52	52.53	25.91	579.68	-263.09	23.32	1.45	1.43	1.57	15.3	22.17	21.88	24.07
113	32	Woman	50	158	20.03	47.53	23.26	453.28	-338.84	19.53	1.59	1.58	1.81	9.5	15.07	14.97	17.18
114	81	Man	67	170	23.18	56.24	27.68	649.24	-352.96	23.13	1.36	1.34	1.58	15.0	20.34	20.10	23.77
115	78	Man	46	142	22.81	47.47	23.15	460.86	-371.62	19.20	1.59	1.58	1.83	9.0	14.29	14.24	16.47
116	65	Woman	50	150	22.22	52.77	25.58	598.06	-235.50	24.13	1.44	1.45	1.53	14.9	21.50	21.56	22.76
117	74	Man	66	170	22.84	55.59	27.02	633.93	-306.45	23.66	1.37	1.37	1.55	15.0	20.58	20.59	23.31
118	63	Woman	46	150	20.44	50.61	24.56	538.17	-336.00	21.33	1.50	1.50	1.69	11.5	17.25	17.28	19.47
119	65	Man	53	172	17.92	49.77	24.15	478.91	-322.03	20.33	1.52	1.53	1.76	9.7	14.77	14.79	17.03
120	63	Man	63	164	23.42	54.3	26.66	608.23	-290.69	23.44	1.40	1.39	1.57	14.3	20.08	19.89	22.40
121	55	Woman	60	154	25.30	54.52	26.55	597.77	-255.20	23.81	1.40	1.40	1.55	15.4	21.53	21.50	23.80
122	76	Man	50	159	19.78	51.13	24.97	510.38	-285.18	21.55	1.49	1.48	1.68	11.3	16.80	16.72	18.97
123	93	Man	70	160	27.34	60.56	29.96	759.23	-270.92	26.55	1.25	1.23	1.40	19.2	24.08	23.66	26.83
124	75	Woman	48	153	20.50	51.38	24.92	524.32	-257.88	22.26	1.48	1.48	1.64	10.6	15.68	15.71	17.34
125	54	Man	46	160	17.97	49.22	24.16	500.75	-330.57	20.66	1.54	1.52	1.73	10.3	15.84	15.71	17.87

No.	Age (Yr)	Gender	BW (kg)	HT (cm)	BMI (kg/m^2)	AP+ LAT (cm)	Effective diameter (cm)	A_{ROI} (cm^2)	CT number (HU)	Dw (cm)	f_{AP+LAT}	f_{EFF}	f_{Dw}	CTDIvol mGy	SSDE (AP+LAT) mGy	SSDE (EFF) mGy	SSDE (Dw) mGy
126	55	Man	61	178	19.25	55.5	27.22	592.54	-372.28	21.76	1.37	1.36	1.67	14.6	20.06	19.90	24.33
127	63	Woman	52	160	20.31	53.76	26.23	599.67	-206.25	24.62	1.42	1.41	1.50	15.6	22.11	22.04	23.40
128	79	Woman	50	156	20.55	52.8	26.27	582.50	-301.60	22.76	1.44	1.41	1.61	12.9	18.61	18.20	20.72
129	85	Man	57	162	21.72	48.15	23.30	478.00	-364.70	19.66	1.57	1.57	1.80	10.0	15.68	15.74	18.00
130	58	Woman	51.7	157	20.97	50.06	24.49	529.56	-318.90	21.43	1.52	1.51	1.69	10.4	15.76	15.67	17.54
131	54	Man	64	170	22.15	54	26.60	610.58	-342.84	22.60	1.41	1.39	1.62	13.8	19.48	19.24	22.29
132	60	Woman	67	167	24.02	59.66	28.80	645.13	-244.30	24.91	1.27	1.29	1.48	16.0	20.40	20.57	23.74
133	79	Woman	45	152	19.48	48.61	23.85	489.24	-221.55	22.02	1.56	1.54	1.65	10.3	16.02	15.88	17.00
134	64	Woman	49	151	21.49	49.76	24.35	531.99	-270.62	22.23	1.52	1.51	1.64	10.9	16.61	16.50	17.85
135	45	Woman	60	156	24.65	51.5	25.06	571.45	-262.51	23.16	1.48	1.48	1.58	13.3	19.64	19.62	21.05
136	81	Woman	45	150	20.00	42.05	20.58	356.10	-320.82	17.55	1.75	1.74	1.94	6.0	10.50	10.43	11.67
137	75	Man	65.2	160	25.47	55.18	26.96	630.44	-343.39	22.96	1.38	1.38	1.59	14.7	20.31	20.22	23.44
138	38	Woman	65	160	25.39	63.14	30.63	808.34	-100.59	30.43	1.20	1.20	1.21	19.1	22.87	22.97	23.15
139	20	Man	60	170	20.76	44.25	21.49	379.74	-207.61	19.57	1.68	1.68	1.81	7.5	12.62	12.61	13.54
140	75	Woman	44.5	154	18.76	48.69	23.39	481.21	-312.40	20.53	1.55	1.57	1.74	11.3	17.55	17.72	19.70
141	58	Man	52	168	18.42	51.97	25.48	526.74	-264.22	22.21	1.46	1.45	1.64	12.4	18.15	18.01	20.32
142	61	Man	58	160	22.66	51.28	25.29	555.95	-296.23	22.32	1.48	1.46	1.63	13.3	19.71	19.45	21.71
143	77	Woman	50	156	20.55	50.99	25.33	561.10	-257.23	23.04	1.49	1.46	1.59	12.2	18.18	17.82	19.40
144	35	Woman	60	160	23.44	46.39	22.32	420.26	-222.20	20.40	1.62	1.63	1.75	9.6	15.54	15.66	16.81
145	51	Woman	52	155	21.64	49.83	24.33	524.20	-154.60	23.75	1.52	1.52	1.55	12.7	19.32	19.24	19.67
146	80	Man	65	165	23.88	47.4	23.26	478.01	-325.70	20.26	1.59	1.58	1.76	9.4	14.94	14.81	16.55
147	26	Man	50	160	19.53	45.07	22.11	423.06	-288.50	19.58	1.66	1.64	1.81	8.9	14.75	14.63	16.07
148	77	Man	70	165	25.71	55.08	26.75	586.65	-167.20	24.94	1.38	1.39	1.48	16.1	22.29	22.32	23.87
149	73	Man	48	162	18.29	52.71	25.71	555.11	-325.39	21.84	1.44	1.44	1.66	11.6	16.76	16.70	19.27
150	54	Man	64	170	22.15	53.76	26.45	617.28	-350.45	22.59	1.42	1.40	1.62	13.8	19.56	19.34	22.30

No.	Age (Yr)	Gender	BW (kg)	HT (cm)	BMI (kg/m²)	AP+ LAT (cm)	Effective diameter (cm)	A_{ROI} (cm²)	CT number (HU)	Dw (cm)	f_{AP+LAT}	f_{EFF}	f_{Dw}	CTDIvol mGy	SSDE (AP+LAT) mGy	SSDE (EFF) mGy	SSDE (Dw) mGy
151	63	Man	70	163	26.35	57.71	28.10	669.65	-271.52	24.92	1.32	1.32	1.48	16.7	22.05	22.03	24.78
152	30	Man	50	168	17.72	48.79	23.92	482.97	-144.54	22.94	1.55	1.54	1.60	12.2	18.91	18.76	19.47
153	68	Woman	54	150	24.00	49.23	23.93	520.70	-291.59	21.67	1.54	1.54	1.67	11.9	18.30	18.30	19.89
154	93	Man	40	155	16.65	46.37	22.31	411.94	-351.92	18.44	1.62	1.63	1.88	8.7	14.09	14.20	16.38
155	72	Woman	57	152	24.67	52.61	25.41	580.82	-285.17	22.99	1.45	1.46	1.59	12.7	18.38	18.49	20.23
156	90	Man	65	170	22.49	50.86	24.66	526.87	-341.00	21.03	1.49	1.50	1.71	11.8	17.62	17.66	20.20
157	70	Man	60	162	22.86	56.35	27.01	614.13	-284.48	23.65	1.35	1.37	1.55	14.8	20.02	20.32	23.00
158	75	Woman	48	160	18.75	54.04	26.11	598.86	-250.00	23.91	1.41	1.42	1.54	12.8	18.05	18.17	19.71
159	59	Man	60	170	20.76	49.91	24.63	505.79	-371.50	20.12	1.52	1.50	1.77	11.3	17.17	16.93	20.00
160	72	Woman	52	149	23.42	50.31	24.90	556.08	-218.69	23.52	1.51	1.48	1.56	13.7	20.67	20.33	21.40
161	61	Man	50	162	19.05	51.46	24.98	499.54	-346.78	20.38	1.48	1.48	1.75	10.3	15.22	15.24	18.05
162	28	Woman	50	158	20.03	48.97	23.14	511.36	-260.30	21.95	1.55	1.58	1.65	10.5	16.23	16.62	17.38
163	76	Man	64	160	25.00	56.45	27.59	627.18	-331.56	23.10	1.35	1.34	1.59	15.3	20.66	20.56	24.27
164	64	Man	60	160	23.44	52.59	25.57	558.78	-250.09	23.10	1.45	1.45	1.59	14.3	20.70	20.70	22.68
165	56	Woman	52	160	20.31	52.09	25.44	555.18	-345.40	21.51	1.46	1.45	1.68	11.1	16.22	16.15	18.67
166	50	Woman	61	157	24.75	54.75	26.23	572.48	-225.20	23.76	1.39	1.41	1.55	14.7	20.47	20.77	22.76
167	51	Man	52	175	16.98	50.09	24.20	484.11	-339.03	20.18	1.51	1.52	1.77	9.4	14.24	14.31	16.60
168	58	Man	65	160	25.39	52.88	25.50	554.13	-278.70	22.56	1.44	1.45	1.62	13.6	19.59	19.74	22.01
169	59	Woman	62	159	24.52	52.07	25.30	601.69	-194.91	24.84	1.46	1.46	1.49	15.8	23.09	23.10	23.52
170	47	Woman	54	155	22.48	51.39	25.00	550.19	-286.30	22.36	1.48	1.48	1.63	12.0	17.75	17.74	19.56
171	56	Man	45	168	15.94	49.17	23.89	498.26	-422.53	19.14	1.54	1.54	1.83	9.1	14.01	14.01	16.69
172	68	Man	50	161	19.29	52.2	24.89	560.63	-340.06	21.70	1.46	1.48	1.67	12.0	17.50	17.81	20.04
173	66	Man	55	178	17.36	49.2	24.18	531.64	-403.28	20.10	1.54	1.52	1.77	12.2	18.77	18.59	21.61
174	58	Woman	50	158	20.03	47.87	23.66	482.91	-107.36	23.43	1.58	1.55	1.57	11.5	18.13	17.85	18.02
175	71	Woman	50.4	158	20.19	49.75	24.15	510.26	-319.50	21.03	1.52	1.53	1.71	10.3	15.69	15.71	17.63

No.	Age (Yr)	Gender	BW (kg)	HT (cm)	BMI (kg/m^2)	AP+ LAT (cm)	Effective diameter (cm)	A_{ROI} (cm^2)	CT number (HU)	Dw (cm)	f_{AP+LAT}	f_{EFF}	f_{Dw}	CTDIvol mGy	SSDE (AP+LAT) mGy	SSDE (EFF) mGy	SSDE (Dw) mGy
176	56	Woman	40	160	15.63	44.95	21.69	397.05	-332.76	18.37	1.66	1.67	1.89	7.5	12.46	12.52	14.16
177	53	Man	67	169	23.46	55.19	26.78	625.93	-304.62	23.54	1.38	1.38	1.56	14.9	20.59	20.63	23.26
178	72	Man	53	167	19.00	51.59	24.91	516.04	-364.99	20.43	1.47	1.48	1.75	10.8	15.92	16.02	18.90
179	57	Woman	45	145	21.40	52.68	25.79	561.83	-224.46	23.55	1.45	1.44	1.56	13.7	19.80	19.67	21.37
180	55	Man	55	170	19.03	48.25	23.11	472.25	-327.48	20.11	1.57	1.58	1.77	10.0	15.65	15.84	17.70
181	55	Woman	56	159	22.15	49.69	24.44	502.62	-305.80	21.08	1.53	1.51	1.71	11.2	17.08	16.90	19.14
182	56	Man	58	175	18.94	50.88	25.16	548.83	-340.34	21.47	1.49	1.47	1.68	11.7	17.47	17.19	19.70
183	29	Woman	45	158	18.03	44.39	21.60	406.87	-318.93	18.78	1.68	1.67	1.86	8.3	13.93	13.90	15.43
184	42	Man	62	168	21.97	53.81	26.05	564.29	-272.07	22.87	1.42	1.42	1.60	13.4	18.98	19.06	21.44
185	65	Man	69	168	24.45	58.36	28.07	691.04	-242.42	25.82	1.30	1.32	1.44	18.0	23.49	23.77	25.84
186	46	Woman	50	158	20.03	49.71	24.26	527.83	-279.19	22.01	1.52	1.52	1.65	10.7	16.32	16.25	17.67
187	75	Man	56	160	21.88	50	24.53	524.04	-334.49	21.07	1.52	1.50	1.71	11.5	17.44	17.29	19.65
188	60	Woman	47	157	19.07	49.48	23.72	459.34	-331.12	19.78	1.53	1.55	1.79	8.9	13.63	13.79	15.95
189	74	Woman	45	145	21.40	46.98	22.72	443.49	-309.50	19.75	1.60	1.61	1.79	8.1	12.97	13.02	14.53
190	35	Woman	57	160	22.27	49.37	24.09	525.95	-345.22	20.94	1.53	1.53	1.72	10.4	15.96	15.90	17.86
191	35	Woman	48	165	17.63	47.21	22.68	487.52	-263.09	21.39	1.59	1.61	1.69	10.6	16.91	17.06	17.91
192	53	Man	50	167	17.93	52.18	25.51	585.33	-319.12	22.53	1.46	1.45	1.62	14.7	21.44	21.33	23.81
193	61	Woman	57.8	150	25.69	48.6	23.39	477.26	-189.89	22.19	1.56	1.57	1.64	12.2	18.98	19.13	20.01
194	65	Man	70	167	25.10	56.01	27.57	636.31	-236.83	24.87	1.36	1.35	1.49	16.2	22.05	21.79	24.08
195	65	Man	54	155	22.48	52.17	25.44	568.19	-205.83	23.97	1.46	1.45	1.54	13.3	19.40	19.35	20.43
196	67	Woman	53	150	23.56	51.96	25.45	560.16	-283.62	22.60	1.46	1.45	1.62	13.6	19.91	19.77	21.97
197	64	Woman	42	153	17.94	47.4	23.56	465.01	-278.46	20.67	1.59	1.56	1.73	9.8	15.58	15.27	17.00
198	81	Man	55	170	19.03	51.05	25.16	534.91	-370.90	20.70	1.49	1.47	1.73	11.5	17.12	16.90	19.92
199	45	Woman	44.5	152	19.26	45.25	21.98	428.81	-315.06	19.34	1.65	1.65	1.82	7.7	12.72	12.72	14.02
200	31	Woman	50	158	20.03	50.06	23.90	510.48	-305.43	21.25	1.52	1.54	1.70	9.9	15.00	15.24	16.81

No.	Age (Yr)	Gender	BW (kg)	HT (cm)	BMI (kg/m^2)	AP+ LAT (cm)	Effective diameter (cm)	A_{ROI} (cm^2)	CT number (HU)	Dw (cm)	f_{AP+LAT}	f_{EFF}	f_{Dw}	CTDIvol mGy	SSDE (AP+LAT) mGy	SSDE (EFF) mGy	SSDE (Dw) mGy
201	77	Woman	61	165	22.41	60.11	28.87	706.35	-255.08	25.88	1.26	1.28	1.43	16.4	20.74	21.03	23.49
202	46	Man	53	158	21.23	50.49	24.78	511.05	-286.56	21.55	1.50	1.49	1.68	11.6	17.44	17.29	19.48
203	67	Man	53	160	20.70	49.16	24.03	508.05	-366.81	20.24	1.54	1.53	1.76	11.1	17.09	17.01	19.56
204	57	man	53	163	19.95	51.9	25.16	526.48	-197.56	23.19	1.47	1.47	1.58	12.2	17.88	17.93	19.29
205	63	Man	57	153	24.35	52.55	25.36	561.55	-267.82	22.88	1.45	1.46	1.60	16.0	23.18	23.34	25.59
206	68	Man	44	167	15.78	47.02	22.66	415.49	-381.74	18.09	1.60	1.61	1.91	8.0	12.80	12.89	15.26
207	73	Man	69	163	25.97	57.09	28.06	705.77	-353.48	24.10	1.34	1.32	1.53	16.4	21.90	21.67	25.07
208	60	Woman	52	152	22.51	50.53	24.64	558.04	-218.80	23.56	1.50	1.50	1.56	13.6	20.43	20.37	21.21
209	69	man	52	167	18.65	49.16	24.33	513.17	-356.05	20.51	1.54	1.51	1.74	9.6	14.78	14.54	16.75
210	68	Man	59	168	20.90	54.28	26.44	538.91	-250.93	22.67	1.40	1.40	1.61	13.5	18.96	18.93	21.75
211	24	Man	59	163	22.21	52.97	25.49	537.38	-315.86	21.64	1.44	1.45	1.67	12.5	17.97	18.15	20.92
212	32	Woman	50	158	20.03	47.1	23.02	458.54	-341.31	19.61	1.60	1.59	1.80	9.5	15.18	15.10	17.13
213	51	Man	68	169	23.81	57.53	28.16	664.63	-270.61	24.84	1.32	1.32	1.49	16.1	21.33	21.19	23.95
214	58	Woman	48	160	18.75	48.25	23.40	458.86	-222.59	21.31	1.57	1.57	1.69	9.7	15.18	15.21	16.43
215	69	man	57	155	23.73	51.17	25.03	528.37	-298.89	21.72	1.49	1.48	1.67	12.6	18.71	18.60	21.03
216	65	Man	62.5	156	25.68	53.05	26.00	549.28	-235.97	23.12	1.44	1.42	1.59	14.4	20.68	20.52	22.83
217	37	Woman	47	157	19.07	47.82	23.39	474.12	-207.90	21.87	1.58	1.57	1.66	12.2	19.25	19.13	20.25
218	51	Woman	44	152	19.04	45.83	22.62	429.04	-288.77	19.71	1.64	1.61	1.80	7.8	12.75	12.58	14.01
219	65	Man	54	165	19.83	48.39	23.37	487.10	-299.72	20.84	1.56	1.57	1.72	11.8	18.43	18.52	20.34
220	45	man	54	160	21.09	53.04	25.53	537.79	-368.13	20.80	1.44	1.45	1.73	10.9	15.65	15.80	18.81
221	70	Man	62	164	23.05	53.84	26.43	579.17	-290.99	22.87	1.42	1.40	1.60	13.7	19.39	19.21	21.92
222	33	Woman	49	158	19.63	45.73	22.40	438.51	-213.11	20.96	1.64	1.63	1.72	8.5	13.92	13.82	14.59
223	64	man	61	165	22.41	54.35	26.52	596.31	-239.22	24.03	1.40	1.40	1.53	14.2	19.92	19.85	21.77
224	70	Man	57	163	21.45	51.85	25.66	570.89	-321.56	22.21	1.47	1.44	1.64	12.6	18.49	18.18	20.65
225	66	Man	51	158	20.43	49.11	24.19	525.32	-303.17	21.59	1.54	1.52	1.68	12.2	18.80	18.58	20.46

No.	Age (Yr)	Gender	BW (kg)	HT (cm)	BMI (kg/m^2)	AP+ LAT (cm)	Effective diameter (cm)	A_{ROI} (cm^2)	CT number (HU)	Dw (cm)	f_{AP+LAT}	f_{EFF}	f_{Dw}	CTDIvol mGy	SSDE (AP+LAT) mGy	SSDE (EFF) mGy	SSDE (Dw) mGy
226	77	Woman	45	155	18.73	48.54	23.47	451.11	-183.17	21.66	1.56	1.56	1.67	12.5	19.47	19.55	20.90
227	18	Woman	50	158	20.03	48.32	23.49	492.19	-286.16	21.15	1.56	1.56	1.70	10.0	15.63	15.62	17.04
228	32	Man	70	175	22.86	58.42	28.17	671.63	-292.31	24.60	1.30	1.32	1.50	16.0	20.86	21.06	24.02
229	62	Woman	43	157	17.44	44.23	21.65	432.41	-328.52	19.23	1.68	1.67	1.83	7.5	12.62	12.54	13.71
230	53	Woman	45.9	155	19.11	49.9	24.38	509.58	-155.60	23.41	1.52	1.51	1.57	12.5	19.00	18.90	19.61

Table A 3 Patient data and radiation dose determined from middle slice of scan range

No.	Age (Yr)	Gender	BW (kg)	HT (cm)	BMI (kg/m^2)	AP+ LAT (cm)	Effective diameter (cm)	A_{ROI} (cm^2)	CT number (HU)	Dw (cm)	f_{AP+LAT}	f_{EFF}	f_{Dw}	CTDIvol mGy	SSDE (AP+LAT) mGy	SSDE (EFF) mGy	SSDE (Dw) mGy
1	55	Male	60	165	22.04	51.28	25.06	555.15	-354.72	21.36	1.48	1.48	1.69	11.7	17.34	17.26	19.79
2	33	Female	53	160	20.70	47.09	23.10	474.56	-300.89	20.55	1.60	1.59	1.74	9.4	15.03	14.90	16.37
3	73	Man	45	167	16.14	49.18	24.02	481.04	-344.04	20.04	1.54	1.53	1.77	9.9	15.24	15.17	17.57
4	69	Woman	54	159	21.36	51.51	25.45	588.34	-280.44	23.22	1.48	1.45	1.58	12.0	17.71	17.45	18.95
5	62	Man	65	173	21.72	54.55	27.07	614.64	-385.96	21.92	1.40	1.37	1.66	12.8	17.89	17.54	21.20
6	47	Man	66	171	22.57	54.77	26.60	576.26	-315.99	22.40	1.39	1.39	1.63	13.1	18.24	18.26	21.32
7	41	Man	67	173	22.39	52.74	25.95	570.87	-314.57	22.32	1.44	1.43	1.63	13.3	19.20	18.98	21.71
8	64	Woman	54	145	25.68	53.77	26.08	589.18	-281.93	23.21	1.42	1.42	1.58	13.6	19.28	19.32	21.49
9	57	Man	52	160	20.31	50.70	24.34	509.76	-227.80	22.39	1.50	1.51	1.63	11.7	17.53	17.72	19.05
10	75	Woman	51	150	22.67	51.54	25.15	516.43	-272.20	21.88	1.48	1.47	1.66	10.7	15.79	15.73	17.75
11	55	Woman	56	156	23.01	47.52	23.35	466.40	-307.05	20.29	1.59	1.57	1.76	10.1	16.02	15.86	17.77
12	65	Man	64	167	22.95	55.41	27.14	611.07	-345.21	22.57	1.38	1.37	1.62	14.4	19.82	19.68	23.29
13	79	Man	65	161	25.08	56.73	28.07	643.75	-258.15	24.66	1.34	1.32	1.50	15.9	21.37	21.00	23.82
14	76	Woman	40	147	18.51	47.02	22.91	436.75	-241.17	20.54	1.60	1.60	1.74	8.0	12.80	12.77	13.94
15	24	Man	58	170	20.07	50.29	23.43	473.48	-245.98	21.32	1.51	1.57	1.69	10.4	15.69	16.29	17.61
16	75	Man	63	165	23.14	57.75	28.44	698.43	-305.71	24.85	1.32	1.30	1.49	16.2	21.37	21.10	24.10
17	77	Man	47	160	18.36	49.10	24.05	486.51	-328.28	20.40	1.54	1.53	1.75	10.4	16.03	15.92	18.22
18	71	Man	65	160	25.39	53.89	26.50	589.86	-172.21	24.93	1.41	1.40	1.48	15.6	22.06	21.82	23.13
19	63	Man	70	163	26.35	57.96	28.23	664.51	-259.60	25.03	1.31	1.31	1.48	16.7	21.95	21.93	24.68
20	57	Man	60	160	23.44	53.72	25.95	598.41	-195.80	24.75	1.42	1.43	1.49	15.9	22.56	22.70	23.74
21	68	Woman	54	150	24.00	48.65	23.79	516.90	-270.03	21.92	1.55	1.55	1.66	11.9	18.49	18.39	19.71
22	79	Woman	42	146	19.70	48.01	23.40	449.09	-247.60	20.74	1.57	1.57	1.73	11.0	17.29	17.24	19.03
23	31	Man	63	186	18.21	50.69	24.17	518.82	-220.30	22.70	1.50	1.52	1.61	12.5	18.73	19.05	20.13
24	93	Man	40	155	16.65	44.74	21.63	413.53	-346.04	18.56	1.67	1.67	1.87	8.7	14.51	14.56	16.31
25	72	Woman	57	152	24.67	53.55	25.95	576.03	-271.38	23.12	1.42	1.43	1.59	12.7	18.07	18.13	20.13

No.	Age (Yr)	Gender	BW (kg)	HT (cm)	BMI (kg/m^2)	AP+ LAT (cm)	Effective diameter (cm)	A_{ROI} (cm^2)	CT number (HU)	Dw (cm)	f_{AP+LAT}	f_{EFF}	f_{Dw}	CTDIvol mGy	SSDE (AP+LAT) mGy	SSDE (EFF) mGy	SSDE (Dw) mGy
26	81	Man	68	173	22.72	50.68	24.98	535.49	-248.03	22.64	1.50	1.48	1.61	13.1	19.63	19.38	21.13
27	62	Man	67	180	20.68	50.61	25.01	550.39	-248.96	22.94	1.50	1.48	1.60	15.4	23.10	22.76	24.57
28	55	Woman	48	148	21.91	51.55	25.02	553.90	-224.90	23.38	1.48	1.48	1.57	13.4	19.77	19.79	21.04
29	60	Man	68	171	23.26	57.41	27.61	616.97	-255.10	24.19	1.33	1.34	1.52	15.2	20.18	20.42	23.16
30	54	Man	50	166	18.14	50.81	24.74	519.91	-355.17	20.66	1.49	1.49	1.73	10.4	15.55	15.52	18.04
31	74	Man	60.2	170	20.83	51.16	25.09	587.20	-274.80	23.29	1.49	1.47	1.58	14.8	21.99	21.80	23.32
32	84	Woman	57	140	29.08	56.70	27.91	589.80	-177.80	24.85	1.34	1.33	1.49	14.2	19.09	18.87	21.12
33	65	Woman	62	152	26.84	52.02	25.68	566.48	-225.30	23.64	1.46	1.44	1.56	14.6	21.36	21.05	22.71
34	62	Woman	54	158	21.63	48.58	24.05	533.97	-225.80	22.94	1.56	1.53	1.60	12.1	18.83	18.52	19.30
35	67	Woman	52	158	20.83	53.73	26.30	599.84	-246.70	23.99	1.42	1.41	1.54	13.0	18.44	18.32	19.96
36	61	Woman	51	165	18.73	48.34	23.46	504.57	-313.50	21.00	1.56	1.56	1.71	10.0	15.63	15.64	17.13
37	84	Woman	51	156	20.96	55.06	27.04	596.12	-179.10	24.96	1.38	1.37	1.48	14.9	20.63	20.44	22.07
38	69	Woman	50	150	22.22	57.95	27.81	649.10	-227.30	25.27	1.31	1.33	1.46	16.0	21.03	21.33	23.44
39	61	Woman	48	153	20.50	49.83	24.49	490.51	-234.30	21.87	1.52	1.51	1.66	10.9	16.58	16.42	18.09
40	62	Woman	62	155	25.81	52.10	25.61	550.71	-243.99	23.02	1.46	1.45	1.59	14.6	21.32	21.10	23.22
41	69	Man	49	162	18.67	46.65	22.67	455.08	-313.06	19.95	1.61	1.61	1.78	10.3	16.59	16.59	18.34
42	49	Woman	43	152	18.61	44.75	22.17	451.52	-296.00	20.12	1.67	1.64	1.77	7.5	12.50	12.30	13.27
43	65	Man	57	160	22.27	50.87	25.07	534.15	-344.07	21.12	1.49	1.47	1.71	11.7	17.47	17.25	19.96
44	75	Man	53	164	19.71	51.48	25.29	536.25	-327.71	21.43	1.48	1.46	1.69	11.8	17.43	17.26	19.91
45	59	Woman	43	145	20.45	47.10	23.04	464.15	-272.20	20.74	1.60	1.59	1.73	8.2	13.10	13.03	14.19
46	68	Man	58	170	20.07	53.01	26.05	580.56	-253.01	23.50	1.44	1.42	1.56	14.5	20.83	20.63	22.67
47	64	Woman	46	150	20.44	50.42	24.77	565.61	-264.09	23.02	1.51	1.49	1.59	13.1	19.72	19.53	20.84
48	62	Woman	70	160	27.34	56.12	26.25	665.96	-221.00	25.70	1.36	1.41	1.44	16.4	22.28	23.15	23.64
49	69	Woman	46	141	23.14	50.01	24.54	501.27	-262.80	21.69	1.52	1.50	1.67	11.5	17.44	17.29	19.21
50	62	Man	52	158	20.83	50.42	24.70	535.04	-358.71	20.90	1.51	1.49	1.72	11.7	17.61	17.49	20.12

No.	Age (Yr)	Gender	BW (kg)	HT (cm)	BMI (kg/m^2)	AP+ LAT (cm)	Effective diameter (cm)	A_{ROI} (cm^2)	CT number (HU)	Dw (cm)	f_{AP+LAT}	f_{EFF}	f_{Dw}	CTDIvol mGy	SSDE (AP+LAT) mGy	SSDE (EFF) mGy	SSDE (Dw) mGy
51	87	Woman	49	140	25.00	49.47	24.34	487.35	-119.48	23.37	1.53	1.51	1.57	10.3	15.77	15.60	16.17
52	66	Woman	54	150	24.00	50.73	25.01	537.16	-102.59	24.77	1.50	1.48	1.49	13.8	20.66	20.39	20.58
53	58	Woman	59	156	24.24	52.56	25.80	588.81	-246.86	23.76	1.45	1.44	1.55	14.8	21.44	21.25	22.91
54	78	Woman	69	155	28.72	60.72	29.84	701.77	-264.00	25.64	1.25	1.24	1.44	16.9	21.14	20.91	24.42
55	53	Woman	66	163	24.84	52.21	25.49	547.22	-255.52	22.78	1.46	1.45	1.61	13.1	19.10	19.02	21.03
56	60	Man	64.5	165	23.69	56.07	27.62	644.74	-288.58	24.17	1.36	1.34	1.53	15.4	20.94	20.67	23.49
57	69	Man	57	166	20.69	51.45	25.30	533.89	-334.35	21.27	1.48	1.46	1.70	11.0	16.26	16.08	18.66
58	54	Woman	46.7	149	21.04	48.35	23.71	503.39	-201.70	22.62	1.56	1.55	1.61	10.9	17.03	16.89	17.60
59	86	Woman	50	150	22.22	50.16	24.09	532.52	-223.09	22.95	1.51	1.53	1.59	13.3	20.12	20.33	21.21
60	50	Woman	60	175	19.59	48.67	23.85	511.18	-310.05	21.19	1.55	1.54	1.70	10.6	16.47	16.35	18.04
61	61	Man	70	168	24.80	56.16	27.61	637.37	-307.00	23.72	1.36	1.34	1.55	15.3	20.77	20.55	23.73
62	67	Woman	60	153	25.63	50.03	24.50	513.35	-306.20	21.30	1.52	1.51	1.69	12.1	18.34	18.22	20.51
63	53	Woman	52	157	21.10	49.52	24.02	533.93	-307.40	21.70	1.53	1.53	1.67	12.5	19.13	19.15	20.87
64	75	Woman	56	156	23.01	57.11	27.80	668.26	-225.50	25.67	1.33	1.33	1.44	15.9	21.22	21.21	22.95
65	71	Woman	56.8	145	27.02	52.99	25.78	578.11	-208.10	24.14	1.44	1.44	1.53	14.4	20.70	20.69	21.98
66	29	Man	50	170	17.30	51.04	24.71	488.06	-362.60	19.90	1.49	1.49	1.78	10.3	15.33	15.39	18.37
67	70	Woman	60	150	26.66	50.40	24.67	534.37	-134.40	24.27	1.51	1.50	1.52	14.1	21.23	21.09	21.43
68	56	Man	57	175	18.61	51.02	25.24	543.51	-341.67	21.34	1.49	1.47	1.69	11.8	17.57	17.29	19.96
69	63	Woman	60	158	24.03	56.53	27.58	667.90	-177.75	26.44	1.35	1.34	1.40	16.6	22.39	22.33	23.29
70	42	Woman	47	154	19.82	45.01	21.69	430.23	-279.77	19.86	1.66	1.67	1.79	9.5	15.76	15.86	16.97
71	74	Woman	56	160	21.88	49.63	24.35	538.28	-228.24	23.00	1.53	1.51	1.59	11.6	17.71	17.56	18.47
72	64	Man	59	171	20.18	51.61	25.39	546.26	-339.48	21.43	1.47	1.46	1.69	11.3	16.65	16.47	19.06
73	75	Woman	56	164	20.82	52.77	25.48	553.84	-262.19	22.81	1.44	1.45	1.60	12.8	18.47	18.59	20.52
74	52	Man	58	165	21.30	54.36	26.74	592.41	-297.71	23.02	1.40	1.39	1.59	13.7	19.21	19.00	21.80
75	56	Woman	67	168	23.74	59.75	28.88	686.14	-121.11	27.71	1.27	1.28	1.34	16.8	21.38	21.54	22.50

No.	Age (Yr)	Gender	BW (kg)	HT (cm)	BMI (kg/m^2)	AP+ LAT (cm)	Effective diameter (cm)	A_{ROI} (cm^2)	CT number (HU)	Dw (cm)	f_{AP+LAT}	f_{EFF}	f_{Dw}	CTDIvol mGy	SSDE (AP+LAT) mGy	SSDE (EFF) mGy	SSDE (Dw) mGy
76	60	Woman	66	165	24.24	57.84	28.29	708.14	-261.75	25.80	1.32	1.31	1.44	16.8	22.13	22.01	24.13
77	58	Woman	62	158	24.84	59.10	29.21	709.44	-246.73	26.09	1.29	1.27	1.42	16.3	20.99	20.65	23.17
78	69	Man	59	164	21.94	55.23	27.32	616.95	-225.82	24.66	1.38	1.36	1.50	15.4	21.26	20.91	23.07
79	54	Man	59	175	19.27	54.96	26.59	607.79	-352.03	22.39	1.39	1.39	1.63	11.7	16.23	16.31	19.05
80	26	Woman	55	170	19.03	47.76	23.29	530.37	-297.37	21.78	1.58	1.57	1.66	11.0	17.37	17.32	18.31
81	50	Man	61	165	22.41	55.41	27.43	606.25	-276.49	23.63	1.38	1.35	1.56	13.6	18.72	18.39	21.16
82	65	Woman	65	155	27.06	56.13	27.47	702.20	-123.87	27.99	1.36	1.35	1.33	18.3	24.86	24.70	24.26
83	55	Woman	48	162	18.29	47.61	23.61	466.08	-358.55	19.51	1.58	1.56	1.81	8.5	13.46	13.22	15.38
84	60	Man	63	173	21.05	53.01	26.28	576.86	-329.15	22.20	1.44	1.41	1.64	13.8	19.83	19.46	22.63
85	58	Man	53	160	20.70	49.15	23.74	506.82	-290.76	21.39	1.54	1.55	1.69	11.9	18.33	18.42	20.10
86	63	Woman	43	158	17.22	43.64	21.24	398.61	-340.89	18.29	1.70	1.70	1.89	7.6	12.93	12.90	14.38
87	61	Man	51	160	19.92	47.80	23.26	487.21	-285.59	21.05	1.58	1.58	1.71	11.0	17.36	17.33	18.81
88	56	Woman	45	160	17.58	45.65	22.08	426.74	-288.69	19.66	1.64	1.65	1.80	8.4	13.78	13.82	15.12
89	51	Man	63	160	24.61	52.25	25.53	577.89	-283.46	22.96	1.46	1.45	1.59	15.0	21.85	21.75	23.92
90	59	Woman	48	153	20.50	47.16	23.33	494.49	-261.99	21.56	1.60	1.57	1.68	10.5	16.76	16.50	17.63
91	37	Woman	43	156	17.67	42.67	20.94	401.35	-316.17	18.69	1.73	1.72	1.86	10.8	18.69	18.53	20.14
92	71	Man	51.3	165	18.84	52.08	25.60	542.19	-300.11	21.98	1.46	1.45	1.65	12.9	18.85	18.65	21.32
93	50	Man	68	176	21.95	53.59	26.12	572.71	-304.14	22.53	1.42	1.42	1.62	12.9	18.34	18.30	20.90
94	68	Man	70	160	27.34	56.93	28.12	672.26	-266.17	25.06	1.34	1.32	1.48	16.6	22.23	21.88	24.50
95	52	Woman	56	150	24.89	51.70	25.30	564.81	-249.53	23.23	1.47	1.46	1.58	14.6	21.48	21.34	23.05
96	70	Woman	60	155	24.97	53.74	26.32	603.57	-227.25	24.37	1.42	1.41	1.51	14.6	20.70	20.56	22.10
97	57	Man	55	170	19.03	52.70	25.44	552.05	-410.98	20.35	1.44	1.45	1.75	10.9	15.75	15.86	19.13
98	72	Woman	54	159	21.36	50.02	24.59	547.46	-297.35	22.13	1.52	1.50	1.64	13.0	19.71	19.51	21.37
99	19	Woman	43	163	16.18	41.43	20.30	360.52	-183.26	19.36	1.77	1.76	1.82	6.9	12.21	12.12	12.56
100	68	Woman	57	157	23.12	47.21	23.38	473.03	-275.56	20.89	1.59	1.57	1.72	10.4	16.59	16.32	17.89

No.	Age (Yr)	Gender	BW (kg)	HT (cm)	BMI (kg/m^2)	AP+ LAT (cm)	Effective diameter (cm)	A_{ROI} (cm^2)	CT number (HU)	Dw (cm)	f_{AP+LAT}	f_{EFF}	f_{Dw}	CTDIvol mGy	SSDE (AP+LAT) mGy	SSDE (EFF) mGy	SSDE (Dw) mGy
101	40	Man	65	165	23.88	51.64	24.97	526.61	-296.07	21.73	1.47	1.48	1.67	12.3	18.11	18.20	20.52
102	55	Woman	63	168	22.32	52.61	25.49	562.42	-310.63	22.22	1.45	1.45	1.64	12.9	18.67	18.73	21.14
103	88	Man	43	150	19.11	46.78	23.01	472.81	-251.78	21.22	1.61	1.59	1.70	10.6	17.04	16.86	18.01
104	77	Woman	42	140	21.43	44.61	21.79	391.42	-231.61	19.57	1.67	1.66	1.81	9.1	15.21	15.13	16.43
105	69	Man	57	160	22.27	50.29	24.63	526.34	-331.08	21.17	1.51	1.50	1.70	12.5	18.86	18.73	21.28
106	20	Man	62	160	24.22	52.87	25.90	545.10	-323.71	21.67	1.44	1.43	1.67	12.5	18.01	17.88	20.90
107	61	Man	62	170	21.45	52.84	25.69	581.30	-322.44	22.39	1.44	1.44	1.63	13.9	20.03	20.03	22.63
108	30	Woman	48.7	155	20.27	46.68	22.68	482.77	-313.96	20.54	1.61	1.61	1.74	9.6	15.46	15.45	16.73
109	60	Woman	54	153	23.07	52.84	26.07	581.89	-158.22	24.97	1.44	1.42	1.48	14.9	21.48	21.18	22.06
110	52	Man	52	167	18.65	51.42	25.33	532.55	-389.61	20.34	1.48	1.46	1.76	10.4	15.38	15.19	18.25
111	48	Woman	65	161	25.08	52.91	26.01	603.57	-280.28	23.52	1.44	1.42	1.56	14.2	20.44	20.22	22.18
112	56	Man	62.5	163	23.52	52.17	25.84	570.88	-256.42	23.25	1.46	1.43	1.58	15.3	22.32	21.93	24.14
113	32	Woman	50	158	20.03	47.03	23.06	453.87	-337.32	19.57	1.60	1.59	1.81	9.5	15.20	15.08	17.16
114	81	Man	67	170	23.18	55.00	27.27	650.13	-339.41	23.38	1.39	1.36	1.57	15.0	20.79	20.40	23.55
115	78	Man	46	142	22.81	47.69	23.31	459.84	-365.73	19.27	1.58	1.57	1.83	9.0	14.23	14.15	16.43
116	65	Woman	50	150	22.22	52.86	25.72	595.21	-237.60	24.04	1.44	1.44	1.53	14.9	21.47	21.45	22.84
117	74	Man	66	170	22.84	56.07	27.43	624.64	-299.63	23.60	1.36	1.35	1.56	15.0	20.40	20.28	23.36
118	63	Woman	46	150	20.44	49.99	24.47	528.60	-330.90	21.22	1.52	1.51	1.70	11.5	17.45	17.33	19.54
119	65	Man	53	172	17.92	48.78	23.91	476.64	-326.44	20.22	1.55	1.54	1.76	9.7	15.04	14.92	17.10
120	63	Man	63	164	23.42	53.91	26.47	604.12	-288.12	23.40	1.41	1.40	1.57	14.3	20.22	20.03	22.43
121	55	Woman	60	154	25.30	53.03	25.94	583.66	-223.50	24.02	1.44	1.43	1.53	15.4	22.12	21.99	23.62
122	76	Man	50	159	19.78	50.57	24.78	514.23	-344.21	20.72	1.50	1.49	1.73	11.3	16.97	16.84	19.56
123	93	Man	70	160	27.34	60.28	29.95	748.85	-277.51	26.25	1.26	1.23	1.41	19.2	24.20	23.67	27.13
124	75	Woman	48	153	20.50	50.54	24.69	517.50	-214.13	22.76	1.50	1.50	1.61	10.6	15.92	15.85	17.03
125	54	Man	46	160	17.97	49.12	24.15	505.45	-321.59	20.90	1.54	1.53	1.72	10.3	15.87	15.71	17.72

No.	Age (Yr)	Gender	BW (kg)	HT (cm)	BMI (kg/m^2)	AP+ LAT (cm)	Effective diameter (cm)	A_{ROI} (cm^2)	CT number (HU)	Dw (cm)	f_{AP+LAT}	f_{EFF}	f_{Dw}	CTDIvol mGy	SSDE (AP+LAT) mGy	SSDE (EFF) mGy	SSDE (Dw) mGy
126	55	Man	61	178	19.25	55.64	27.19	602.26	-359.69	22.16	1.37	1.36	1.64	14.6	20.01	19.91	23.97
127	63	Woman	52	160	20.31	53.90	26.28	602.02	-203.43	24.71	1.41	1.41	1.50	15.6	22.06	22.00	23.32
128	79	Woman	50	156	20.55	52.79	26.29	580.66	-279.30	23.08	1.44	1.41	1.59	12.9	18.61	18.19	20.48
129	85	Man	57	162	21.72	47.11	23.05	481.04	-343.45	20.05	1.60	1.59	1.77	10.0	15.98	15.88	17.74
130	58	Woman	51.7	157	20.97	49.67	24.47	528.35	-296.70	21.75	1.53	1.51	1.67	10.4	15.87	15.67	17.33
131	54	Man	64	170	22.15	53.25	26.25	607.85	-339.11	22.62	1.43	1.41	1.61	13.8	19.74	19.49	22.28
132	60	Woman	67	167	24.02	57.64	28.02	660.72	-231.50	25.43	1.32	1.32	1.46	16.0	21.15	21.17	23.30
133	79	Woman	45	152	19.48	48.24	23.74	486.30	-194.84	22.33	1.57	1.55	1.63	10.3	16.13	15.95	16.81
134	64	Woman	49	151	21.49	49.90	24.43	519.03	-277.42	21.85	1.52	1.51	1.66	10.9	16.56	16.45	18.10
135	45	Woman	60	156	24.65	51.31	25.05	566.07	-261.42	23.07	1.48	1.48	1.59	13.3	19.70	19.63	21.12
136	81	Woman	45	150	20.00	40.30	19.87	352.53	-250.25	18.35	1.81	1.78	1.89	6.0	10.84	10.71	11.33
137	75	Man	65.2	160	25.47	55.33	27.11	628.84	-347.44	22.86	1.38	1.37	1.60	14.7	20.26	20.11	23.53
138	38	Woman	65	160	25.39	63.11	30.72	798.70	-108.10	30.12	1.20	1.20	1.23	19.1	22.88	22.89	23.42
139	20	Man	60	170	20.76	43.63	21.28	382.94	-218.97	19.51	1.70	1.69	1.81	7.5	12.76	12.71	13.57
140	75	Woman	44.5	154	18.76	47.96	23.33	471.76	-331.38	20.04	1.57	1.57	1.77	11.3	17.78	17.76	20.06
141	58	Man	52	168	18.42	49.57	24.48	528.86	-241.82	22.60	1.53	1.51	1.62	12.4	18.96	18.68	20.04
142	61	Man	58	160	22.66	51.69	25.46	552.16	-301.69	22.16	1.47	1.45	1.64	13.3	19.57	19.33	21.84
143	77	Woman	50	156	20.55	51.07	25.37	558.25	-237.58	23.28	1.49	1.46	1.58	12.2	18.15	17.79	19.23
144	35	Woman	60	160	23.44	45.69	22.01	416.62	-206.20	20.52	1.64	1.65	1.74	9.6	15.74	15.84	16.74
145	51	Woman	52	155	21.64	49.91	24.43	526.58	-155.50	23.80	1.52	1.51	1.55	12.7	19.30	19.17	19.64
146	80	Man	65	165	23.88	47.17	23.11	478.72	-326.30	20.26	1.60	1.58	1.76	9.4	15.00	14.89	16.55
147	26	Man	50	160	19.53	44.59	21.96	425.60	-273.10	19.85	1.67	1.65	1.79	8.9	14.88	14.71	15.91
148	77	Man	70	165	25.71	54.07	26.50	588.44	-160.50	25.08	1.41	1.40	1.48	16.1	22.70	22.52	23.75
149	73	Man	48	162	18.29	52.71	25.75	553.33	-327.21	21.77	1.44	1.44	1.67	11.6	16.76	16.68	19.32
150	54	Man	64	170	22.15	53.69	26.46	616.25	-346.41	22.65	1.42	1.40	1.61	13.8	19.59	19.33	22.26

No.	Age (Yr)	Gender	BW (kg)	HT (cm)	BMI (kg/m^2)	AP+ LAT (cm)	Effective diameter (cm)	A_{ROI} (cm^2)	CT number (HU)	Dw (cm)	f_{AP+LAT}	f_{EFF}	f_{Dw}	CTDIvol mGy	SSDE (AP+LAT) mGy	SSDE (EFF) mGy	SSDE (Dw) mGy
151	63	Man	70	163	26.35	57.88	28.21	674.91	-261.52	25.19	1.32	1.31	1.47	16.7	21.98	21.95	24.53
152	30	Man	50	168	17.72	49.42	24.30	488.35	-139.76	23.13	1.53	1.52	1.58	12.2	18.70	18.50	19.33
153	68	Woman	54	150	24.00	48.94	23.90	512.53	-270.34	21.82	1.55	1.54	1.66	11.9	18.40	18.32	19.78
154	93	Man	40	155	16.65	45.89	22.03	418.86	-345.25	18.69	1.63	1.65	1.87	8.7	14.21	14.34	16.23
155	72	Woman	57	152	24.67	52.86	25.56	569.80	-272.24	22.98	1.44	1.45	1.59	12.7	18.30	18.39	20.24
156	90	Man	65	170	22.49	51.01	24.80	527.44	-345.90	20.96	1.49	1.49	1.72	11.8	17.58	17.57	20.25
157	70	Man	60	162	22.86	54.35	26.44	598.62	-273.17	23.54	1.40	1.40	1.56	14.8	20.76	20.75	23.10
158	75	Woman	48	160	18.75	55.39	26.80	598.76	-225.40	24.30	1.38	1.38	1.52	12.8	17.62	17.71	19.43
159	59	Man	60	170	20.76	49.74	24.61	509.08	-360.22	20.36	1.52	1.50	1.75	11.3	17.22	16.95	19.82
160	72	Woman	52	149	23.42	50.56	25.07	562.35	-216.20	23.69	1.50	1.47	1.55	13.7	20.57	20.20	21.27
161	61	Man	50	162	19.05	51.51	24.97	494.87	-357.49	20.12	1.48	1.48	1.77	10.3	15.20	15.24	18.23
162	28	Woman	50	158	20.03	46.08	22.15	488.25	-231.40	21.86	1.63	1.64	1.66	10.5	17.09	17.23	17.43
163	76	Man	64	160	25.00	56.47	27.72	631.94	-309.20	23.58	1.35	1.34	1.56	15.3	20.66	20.47	23.85
164	64	Man	60	160	23.44	51.93	25.36	555.03	-256.48	22.92	1.47	1.46	1.60	14.3	20.95	20.86	22.83
165	56	Woman	52	160	20.31	51.55	25.41	552.72	-317.90	21.91	1.48	1.46	1.66	11.1	16.37	16.16	18.39
166	50	Woman	61	157	24.75	54.05	25.96	572.57	-207.80	24.03	1.41	1.43	1.53	14.7	20.73	20.97	22.53
167	51	Man	52	175	16.98	47.94	23.22	471.77	-354.13	19.70	1.57	1.58	1.80	9.4	14.80	14.83	16.90
168	58	Man	65	160	25.39	52.87	25.68	554.74	-288.90	22.41	1.44	1.44	1.63	13.6	19.59	19.61	22.13
169	59	Woman	62	159	24.52	52.27	25.58	583.83	-100.02	25.87	1.46	1.45	1.43	15.8	23.01	22.86	22.64
170	47	Woman	54	155	22.48	50.22	24.57	530.07	-257.50	22.39	1.51	1.50	1.63	12.0	18.13	18.02	19.54
171	56	Man	45	168	15.94	49.58	24.11	503.56	-410.30	19.44	1.53	1.53	1.81	9.1	13.91	13.90	16.51
172	68	Man	50	161	19.29	52.26	25.16	565.84	-355.23	21.55	1.46	1.47	1.68	12.0	17.48	17.64	20.15
173	66	Man	55	178	17.36	50.27	24.74	541.01	-387.69	20.54	1.51	1.49	1.74	12.2	18.42	18.20	21.26
174	58	Woman	50	158	20.03	47.68	23.69	496.11	-113.28	23.67	1.58	1.55	1.55	11.5	18.19	17.83	17.87
175	71	Woman	50.4	158	20.19	47.56	23.31	489.90	-265.40	21.41	1.58	1.57	1.69	10.3	16.33	16.20	17.39

No.	Age (Yr)	Gender	BW (kg)	HT (cm)	BMI (kg/m^2)	AP+ LAT (cm)	Effective diameter (cm)	A_{ROI} (cm^2)	CT number (HU)	Dw (cm)	f_{AP+LAT}	f_{EFF}	f_{Dw}	CTDIvol mGy	SSDE (AP+LAT) mGy	SSDE (EFF) mGy	SSDE (Dw) mGy
176	56	Woman	40	160	15.63	44.36	21.47	399.13	-280.91	19.12	1.68	1.68	1.84	7.5	12.59	12.62	13.77
177	53	Man	67	169	23.46	54.10	26.40	609.60	-217.06	24.65	1.41	1.40	1.50	14.9	20.99	20.92	22.33
178	72	Man	53	167	19.00	50.43	24.53	514.41	-369.63	20.32	1.51	1.50	1.76	10.8	16.26	16.24	18.97
179	57	Woman	45	145	21.40	51.54	25.44	547.42	-216.19	23.37	1.48	1.45	1.57	13.7	20.21	19.93	21.51
180	55	Man	55	170	19.03	47.17	22.75	469.38	-297.79	20.49	1.60	1.61	1.75	10.0	15.96	16.05	17.46
181	55	Woman	56	159	22.15	49.10	24.21	494.52	-288.97	21.16	1.54	1.52	1.70	11.2	17.27	17.05	19.08
182	56	Man	58	175	18.94	50.72	25.11	536.82	-337.77	21.28	1.50	1.47	1.70	11.7	17.52	17.23	19.85
183	29	Woman	45	158	18.03	43.95	21.46	403.10	-302.80	18.92	1.69	1.68	1.85	8.3	14.04	13.97	15.35
184	42	Man	62	168	21.97	53.03	25.86	547.93	-258.69	22.74	1.44	1.43	1.61	13.4	19.25	19.19	21.54
185	65	Man	69	168	24.45	58.02	28.02	688.68	-235.05	25.90	1.31	1.32	1.43	18.0	23.63	23.82	25.76
186	46	Woman	50	158	20.03	49.94	24.50	524.82	-269.99	22.09	1.52	1.51	1.65	10.7	16.25	16.11	17.62
187	75	Man	56	160	21.88	49.74	24.44	519.50	-326.49	21.11	1.52	1.51	1.71	11.5	17.53	17.35	19.63
188	60	Woman	47	157	19.07	47.87	23.34	453.57	-308.37	19.99	1.58	1.57	1.78	8.9	14.03	13.98	15.83
189	74	Woman	45	145	21.40	47.22	22.83	448.07	-320.92	19.68	1.59	1.60	1.80	8.1	12.92	12.96	14.57
190	35	Woman	57	160	22.27	49.02	24.02	489.73	-347.31	20.17	1.54	1.53	1.77	10.4	16.06	15.94	18.37
191	35	Woman	48	165	17.63	46.24	22.36	470.24	-249.79	21.19	1.62	1.63	1.70	10.6	17.20	17.26	18.03
192	53	Man	50	167	17.93	52.49	25.69	585.86	-306.85	22.74	1.45	1.44	1.61	14.7	21.32	21.19	23.63
193	61	Woman	57.8	150	25.69	48.30	23.45	484.77	-160.90	22.76	1.56	1.56	1.61	12.2	19.08	19.09	19.60
194	65	Man	70	167	25.10	56.35	27.81	637.39	-218.93	25.18	1.35	1.33	1.47	16.2	21.92	21.60	23.81
195	65	Man	54	155	22.48	52.17	25.51	565.17	-214.79	23.77	1.46	1.45	1.55	13.3	19.40	19.30	20.58
196	67	Woman	53	150	23.56	51.80	25.46	561.85	-271.19	22.83	1.47	1.45	1.60	13.6	19.97	19.77	21.79
197	64	Woman	42	153	17.94	47.18	23.46	461.76	-254.33	20.94	1.60	1.56	1.72	9.8	15.64	15.33	16.83
198	81	Man	55	170	19.03	51.27	25.32	538.78	-368.30	20.82	1.48	1.46	1.72	11.5	17.05	16.80	19.84
199	45	Woman	44.5	152	19.26	45.14	22.02	413.32	-318.27	18.94	1.66	1.65	1.85	7.7	12.75	12.70	14.23
200	31	Woman	50	158	20.03	48.47	23.39	488.94	-307.53	20.76	1.56	1.57	1.73	9.9	15.44	15.52	17.11

No.	Age (Yr)	Gender	BW (kg)	HT (cm)	BMI (kg/m^2)	AP+ LAT (cm)	Effective diameter (cm)	A_{ROI} (cm^2)	CT number (HU)	Dw (cm)	f_{AP+LAT}	f_{EFF}	f_{Dw}	CTDIvol mGy	SSDE (AP+LAT) mGy	SSDE (EFF) mGy	SSDE (Dw) mGy
201	77	Woman	61	165	22.41	60.19	28.93	708.15	-238.01	26.21	1.26	1.28	1.41	16.4	20.71	20.99	23.21
202	46	Man	53	158	21.23	50.19	24.60	514.12	-297.83	21.44	1.51	1.50	1.69	11.6	17.54	17.40	19.56
203	67	Man	53	160	20.70	49.49	24.33	512.61	-383.14	20.07	1.53	1.52	1.77	11.1	16.99	16.82	19.68
204	57	man	53	163	19.95	52.21	25.39	526.84	-197.07	23.21	1.46	1.46	1.58	12.2	17.78	17.78	19.28
205	63	Man	57	153	24.35	52.91	25.67	568.08	-265.43	23.05	1.44	1.44	1.59	16.0	23.03	23.08	25.43
206	68	Man	44	167	15.78	46.46	22.44	420.27	-378.82	18.23	1.62	1.62	1.90	8.0	12.93	12.99	15.17
207	73	Man	69	163	25.97	57.37	28.22	401.36	-355.75	18.14	1.33	1.31	1.90	16.4	21.79	21.54	31.21
208	60	Woman	52	152	22.51	50.22	24.65	539.07	-225.60	23.06	1.51	1.50	1.59	13.6	20.55	20.37	21.61
209	69	man	52	167	18.65	48.81	24.18	510.17	-354.62	20.48	1.55	1.52	1.75	9.6	14.88	14.62	16.77
210	68	Man	59	168	20.90	50.73	24.94	543.54	-260.31	22.63	1.50	1.48	1.61	13.5	20.21	20.00	21.79
211	24	Man	59	163	22.21	52.24	25.12	528.59	-308.15	21.58	1.46	1.47	1.68	12.5	18.21	18.40	20.97
212	32	Woman	50	158	20.03	46.55	22.86	463.49	-338.72	19.75	1.61	1.60	1.79	9.5	15.33	15.19	17.04
213	51	Man	68	169	23.81	56.53	27.80	655.10	-275.09	24.59	1.35	1.33	1.50	16.1	21.71	21.47	24.18
214	58	Woman	48	160	18.75	48.26	23.39	459.71	-234.53	21.17	1.57	1.57	1.70	9.7	15.18	15.21	16.52
215	69	man	57	155	23.73	50.89	25.02	521.62	-300.28	21.56	1.49	1.48	1.68	12.6	18.81	18.61	21.15
216	65	Man	62.5	156	25.68	51.95	25.62	542.51	-190.57	23.65	1.46	1.45	1.55	14.4	21.09	20.81	22.39
217	37	Woman	47	157	19.07	48.00	23.54	462.14	-200.49	21.69	1.57	1.56	1.67	12.2	19.18	19.03	20.38
218	51	Woman	44	152	19.04	45.68	22.54	421.73	-280.98	19.65	1.64	1.62	1.80	7.8	12.79	12.62	14.04
219	65	Man	54	165	19.83	48.88	23.66	486.80	-300.09	20.83	1.55	1.55	1.72	11.8	18.26	18.32	20.35
220	45	man	54	160	21.09	52.79	25.13	527.18	-355.62	20.80	1.44	1.47	1.73	10.9	15.72	16.04	18.82
221	70	Man	62	164	23.05	53.29	26.17	580.39	-295.55	22.82	1.43	1.42	1.60	13.7	19.59	19.40	21.96
222	33	Woman	49	158	19.63	45.84	22.40	443.06	-217.30	21.01	1.63	1.63	1.71	8.5	13.90	13.82	14.56
223	64	man	61	165	22.41	54.75	26.73	596.51	-237.83	24.06	1.39	1.39	1.53	14.2	19.77	19.70	21.74
224	70	Man	57	163	21.45	51.50	25.49	566.71	-322.36	22.11	1.48	1.45	1.64	12.6	18.60	18.29	20.72
225	66	Man	51	158	20.43	49.15	24.18	525.63	-305.21	21.56	1.54	1.52	1.68	12.2	18.79	18.58	20.48

No.	Age (Yr)	Gender	BW (kg)	HT (cm)	BMI (kg/m^2)	AP+ LAT (cm)	Effective diameter (cm)	A_{ROI} (cm^2)	CT number (HU)	Dw (cm)	f_{AP+LAT}	f_{EFF}	f_{Dw}	CTDIvol mGy	SSDE (AP+LAT) mGy	SSDE (EFF) mGy	SSDE (Dw) mGy
226	77	Woman	45	155	18.73	38.17	19.08	460.95	-132.82	22.56	1.88	1.84	1.62	12.5	23.46	22.96	20.23
227	18	Woman	50	158	20.03	47.42	23.16	492.60	-277.42	21.29	1.59	1.58	1.70	10.0	15.89	15.81	16.95
228	32	Man	70	175	22.86	58.67	28.36	670.28	-285.80	24.69	1.30	1.31	1.50	16.0	20.76	20.91	23.94
229	62	Woman	43	157	17.44	44.78	21.95	425.34	-303.85	19.42	1.67	1.65	1.82	7.5	12.50	12.40	13.62
230	53	Woman	45.9	155	19.11	49.98	24.44	509.73	-144.90	23.56	1.52	1.51	1.56	12.5	18.97	18.86	19.50

Appendix B: Quality Control of Multi-Detector Computed Tomography System

Location	**:** Bhumi Siri Building (2nd floor) King Chulalongkorn Memorial Hospital
Date	**:** 1 June 2016
Manufacturer	**:** Toshiba Aquilion ONE; 11/2011
M/N and S/N	**:** m/n TSX-3014 s/n LCC10Y2249

Pass	Scan Localization Light Accuracy
Pass	Alignment of Table to Gantry
Pass	Table Increments Accuracy
Pass	Gantry Tilt
Pass	C.T.# Position Dependence and S/N
Pass	Reproducibility of C.T. Numbers
Pass	mAs Linearity
Pass	Linearity of C.T. Numbers
Pass	High Contrast Resolution
Pass	Low Contrast Resolution
Pass	Slice Thickness Accuracy
Pass	Image Uniformity
Pass	Accuracy of distance measurement
Pass	CTDI Measurement

1. General and mechanical tests

1.1. Scan localization light accuracy

Purpose: To test congruency of scan localization light and scan plane.

Method:

1.Place the tape measurement vertically along the midline the couch aligned with the longitudinal axis.

2. Set external light align with the reference point on the tape measurement.

3. Set table position to zero. Move table by monitor scanner, the table position move from external to internal localization light. Measure and record deviation position.

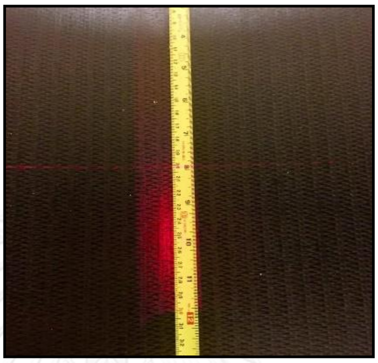

Figure B 1 Localization light accuracy setting on the tape measurement.

Results:

Table B 1 Scan Localization Light Accuracy

Measured Deviation	External	0 mm
	Internal	0 mm

Tolerance: The center of the irradiation field from internal laser should be less than 2 mm.

Comment: **Pass**

1.2. Alignment of table to gantry

Purpose: To ensure that long axis of the table is horizontally aligned with a vertical line passing through the rotational axis of the scanner**.**

Method:

1**.** Locate the table midline using a ruler and mark it on a tape affixed to the table. With the gantry untitled, extend the table top into gantry to tape position.

2. Measure the horizontal deviation between the gantry aperture center and the table midline.

Results:

Table B 2 Alignment of table to gantry

	Table	Bore
Distance from Right to Centre (mm)	237	359
Distance from Centre to Left (mm)	235	361
Measured Deviation	1	1

Measured deviation: (Distance from right to center – Distance from center to left)/2

Tolerance: The Deviation should be within 5 mm
Comment: **Pass**

1.3. Table increment accuracy
Purpose: To determine accuracy and reproducibility of table longitudinal motion
Method:
1. Tape a measuring tape at the foot end of the table.
2. Place a paper clip at the center of the tape to function as an indicator.
3. Load the table uniformly with 150 lbs. From the initial position move the table 300, 400 and 500 mm into the gantry under software control (+ ve).
4. Record the relative displacement of the pointer on the ruler. Reverse the direction of motion (-ve) and repeat.
5. Repeat the measurements four times.

Results:

Table B 3 Table increment accuracy

Indicated	Measured	Deviation
300	300	0
400	400	0
500	500	0
-300	300	0
-400	400.5	0.5
-500	500	0

Deviation = | Indicated – Measured|
Tolerance: Positional errors should be less than 3 mm.
Comment: Pass

1.4. Gantry angle tilt
Purpose: To determine the limit of gantry tilt and the accuracy of tilt angle indicator
Method:
1. Raise the table to the head position and move the table into the gantry.
2. Tilt the gantry towards and away from the table. Measure the clearance from the close point of gantry to midline of table.

Results:

Table B 4 Gantry Angle Tilt

	Away	**Towards**
Clearance	32	30.5

Tolerance: Gantry clearance should be ≥30cm
Comment: Pass

1.5. Position dependence and S/N ratio of C.T. numbers
Method:
1. Position the C.T. head phantom centered in the gantry.
2. Using 1 cm slice thickness obtain one scan using typical head technique.
3. Select a circular region of interest of approximately 400 sq. mm.
4. Record the mean C.T. number and standard deviation for each of the positions 1 through 5.

Technique: 120 kV, 300 mA, 1 second, 250 mm. FOV

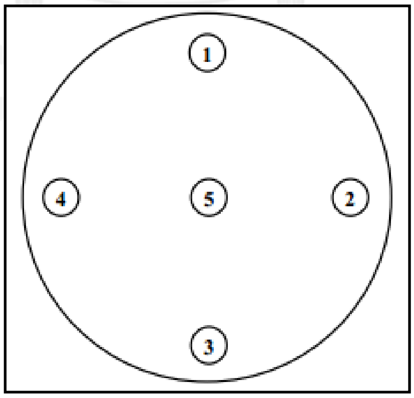

Figure B 2 Draw region of interest for each of the positions 1 through 5.

Results:

Table B 5 Position dependence and S/N ratio of C.T. numbers

Position	Mean C.T.	S.D.	C.V.
1	121.7	13	-
2	121.9	7.9	0.065
3	121.5	7.4	0.061
4	121.6	7.8	0.064
5	118.1	8.6	0.073

***CV = Standard deviation/mean CT number**

Tolerance: The coefficient of variation of mean CT numbers of the four scans should be less than 0.2.

Comment: Pass

1.6. Reproducibility of C.T. numbers

Method:

1. Using the same set up and technique as position dependence, obtain three scans.
2. Using the same ROI as position dependence in location 5, which is the center of the phantom, obtain mean C.T. numbers for each of the four scans

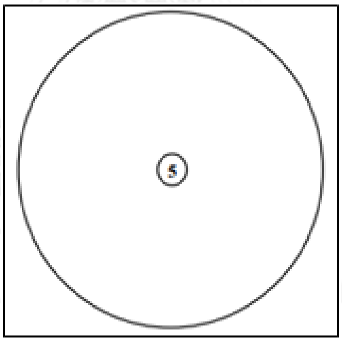

Figure B 3 Draw region of interest of the positions 5.

Results:

Table B 6 Reproducibility of C.T. numbers

Run Number	**1**	**2**	**3**	**4**
Mean C.T	118.1	118.1	118.0	118.4
Mean Global C.T Number	118.15			
Standard Deviation	0.173			
Coefficient of variation	0.001			

Tolerance: The coefficient of variation of mean C.T. numbers of the four scans should be less than 0.002

Comment: Pass

2. Electrical test

2.1. mAs linearity

Method:

1. Set up the same as position dependence and insert 10 cm long pencil chamber in the center slot of the C.T. dose head phantom.
2. Select the same kVp and time as used for head scan. Obtain four scans in each of the mA stations normally used in the clinic. For each mA station record the exposure in mGy for each scan. Scans should be performed in the increasing order of mA. Compute mGy/mAs for each mA setting.

Technique: 120 kV, 300 mA, 1 second, 250 mm. FOV, slice collimation 8 mm

Table B 7 mAs linearity

mA	Exposure in mGy				mGy/mAs	C.V.
	Run 1	Run 2	Run 3	Run 4		
50	1.648	1.642	1.649	1.644	0.03	-
100	3.282	3.292	3.290	3.286	0.03	0.0006
200	6.568	6.556	6.555	6.565	0.03	0.0011
250	8.211	8.206	8.204	8.195	0.03	0.0002
300	11.41	11.39	11.40	11.40	0.04	0.0732
400	15.21	15.20	15.20	15.21	0.04	0.0002
500	19.02	19.00	19.00	19.01	0.04	0.0000

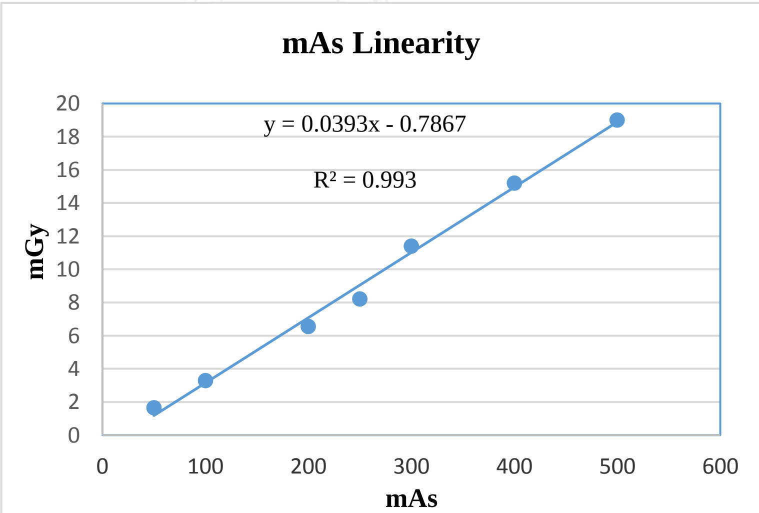

Figure B 4 The relationship of mGy and mAs.

Comment: Pass

1.7. Linearity of C.T. numbers

Method:

1. Set up the CATPHAN performance phantom as described in beam alignment.
2. Select the section containing the test objects of different C.T. numbers.

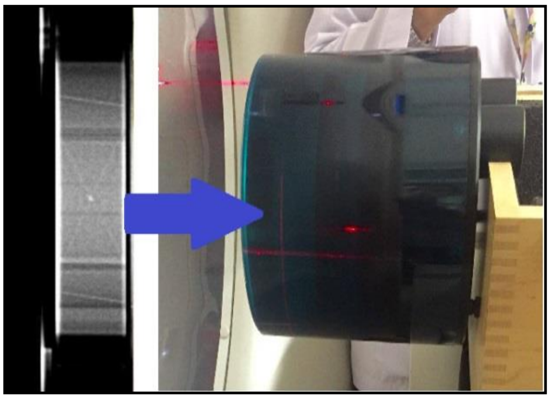

Figure B 5 Catphan phantom setting and reference line of CTP 404 section.

3. Select the head technique and perform a single transverse scan.
4. Select a region of interest (ROI) of sufficient size to cover the test objects.
5. Place the ROI in the middle of each test object and record the mean C.T. number.

Technique: 120kVp, 300 mA, 1sec, 300mm FOV, slice collimation 8 mm

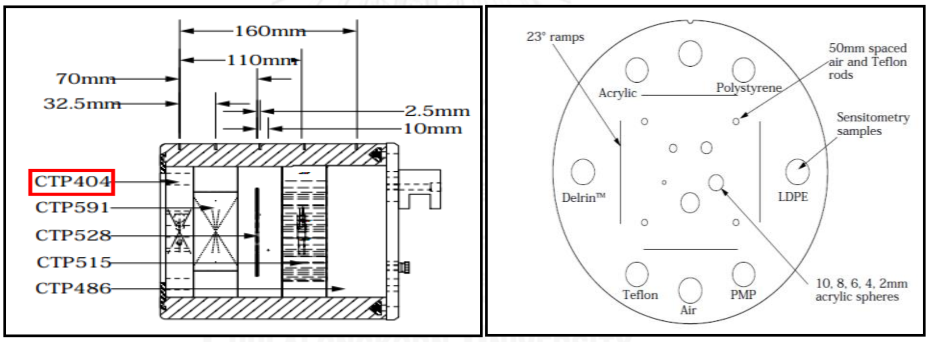

Figure B 6 The section containing the test objects of different CT numbers**.**

Results:

Material	Expected CT Number #	Measured CT Number #
Acrylic	120	115.4
Polystyrene	-35	-46.7
LDPE	-100	-103.3
PMP	-200	-188.6
Delrin	340	350.0
Teflon	990	1032.0
Air (inferior)	-1000	-1007.8
Air (superior)	-1000	-1007.8

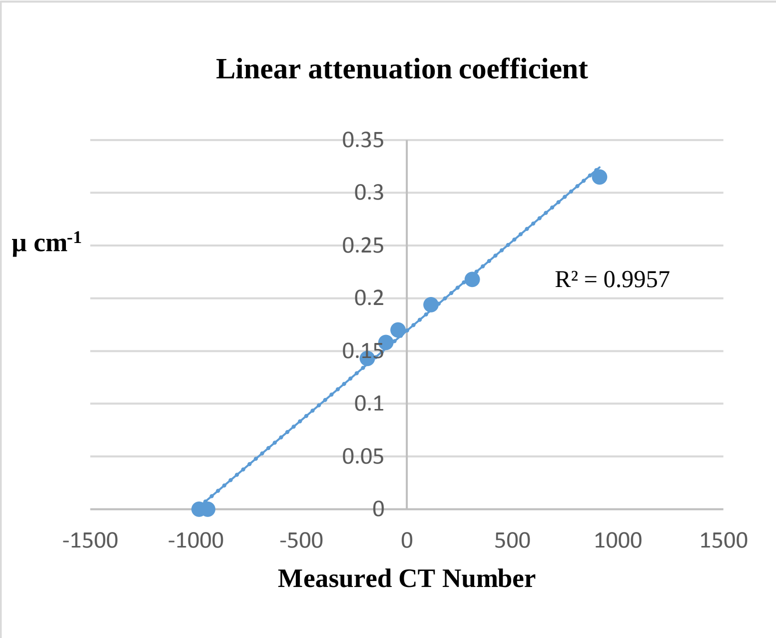

Figure B 7 Linearity of CT number.

Tolerance: R-square between measured CT number and linear attenuation coefficient (µ) more than 0.9
Comment: Pass

1.8. Slice thickness accuracy

Purpose: To Determine the accuracy of the slice thickness.
Method:
1. Set up the catphan phantom as described in beam alignment set up as you would for beam profile measurement.
2. Select the section containing the accuracy of the slice thickness test objects (CTP404 slice width Module)

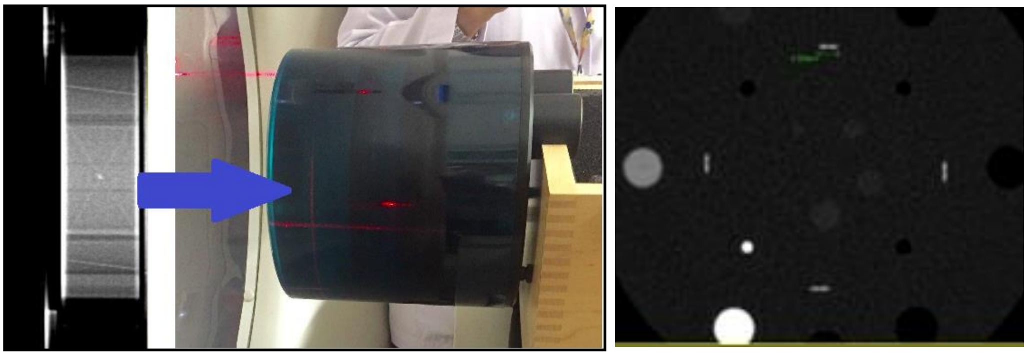

Figure B 8 Catphan phantom setting and reference line of CTP 404 section.

3. Select the head technique, 120 kVp, 300 mAs, smallest slit width.
4. Perform several scans with different programmed slice thicknesses under auto control.
5. Perform scan following catphan manual in each slice collimation.
6. Calculate the real slice thickness.

Result:

Table B 8 Slice thickness accuracy

Slice Thickness (mm)	1	4	8
Peak	577.20	195.67	157.75
BG	101.42	95.53	97.09
Net peak(NP)	475.78	100.14	60.66
50% NP	237.89	50.07	30.33
HM(50%NP+BG)	339.31	145.60	127.42
FWHM L1	2.55	9.82	19.71
FWHM L2	2.78	10.28	19.33
FWHM L3	2.65	9.79	19.50
FWHM L4	2.68	9.93	19.70
Average FWHM	2.665	9.955	19.56
SL=Avg FWHM x 0.42	1.119	4.181	8.215
%Diff (set vs calculate)	0.119	0.181	0.215

Slice Thick in mm	Measured Thick in mm	Deviation (mm)	Slice Thick in mm
1	1.119	0.119	**1**
4	4.181	0.181	**4**
8	8.215	0.215	**8**

Tolerance: Deviation should be < 1mm
Comment: Pass

3. Image quality test

3.1. High contrast resolution
Method:

1. Set up the Catphan phantom in beam alignment.
2. Select the section containing the high resolution test object. (CTP528 21 line pair high resolution Module).

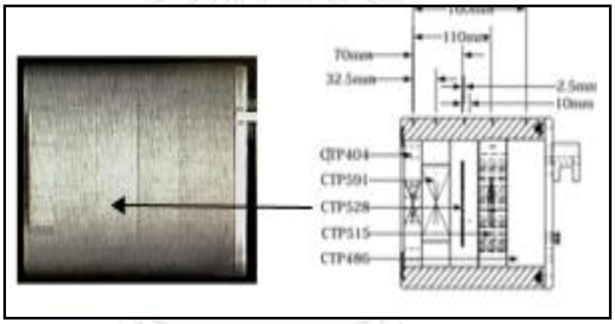

Figure B 9 Catphan phantom setting and reference line of CTP 528 section.

3. Select the head technique and perform a single transverse scan.
4. Select the area containing the high resolution test objects.
5. Select appropriate window and level for the best visualization of the test objects.

Technique: kVp: 120 mA: 300Seconds: 1.0 FOV: 300 mm Slice Thickness :4,8,12mm

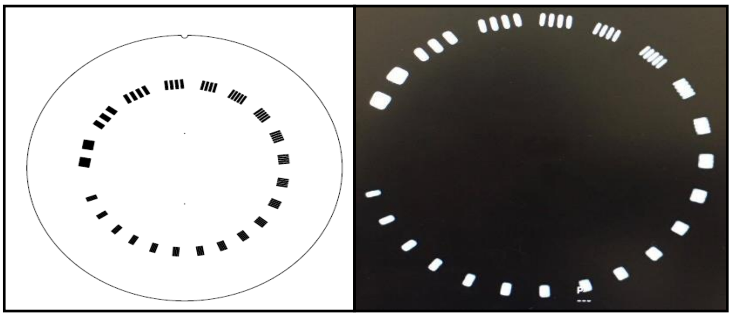

Figure B 10 The number of line pair per centimeter (1 to 21 line pair per centimeter) of high resolution test.

Results:

Table B 9 High contrast resolution

Slice Thickness in mm	Resolution	Gap size
4 mm	8 line pair/cm	0.063 cm
8 mm	8 line pair/cm	0.063 cm
12 mm	8 line pair/cm	0.063 cm

Tolerance: > 5 lp/cm visible
Comment: Pass

3.2. Low contrast resolution
Method:

1. Set up the Catphan 600 phantom in beam alignment.
2. Select the section containing the low resolution test object CTP515 Sub-slice and supra-slice low contrast Module).

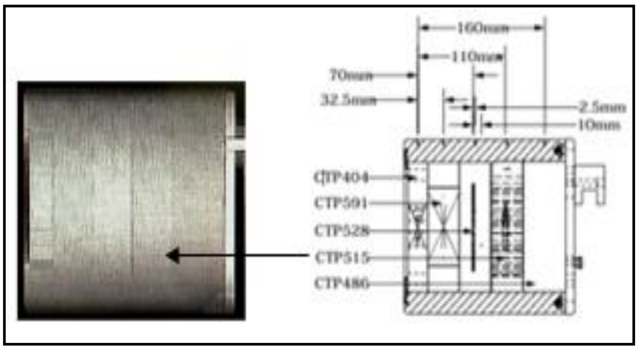

Figure B 11 Catphan phantom setting and reference line of CTP 515 section.

3. Select the head technique and perform a single transverse scan.
4. Select the area containing the low resolution test objects.
5. Select appropriate window and level for the best visualization of the test objects.
6. Record the smallest test object visualized.

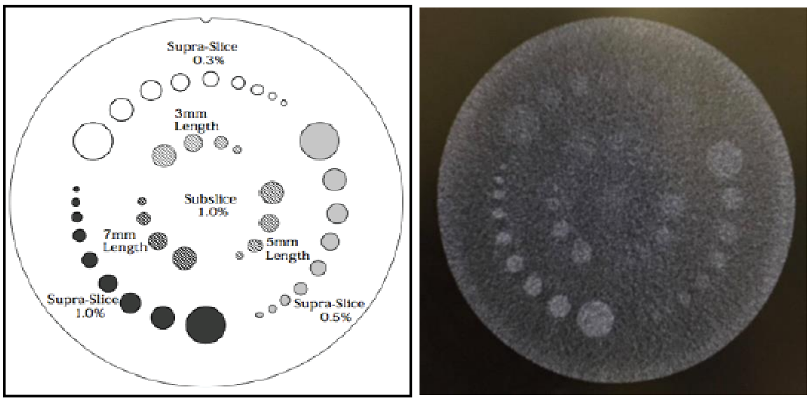

Figure B 12 Low contrast resolution measurement.

Result:

Table B 10 Low contrast resolution

Slice thickness in mm	**Smallest target(spokes) diameter (mm) should been seen**					
	Contrast level of supra-slice			**Length of sub-slice 1.0%**		
	1.00%	0.50%	0.30%	7 mm	5 mm	3 mm
4	8	5	4	4	3	3
8	9	7	5	4	3	3
12	9	8	6	4	3	3

Tolerance: The smallest target diameter at 0.5% contrast level of supra-slice should be seen 4 spokes.

Comment: Pass

3.3. Image uniformity

Method:
1. Set up the Catphan phantom as described in beam alignment.
2. Select the CTP486 solid image uniformity module.
3. Select the head technique and perform a single transverse scan.
4. Select a region of interest (ROI) of sufficient size to cover the test objects.
5. Place the ROI in the middle of each test object and record the mean C.T. number

Technique: 120kVp, 300 mA, 1sec, 250mm FOV, slice collimation 1 mm

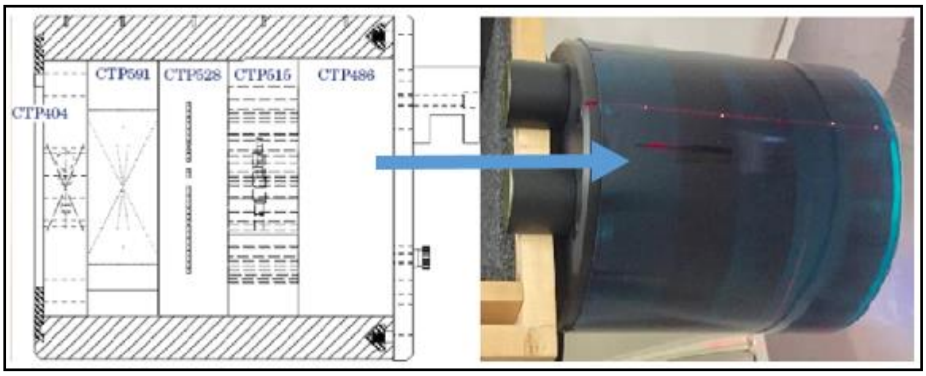

Figure B 13 Image uniformity measurement.

Results:

Table B 11 Image uniformity

Position	Mean C.T Number	S.D.	Difference (HU)
1	1.5	9.1	0.3
2	1.3	8.7	0.5
3	0.9	8.7	0.9
4	0.3	9.1	1.5
5(center)	1.8	10.1	-

Different = |CT number center – CT number peripheral
Tolerance: Less than 5 HU
Comment: Pass

3.4 Accuracy of distance measurement
Purpose: To test accuracy of distance measurement and for circular symmetry of the CT image.
Method:
1. Set up the Catphan phantom as described in beam alignment.
2. Select the section containing the test accuracy of distance measurement.
3. Select the head technique and perform a single transverse scan.
4. Measured object in x and y axes.

Result:

Table B 12 Accuracy of distance measurement

Indicated distance (mm)	Measured distance (mm)	Difference (mm)
50 mm	50.32	0.32
50 mm	50.03	0.03
50 mm	50.20	0.20
50 mm	50.49	0.49

Tolerance: The measured distance should be within ± 1 mm (NCRP No.99: Quality control test for CT scanner, section 14).
Comment: Pass

4. Verification of Computed Tomography Dose Index (CTDI)

4.1 Measurement of $C_{a,100}$ free in air (C_{air} or $CTDI_{air}$)
Purpose: To verification of Computed Tomography Dose Index (CTDI)
Method:
1. Set the 100 mm pencil chamber at the iso-center of the CT bore.
2. Using head and body protocols.
3. Set scan parameter at 100 mA, 1 sec scan time and 1, 2, 4,8,12,16,20,32 mm slice thickness.
4. Change kilovoltage at 80,100,120 and 135.
5. Record CT dose in unit of mGy.
6. Calculate $C_{a,100}$ and ${}_nC_{a,100}$ following;

$$C_{a,100} = \frac{1}{NT}\overline{M}N_{KLQ_0}k_Q k_{TP}$$

Where; $\overline{M}$: Mean value of dosimeter readings
kTP : Correction factor for temperature and pressure
$N_{P_{KL}Q_o}$: Dosimeter calibration coefficient
k_Q : Beam quality correction factor
NT : Nominal width of irradiation beam

$${}_nC_{a,100} = \frac{C_{a,100}}{P_{lt}}$$

Where; P_{lt} : Tube loading for 1 complete rotation

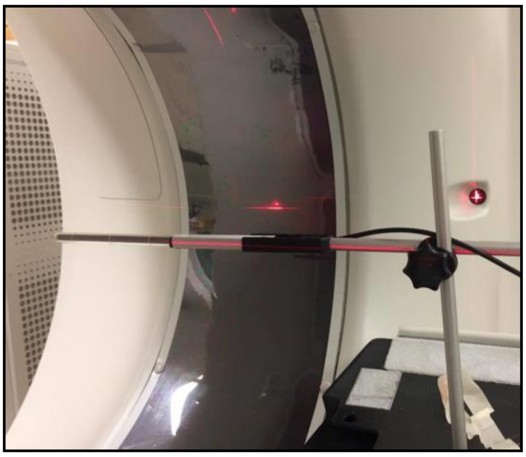

Figure B 14 $CTDI_{100}$ in air measurement using 100 mm pencil ion chamber.

Result:

Table B 13 The measured $CTDI_{100}$ in air for head protocol with 180 mm FOV(s)

$C_{a,100}$ (mGy) in air, Head protocol								
kVp	**1 (1x1)**	**2 (0.5x4)**	**4 (1X4)**	**8 (2x4)**	**12 (3x4)**	**16 (4x4)**	**20 (5x4)**	**32 (8x4)**
80	5.12	3.25	2.24	1.71	1.53	1.44	1.39	1.30
100	8.49	5.35	3.69	2.81	2.51	2.37	2.29	2.14
120	12.82	8.02	6.14	4.14	3.67	3.46	3.33	3.10
135	17.29	10.66	7.22	5.43	4.71	4.42	4.29	3.93

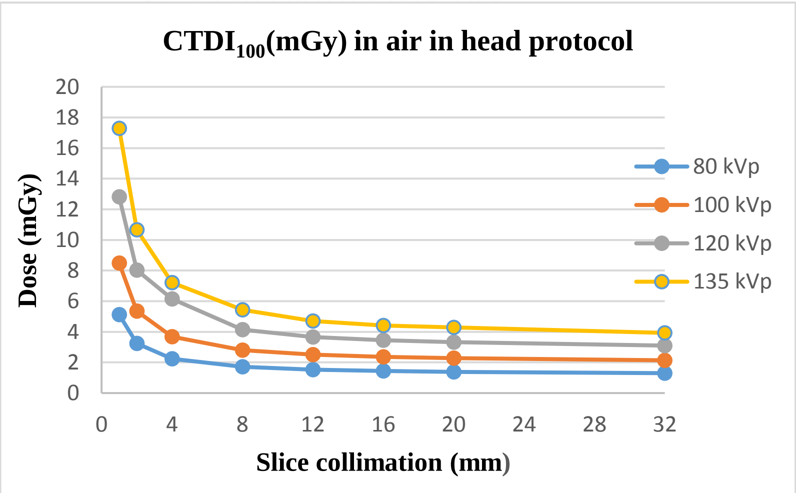

Figure B 15 $CTDI_{100}$ in air for head protocol.

Table B 14 The measured $CTDI_{100}$ in air for body protocol with 500 mm FOV (L).

$C_{a,100}$ (mGy) in air, body protocol								
kVp	**1 (1x1)**	**2 (0.5x4)**	**4 (1X4)**	**8 (2x4)**	**12 (3x4)**	**16 (4x4)**	**20 (5x4)**	**32 (8x4)**
80	5.80	3.45	2.24	1.60	1.35	1.26	1.20	1.11
100	7.07	5.94	3.11	2.37	2.33	2.15	2.04	1.89
120	15.45	9.12	5.86	4.15	3.50	3.24	3.08	2.84
135	20.96	12.24	7.79	5.44	4.56	4.22	3.74	3.65

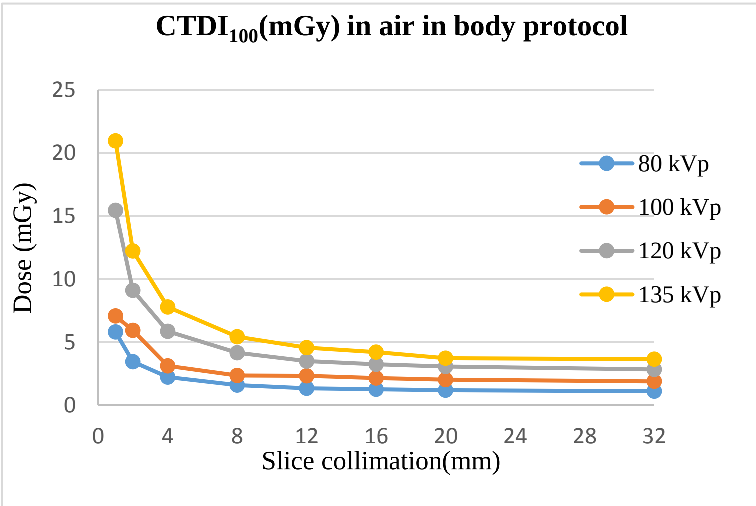

Figure B 16 $CTDI_{100}$ in air for body protocol.

4.2 Measurement of $CTDI_{100}$ in PMMA phantom
Purpose: To verification of Computed Tomography Dose Index (CTDI)
Method:
1. The $CTDI_{100}$ in head and body PMMA phantom by using a 100 mm pencil chamber place in each hole of 16(32) cm diameter PMMA phantom at the iso-center of C.T. bore.
2. Using head and body protocols.
3. The scan parameters were 100 mA, 1 sec scan time, 180 and 500 mm FOV for all measurements at each kVp setting of 80, 100, 120 and 135 in axial volume mode.
4. Record C.T. dose in unit of mGy.
3. Calculate C_w and ${}_nC_w$ following

$$C_w = \frac{1}{3}\left(C_{PMMA,100,C} + 2_{PMMA,100,P}\right)$$

$$_nC_w = \frac{C_w}{P_{lt}}$$

Figure B 17 $CTDI_{100}$ measurement in body and head PMMA phantoms using 100 mm pencil ion chamber.

Table B 15 $CTDI_{100}$ measurement in head PMMA phantom with 180 mm FOV (S).

$CTDI_{100}$ in head PMMA phantom (mGy)								
kVp	**At center**	**At peripheral**					**$CTDI_w$ or C_w (mGy at 100 mAs)**	**$_nCTDI_w$ or $_nC_w$ (mGy/ mAs)**
		3 o'clock	**6 o'clock**	**9 o'clock**	**12 o'clock**	**Average**		
80	0.6958	0.7640	0.8055	0.7676	0.7758	0.7618	9.3851	0.0939
100	1.2133	1.3650	1.4429	1.3751	1.4449	1.3682	16.7809	0.1678
120	2.0627	2.3347	2.3458	2.1689	2.1891	2.2202	27.4254	0.2743
135	2.6805	2.9818	3.0820	2.8797	3.0425	2.9333	36.1403	0.3614

Table B 16 $CTDI_{100}$ measurement in body PMMA phantom with 500 mm FOV (L).

$CTDI_{100}$ in body PMMA phantom (mGy)								
kVp	**At center**	**At peripheral**					**$CTDI_w$ or C_w (mGyat100 mAs)**	**$_nCTDI_w$ or $_nCw$ (mGy/ mAs)**
		3 o'clock	**6 o'clock**	**9 o'clock**	**12 o'clock**	**Average**		
80	0.1760	0.4166	0.3729	0.4081	0.4157	0.3579	4.0409	0.0409
100	0.3817	0.8061	0.9634	0.7321	0.8970	0.7561	8.6714	0.0867
120	0.6773	1.4692	1.2133	1.2902	1.3276	1.1955	13.8650	0.1387
135	0.9653	1.7937	1.9050	1.7836	1.8585	1.6612	19.3159	0.1932

4.3 $CTDI_{vol}$ on monitor and calculated $CTDI_w$

Purpose: To compare the $CTDI_{vol}$ displayed on CT monitor with calculated $CTDI_w$.

Method:

1. Determine the $CTDI_w$ by using the results in Table 3 and 4.
2. The $CTDI_{vol}$ displayed on CT monitor were recorded to compare percentage difference with the calculated values as shown in Table5 for $CTDI_{vol}$ in head phantom and table 6 for $CTDI_{vol}$ in body phantom.

Results:

Table B 17 $CTDI_{vol}$ displayed on monitor and calculated $CTDI_w$ in head phantom using head techniques: mAs 100, collimation 8 mm and 180 mm FOV.

kVp	$CTDI_{vol}$ (mGy) in 16 cm head phantom		
	Calculated $CTDI_w$	**Displayed $CTDI_{vol}$**	**% Difference**
80	9.38	10	6.60
100	16.78	18.3	9.05
120	27.42	28.1	2.11
135	36.14	37.1	2.65

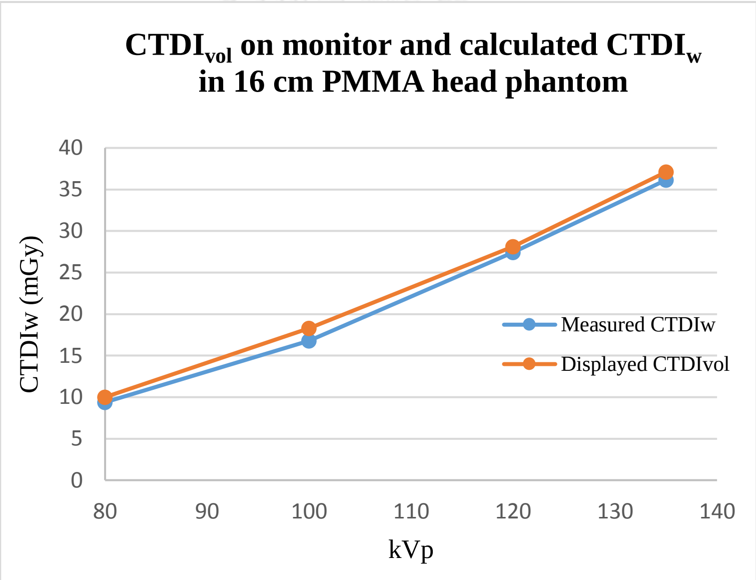

Figure B 18 $CTDI_{vol}$ on monitor and calculated $CTDI_w$ in 16 cm PMMA head phantom.

Tolerance: The difference between measured $CTDI_w$ and display should be less than ±10%

Comment: Pass

Table B 18 $CTDI_{vol}$ displayed on monitor and calculated $CTDI_w$ in body phantom using body techniques: mAs 100, collimation 8 mm and 500 mm FOV.

kVp	$CTDI_{vol}$ (mGy) in 32 cm body phantom		
	Calculated $CTDI_w$	**Displayed $CTDI_{vol}$**	**% Difference**

80	4.04	4.4	8.91
100	8.67	9	3.80
120	13.86	14.7	6.06
135	19.31	20.4	5.64

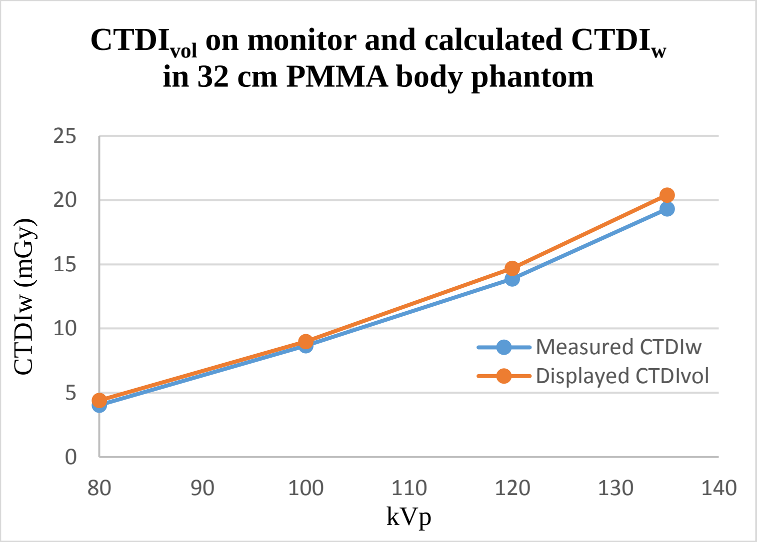

Figure B 19 $CTDI_{vol}$ on monitor and calculated $CTDI_w$ in 32 cm PMMA body phantom.

Tolerance: The difference between measured $CTDI_w$ and display should be less than ±10%
Comment: Pass

VITA

Name : MissSaowapark Yoykaew

Sex : Female

Date of birth : March 24,1990

Place of birth : Phattalung, Thailand

Qualification : Bachelor of Science Faculty of Medical Technology(Radiological Technology) Mahidol University, 2011

Job experience : Radiological Technologist, Songklanagarind Hospital

Home address : 92 Tambon Phanangtung, Amphoe Khuan Khanun,Phatthalung province, Thailand93150

Email : Lovelying1@hotmail.com